

**NOAA Technical Memorandum
NWS ER-98**



**CLIMATOLOGY OF HEAVY RAINFALL ASSOCIATED WITH
TROPICAL CYCLONES AFFECTING THE CENTRAL APPALACHIANS**

James Hudgins, Steve Keighton, Kenneth Kostura, Jan Jackson
National Weather Service Office
Blacksburg, Virginia

Scientific Services Division
Eastern Region Headquarters
Bohemia, New York
September 2005

**U.S. DEPARTMENT OF
COMMERCE**

**National Oceanic and
Atmospheric Administration**

National Weather Service

NOAA TECHNICAL MEMORANDA
National Weather Service, Eastern Region Subseries

The National Weather Service Eastern Region (ER) Subseries provides an informal medium for the documentation and quick dissemination of results not appropriate, or not yet ready for formal publications. The series is used to report on work in progress, to describe technical procedures and practices, or to relate progress to a limited audience. These Technical Memoranda will report on investigations devoted primarily to regional and local problems of interest mainly to ER personnel, and usually will not be widely distributed.

Papers 1 to 22 are in the former series, ESSA Technical Memoranda, Eastern Region Technical Memoranda (ERTM); papers 23 to 37 are in the former series, ESSA Technical Memoranda, Weather Bureau Technical Memoranda (WBTM). Beginning with 38, the papers are now part of the series, NOAA Technical Memoranda NWS.

Papers 1 to 22 are available from the National Weather Service Eastern Region, Scientific Services Division, 630 Johnson Avenue, Bohemia, NY, 11716. Beginning with 23, the papers are available from the National Technical Information Service, U.S. Department of Commerce, Sills Bldg., 5285 Port Royal Road, Springfield, VA 22161. Prices vary for paper copy and for microfiche. Order by accession number shown in parentheses at end of each entry.

ESSA Technical Memoranda

ERTM	1	Local Uses of Vorticity Prognoses in Weather Prediction. Carlos R. Dunn. April 1965.
ERTM	2	Application of the Barotropic Vorticity Prognostic Field to the Surface Forecast Problem. Silvio G. Simplicio. July 1965.
ERTM	3	A Technique for Deriving an Objective Precipitation Forecast Scheme for Columbus, Ohio. Robert Kuessner. September 1965.
ERTM	4	Stepwise Procedures for Developing Objective Aids for Forecasting the Probability of Precipitation. Carlos R. Dunn. November 1965.
ERTM	5	A Comparative Verification of 300 mb. Winds and Temperatures Based on NMC Computer Products Before and After Manual Processing. Silvio G. Simplicio. March 1966.
ERTM	6	Evaluation of OFDEV Technical Note No. 17. Richard M. DeAngelis. March 1966.
ERTM	7	Verification of Probability of Forecasts at Hartford, Connecticut, for the Period 1963-1965. Robert B. Wassall. March 1966.
ERTM	8	Forest-Fire Pollution Episode in West Virginia, November 8-12, 1964. Robert O. Weedfall. April 1966.
ERTM	9	The Utilization of Radar in Meso-Scale Synoptic Analysis and Forecasting. Jerry D. Hill. March 1966.
ERTM	10	Preliminary Evaluation of Probability of Precipitation Experiment. Carlos R. Dunn. May 1966.
ERTM	11	Final Report. A Comparative Verification of 300 mb. Winds and Temperatures Based on NMC Computer Products Before and After Manual Processing. Silvio G. Simplicio. May 1966.
ERTM	12	Summary of Scientific Services Division Development Work in Sub-Synoptic Scale Analysis and Prediction - Fiscal Year 1966. Fred L. Zuckerberg. May 1966.
ERTM	13	A Survey of the Role of Non-Adiabatic Heating and Cooling in Relation of the Development of Mid-Latitude Synoptic Systems. Constantine Zois. July 1966.
ERTM	14	The Forecasting of Extratropical Onshore Gales at the Virginia Capes. Glen V. Sachse. August 1966.
ERTM	15	Solar Radiation and Clover Temperatures. Alex J. Kish. September 1966.
ERTM	16	The Effects of Dams, Reservoirs and Levees on River Forecasting. Richard M. Greening. September 1966.
ERTM	17	Use of Reflectivity Measurements and Reflectivity Profiles for Determining Severe Storms. Robert E. Hamilton. October 1966.
ERTM	18	Procedure for Developing a Nomograph for Use in Forecasting Phenological Events from Growing Degree Days. John C. Purvis and Milton Brown. December 1966.
ERTM	19	Snowfall Statistics for Williamsport, Pa. Jack Hummel. January 1967
ERTM	20	Forecasting Maturity Date of Snap Beans in South Carolina. Alex J. Kish. March 1967.
ERTM	21	New England Coastal Fog. Richard Fay. April 1967.
ERTM	22	Rainfall Probability at Five Stations Near Pickens, South Carolina, 1957-1963. John C. Purvis. April 1967.
WBTM ER 23		A Study of the Effect of Sea Surface Temperature on the Areal Distribution of Radar Detected Precipitation Over the South Carolina Coastal Waters. Edward Paquet. June 1967. (PB-180-612).
WBTM ER 24		An Example of Radar as a Tool in Forecasting Tidal Flooding. Edward P. Johnson. August 1967 (PB-180-613).
WBTM ER 25		Average Mixing Depths and Transport Wind Speeds over Eastern United States in 1965. Marvin E. Miller. August 1967. (PB-180-614).
WBTM ER 26		The Sleet Bright Band. Donald Marier. October 1967. (PB-180-615).
WBTM ER 27		A Study of Areas of Maximum Echo Tops in the Washington, D.C. Area During the Spring and Fall Months. Marie D. Fellechner. April 1968. (PB-179-339).
WBTM ER 28		Washington Metropolitan Area Precipitation and Temperature Patterns. C.A. Woollum and N.L. Canfield. June 1968. (PB-179-340).
WBTM ER 29		Climatological Regime of Rainfall Associated with Hurricanes after Landfall. Robert W. Schoner. June 1968. (PB-179-341).
WBTM ER 30		Monthly Precipitation - Amount Probabilities for Selected Stations in Virginia. M.H. Bailey. June 1968. (PB-179-342).
WBTM ER 31		A Study of the Areal Distribution of Radar Detected Precipitation at Charleston, S.C. S.K. Parrish and M.A. Lopez. October 1968. (PB-180-480).
WBTM ER 32		The Meteorological and Hydrological Aspects of the May 1968 New Jersey Floods. Albert S. Kachic and William Long. February 1969. (Revised July 1970). (PB-194-222).
WBTM ER 33		A Climatology of Weather that Affects Prescribed Burning Operations at Columbia, South Carolina. S.E. Wasserman and J.D. Kanupp. December 1968. (COM-71-00194).
WBTM ER 34		A Review of Use of Radar in Detection of Tornadoes and Hail. R.E. Hamilton. December 1969. (PB-188-315).
WBTM ER 35		Objective Forecasts of Precipitation Using PE Model Output. Stanley E. Wasserman. July 1970. (PB-193-378).
WBTM ER 36		Summary of Radar Echoes in 1967 Near Buffalo, N.Y. Richard K. Sheffield. September 1970. (COM-71-00310).
WBTM ER 37		Objective Mesoscale Temperature Forecasts. Joseph P. Sobel. September 1970. (COM-71-0074).

NOAA Technical Memoranda NWS

NWS	ER 38	Use of Primitive Equation Model Output to Forecast Winter Precipitation in the Northeast Coastal Sections of the United States. Stanley E. Wasserman and Harvey Rosenblum. December 1970. (COM-71-00138).
NWS	ER 39	A Preliminary Climatology of Air Quality in Ohio. Marvin E. Miller. January 1971. (COM-71-00204).
NWS	ER 40	Use of Detailed Radar Intensity Data in Mesoscale Surface Analysis. Robert E. Hamilton. March 1971. (COM-71-00573).
NWS	ER 41	A Relationship Between Snow Accumulation and Snow Intensity as Determined from Visibility. Stanley E. Wasserman and Daniel J. Monte. (COM-71-00763). January 1971.
NWS	ER 42	A Case Study of Radar Determined Rainfall as Compared to Rain Gage Measurements. Martin Ross. July 1971. (COM-71-00897).
NWS	ER 43	Snow Squalls in the Lee of Lake Erie and Lake Ontario. Jerry D. Hill. August 1971. (COM-72-00959).
NWS	ER 44	Forecasting Precipitation Type at Greer, South Carolina. John C. Purvis. December 1971. (COM-72-10332).
NWS	ER 45	Forecasting Type of Precipitation. Stanley E. Wasserman. January 1972. (COM-72-10316).

(CONTINUED ON INSIDE REAR COVER)

NOAA Technical Memorandum NWS ER-98

**CLIMATOLOGY OF HEAVY RAINFALL ASSOCIATED WITH
TROPICAL CYCLONES AFFECTING THE CENTRAL APPALACHIANS**

James Hudgins, Steve Keighton, Kenneth Kostura, Jan Jackson

NOAA/National Weather Service Office
Blacksburg, Virginia

Scientific Services Division
Eastern Region Headquarters
Bohemia, New York
September 2005

United States
Department of Commerce
Carlos M. Gutierrez
Secretary

National Oceanic and
Atmospheric Administration
Conrad C. Lautenbaucher, Jr.
Under Secretary and Administrator

National Weather Service
David L. Johnson
Assistant Administrator



Table of Contents

ABSTRACT	1
1. INTRODUCTION	1
2. TOPOGRAPHY	1
3. DATA AND METHODOLOGY	2
4. STRATIFICATION OF STORMS	3
5. MONTHLY CLIMATOLOGY	4
6. RAINFALL DISTRIBUTION	4
6.1 Atlantic Coast Landfalls	4
6.1.1 Carolina Coast.....	4
6.1.2 SE Coast.....	5
6.1.3 From East.....	5
6.2 Gulf Coast Landfalls	5
6.2.1 West of Mountains.....	6
6.2.2 Across the Mountains from the West.....	6
6.2.3 Paralleling SE of the Mountains.....	6
6.2.4 Along Appalachian Spine.....	7
6.3 Outlier Storms	7
7. FACTORS INFLUENCING HEAVY RAIN	7
8. CONCLUSION	8
ACKNOWLEDGEMENTS	9
REFERENCES	10
FIGURES	11
TABLES	21
APPENDIX A	22

ABSTRACT

Over 50 years (1950-2004) of rainfall events associated with tropical cyclones that affected the central Appalachians were examined. Tracks of tropical cyclones (or tropical depression remnants) that passed within 500 km of the National Weather Service Office in Blacksburg, VA were compared with associated rainfall analyses of the Appalachian region in Virginia, West Virginia, and northwest North Carolina. In addition, surface and upper air analyses were examined for each event to help determine the relative influence of factors such as upslope flow, overrunning, and boundary interaction in relation to the cyclone track on the specific location and amounts of precipitation. The speed of movement across or along the Appalachians, as well as intensity of the cyclone (maximum wind speeds) as it passed through the analysis area, was also considered. The events were divided into categories based on the location the tropical cyclone made landfall. The seasonal distribution, e.g., which specific months are favored for tropical cyclone activity in the region, is also shown.

These data were compiled in order to provide forecasters with a climatological database of tropical cyclones affecting the area, as well as the rainfall from these events. Results of the study will aid forecasters when assessing the potential effects of future tropical cyclone tracks and their rainfall impact on the Central Appalachians.

1. INTRODUCTION

NOAA's National Weather Service (NWS) Weather Forecast Offices (WFOs) have the responsibility for issuing flood or flash flood warnings for the protection of life and property across their County Warning Areas (CWAs). During the summer and early fall months, a substantial percentage of heavy rain events in the Central Appalachians requiring these warnings are associated with land-falling tropical cyclones. Since tropical cyclones can deliver catastrophic amounts of rain, an examination of data detailing the patterns and effects of past storms is critical to understanding the impact of these systems. The purpose of this study is to establish a database of tropical cyclone tracks and associated rainfall affecting the Central Appalachians, and to determine which factors are the most influential in producing substantial rainfall. This tropical rainfall climatology will be an important operational and training reference for forecasters in the Central Appalachian region, and will supplement current references which focus on track climatology (Hudgins 2000). Results of this study will allow forecasters to better assess the potential rainfall impact of future tropical cyclones on the Central Appalachians, in order to issue more accurate and timely flood and flash flood watches and warnings. Analyses of each of the rainfall events and the associated tropical cyclone tracks as well as the depiction of other key factors including surface and upper air charts, is contained in the Appendix.

2. TOPOGRAPHY

Figures 1 and 2 show geographical and political features and names within the analysis area referred to in the discussion, including topography, rivers, mountain ridges, valleys, and counties. The topography of the Central Appalachians is characterized by a rapid increase in elevation from southeast to northwest, starting from less than 1,000 feet in the Piedmont, to mountainous terrain of 3,200-5,000 feet in the higher elevations of the Blue Ridge, and Appalachian mountains of western Virginia (VA), southeastern West Virginia (WV), and northwestern North Carolina (NC). Incorporated within the two mountain ranges exists a number of high elevation valley locations. Topography appeared to be one of the biggest factors in contributing to heavy rainfall and the overall distribution of the rainfall for all the events examined, and indeed is generally a major influence in this region on most precipitation events, tropical or not. This is because upslope low-

level flow can initiate and enhance rainfall development. Perpendicular trajectories into higher mountain ridges often produces the heaviest rain, especially along east and southeast facing slopes of the Blue Ridge and Appalachian mountain chains. We believe this is the case for a couple of reasons: 1) these are the first ridges to produce upslope flow for storms moving in from the nearby Atlantic, and often the movement of the storm contributes to the ground-relative wind speed from the southeast direction; 2) the upslope component on the western side of the Appalachians is not as significant as on the east since the mountains rise more gradually from the west; 3) storms moving in from the west have usually traveled farther over land and may be much weaker, yet when crossing the Appalachians still often produce more rainfall on the southeastern slopes due to more abrupt upslope from southeasterly winds circulating around the cyclone, and possibly advecting in more moisture from the Atlantic.

3. DATA AND METHODOLOGY

Tropical storm tracks and rainfall data from 1950-2004 were gathered using data archives from NOAA's NWS Tropical Prediction Center (TPC), Unisys, and the National Climatic Data Center (NCDC). Additional weather parameters were provided by the NWS Daily Weather Map Series and the Plymouth State University meteorology web site. All the data were compiled and incorporated into a graphical database using Global Tracks hurricane software (JincSolutions 2004).

The paper examines tracks of tropical cyclones that passed within 500 km of the NWS Blacksburg, VA (RNK), located in the heart of the Appalachians (see Fig. 1), with comparison to the associated rainfall analyses of the Central Appalachian region in Virginia, West Virginia, and Northwest North Carolina. The radius of 500km was chosen as the boundary that within which tropical cyclone tracks had a major flooding impact on the Central Appalachians. Outside of this radius no rainfall influenced the Central Appalachian region. Location of tropical cyclone landfall and inland storm track were used to divide the events into different categories. Surface and upper air maps were then examined for all events to help determine if any of the following factors may have been more important for a particular category:

1. Upslope flow: Air flow perpendicular to the northeast to southwest oriented Appalachians producing rising atmospheric motion, enhancing condensation and precipitation.
2. Overrunning: Warm air riding up over a layer of colder air producing rising atmospheric motion and widespread precipitation.
3. Frontal boundary interaction: A boundary contributing to rising motion and heavier precipitation, and also focusing heavier precipitation along or near a quasi-stationary linear zone.
4. Speed of movement: Average motion of each of the inland remnant tropical cyclones as they passed through the region were determined by the tracking software, and ranged from less than 10 mph to greater than 45 mph. Storms moving 15 mph or less were classified as slow movers, and greater than 20 mph as fast movers. These thresholds were chosen subjectively based on a strong weighting of distributions on either side of these values, with only a few events in between.

Seasonal aspects including which specific months were favored for tropical cyclone activity and the most extreme rainfall were also analyzed.

4. STRATIFICATION OF STORMS

The climatological analysis considered all 32 land-falling tropical cyclones that tracked within 500 km of NWS WFO Blacksburg from 1950-2004 (Fig. 3). It is important to point out that not all of these events resulted in flooding rains, (a couple only produced 1-2 inches maximum rainfall). The 32 events were then examined more closely in order to discriminate between Atlantic and Gulf Coast land-falling tropical cyclone tracks, and to determine the relative importance of a number of factors, including speed of movement, degree of upslope, overrunning, and boundary interaction as it passed through the region.

Atlantic land falling storms affecting the Central Appalachians favored more of a perpendicular track, making landfall along the southeast U.S. coast, and producing a trajectory directly into or just parallel to the mountains. There were three distinct groups based upon the inland track:

1. **Carolina Coast:** Making landfall north of Charleston, SC, and continuing on a northwest to north track (Hazel, Connie, Diane, Hugo, Fran, Gaston, and Isabel; Fig. 4a).
2. **SE Coast:** Making landfall south of Charleston SC, and continuing on a north to northeast track (Able, Abby, David, Bob (85), Chris, Gracie, Jeanne, and Subtropical Storm 3; Fig. 4c).
3. **From the East:** Tracking westward into the area, and then dissipating (Bret and Dennis; Fig. 4e).

Gulf Coast system tracks tended to have the most variability, with four distinct subgroups defined according to their inland track:

1. **West of the Mountains:** Tracking northeastward on the west side of the Appalachians (Audrey, Opal and Frederic; Fig. 5a).
2. **Across Mountains from the West:** Tracking eastward across the Central Appalachians in West Virginia and Virginia (Camille, Bob (79), and Claudette; Fig. 5c).
3. **Paralleling SE of the Mountains:** Tracking east-northeast across the Carolinas (Agnes and Danny [97]; Fig. 5e).
4. **Along Appalachian Spine:** Tracking parallel to and along the Appalachian Mountains (Eloise, Danny (85), Beryl, Frances, and Ivan; Fig. 5g).

These categories, along with two storms considered to be outlier events since they did not fit in any of the above categories (see Fig. 6), will be discussed further in Section 7.

Several figures for each event are shown in the Appendix, and the index of events, their dates, categories, and where they can be found in the Appendix are listed in Table 1. The figures for each storm include a map of the storm track and strength, along with the rainfall analysis overlaid on a terrain background image. The track map also indicates the most important features of the event, such as important contributing factors to heavy rainfall, or in some cases, lack there of. These

figures together provide a relative sense for how the rainfall distribution was related to the path and intensity of the storm. Additionally, figures for each storm depict the observed surface station plot with frontal positions and precipitation at two different times as the storm moved across the area of study, as well as one representative observed 500 hPa chart with height contours and winds. These two figures provide the overall synoptic pattern, as well as an indication for potential boundary interaction.

5. MONTHLY CLIMATOLOGY

The seasonal distribution of tropical cyclones shows that the Central Appalachians can experience effects from tropical systems between May and October. However, tropical cyclones are most apt to make an impact during the mid and late summer months of August and September (Fig. 7), which corresponds to the overall peak of the North Atlantic tropical storm season (Neumann et. al 1993). This study and the seasonal distribution shown in Fig. 7 only includes the 32 storms from the 1950-2004 period since this was the time that data was more readily available.

6. RAINFALL DISTRIBUTION

Rainfall distributions showed a wide variation in totals ranging from 10 to 14 inches (and even higher single maximum reports in a few events) to some storms with only 1 to 2 inches maximum rainfall amounts. This variability was at least partially dependent upon where systems made landfall and how they eventually tracked in relation to the Central Appalachians. The tropical cyclone tracks were divided into two categories: Atlantic and Gulf Coast land falls. Each category was then sub-divided based on cyclone track relative to topography (section 5). In addition, rainfall composite depictions were included to show where the heaviest rainfall would typically occur with each of the different track categories. The maximum amounts represent the locations that would normally receive the greatest rainfall totals. Surrounding these areas are regions where on average substantial rainfall (2 inches or more) might occur. However, some of the categories were limited to a small number of storms and thus the depicted rainfall composites may not be representative due to the sample size. A rainfall composite for the outlier category was not produced since rainfall amounts were inconclusive based on the nature of varying tracks. Refer to Figure 2 for any descriptions of geographic regions, counties, or river names.

6.1 Atlantic Coast Landfalls

Rainfall characteristics of Atlantic Coast land-falling storms were divided into three subcategories (Fig. 4), Carolina Coast, SE Coast, and those that moved directly inland from the east.

6.1.1 Carolina Coast

Systems moving inland across the Carolina Coast (Fig. 4a) and then along or parallel to the mountains brought the heaviest rainfall of those making landfall along the Atlantic Seaboard. Five of the six storms studied (Connie, Diane, Fran, Hazel, and Isabel), all produced areas of rainfall in excess of 3 inches, with heavier amounts in northeast to southeast upslope areas along the Blue Ridge, especially from the Southern Shenandoah Valley northward. Maximum totals between 10

and 14 inches were observed in the Shenandoah Valley with Diane, Fran, Hazel, and Isabel. Common maximum rainfall total locations included Nelson, Albemarle, Augusta, Rockingham, Page, and Madison counties where several systems caused flooding rainfall (Fig. 4b). Hugo was the exception as it confined most of its heavy rain of a 2 to 6 inch narrow axis in southeast upslope areas across northwest NC and parts of southwestern VA. The smaller area of heavier rain associated with Hugo is attributable to its fast movement and track across the mountains before turning north (average speed 25 to 30 mph). Gaston's more eastward track focused its heavy rain across the Piedmont where totals greater than 3 inches occurred, while nearly null amounts of less than one quarter of an inch fell over the Blue Ridge and Central Appalachians.

6.1.2 SE Coast

Most common were storms making landfall on the SE Coast (Fig. 4c) and then tracking parallel to the mountains. These, with the exception of the subtropical storm, tended to produce the most expansive areas of heavy rain, with maximums of 3 to 9 inches along the east to southeast facing portions of the Blue Ridge from northwest NC into west-central VA (Fig. 4d).

Specifically, the highest totals were observed across Watauga and Ashe counties in northwest NC, and across Grayson, Carroll, Patrick, Floyd, Roanoke, and Franklin counties in southwest VA. A secondary rainfall maximum was also seen from Botetourt, Rockbridge, Amherst and Nelson counties, and across Albemarle, Madison, Page and Rockingham counties (or the area surrounding much of the Shenandoah Valley). Both David and Gracie were slow moving storms with average speeds less than 15 mph, and they resulted in the highest totals, with widespread 3 to 7 inch amounts and local reports of isolated higher amounts along the Blue Ridge and Shenandoah Valley. Able, Bob, and Chris were faster moving storms of 20 mph or more, with similar locations of the heaviest rain to the previous two storms, but had lighter 2 to 6 inch totals. Despite being slow moving systems, with average speeds less than 10 mph, Abby and Subtropical Storm Three were both smaller and weaker storms, focusing the heavier rainfall mainly on the Northwest NC mountains, where between 2 and 4 inches occurred. Jeanne's rainfall was focused more along the track of the remnant system. Although Jeanne moved faster than 20 mph, it did produce a narrow swath of 5 to 7 inches along the Blue Ridge. This resulted in major, river flooding along the Roanoke River at Roanoke VA, and moderate flooding on the Dan River near South Boston VA.

6.1.3 From the East

Tropical cyclones tracking inland perpendicular from the east (Fig. 4e) focused their heavy rain along the Blue Ridge, Alleghany Highlands and Shenandoah Valley of VA (Fig. 4f). Given the limited number of cases (Bret and Dennis), a true representation of rainfall distribution over time is quite limited. However, Dennis did produce between 3 and 8 inches across much of the region with lighter 1 to 2 inch amounts along the western slopes of the Appalachians. Bret, on the other hand, resulted in overall minimal totals, with only a 1 to 2 inch swath across parts of eastern WV, as well as the Alleghany Highlands and Shenandoah Valley in VA.

6.2 Gulf Coast Landfalls

Rainfall distribution with Gulf Coast land-falling storms was divided into four track categories (Fig. 5): west of mountains, across the mountains from the west, paralleling southeast of the mountains, and tracking along spine of the Appalachians.

6.2.1 West of Mountains

Maximum rainfall associated with storms tracking west of the mountains (Fig. 5a) tended to focus heavy rain (>2 inches) across the Northwest NC mountains, as well as parts of the Blue Ridge and Shenandoah Valley of VA (Fig. 5b). The counties of Watauga and Ashe in northwest NC as well as Grayson County VA bordering immediately to the north had the highest occurrence of heavy rain in these situations. Hurricane Opal was one of the most prolific rain producers associated with this track. Maximum totals of around 8 inches were observed across the northwest NC Mountains with Opal. Frederic and Audrey, although closer to the Central Appalachians, were fast moving storms with average speeds near 50 mph, and only responsible for maximum rainfall amounts of 1 to 3 inches from northwest NC into the Alleghany Highlands of VA, as well as eastern WV.

6.2.2 Across the Mountains from the West

Storms moving across the Appalachians from the west (Fig. 5c) were limited to just a few systems, while producing one of the most catastrophic rainfall events ever in the Central Appalachian region. In 1969, Camille interacted with a stationary front as it crossed the mountains to produce a 6 to 20 inch rain swath over the VA Alleghany Highlands, Blue Ridge and Southern Shenandoah Valley. More specific locations receiving the brunt of Camille's flooding rainfall included Rockbridge, Nelson, and Albemarle counties across the Southern Shenandoah Valley in VA, where an isolated 27 inch total was observed. The 27 inches was found on a bucket survey by the National Weather Service (at the time the Weather Bureau) and occurred in an 8-hour period. This torrential rainfall from Camille resulted in the worst flash flood in Virginia's history, killing 117 (Schwarz 1970).

Other storms tracking across the Appalachians from the west, such as Bob and Claudette, were much less impressive and produced near null event totals. Their rainfall totals of around one inch across far northeast VA were much less than the excessive amount seen from Camille, whose rainfall total heavily weighted the rainfall composite for this category (Fig. 5d).

6.2.3 Paralleling SE of the Mountains

There were only two tropical cyclones from the Gulf that paralleled the Appalachians well to the southeast (Fig. 5e) over the past 54 years, but both were associated with heavy rainfall. Those storms were Danny in 1997 and Agnes (1972), and they both focused the heavier rain totals along the Blue Ridge and Shenandoah Valley regions where large swaths of 3 to 8 inches were noted. The heaviest rain was associated with upslope enhancement on east to southeast facing slopes. This region incorporated the counties of Floyd, Franklin, and Patrick along the Blue Ridge, to Rockbridge, Nelson, Albemarle, Page, and Madison counties in the Shenandoah Valley (Fig. 5f).

Both Agnes and Danny were slow moving storms, with average speeds less than 15 mph. Agnes, despite being a minimal hurricane at landfall, was particularly devastating to the area due to its extremely large size and slow movement. Record flooding occurred along the Dan River and middle to lower James River in VA (Fig. 2). Widespread rainfall also occurred farther west into parts of the Appalachians, but of lighter intensity with rainfall amounts totaling between 1 and 3 inches.

6.2.4 Along Appalachian Spine

Systems tracking along the spine of the Appalachians (Fig. 5g) produced the most widespread heavy rain of those systems making landfall along the Gulf Coast. The heaviest rain was associated with upslope enhancement on southeast to south facing slopes from the northwest NC Mountains, across parts of Southwest VA, including the Blue Ridge and into the Southern Shenandoah Valley (Fig. 5h). More specifically, this included Watauga and Ashe counties in NC, to Floyd, Franklin, and Patrick counties along the Blue Ridge, to Rockbridge and Nelson counties in the Southern Shenandoah Valley of VA. Both Danny and Beryl gave small corridors of 8 to 10 inches across parts of the southern Blue Ridge in VA and NC, while Eloise focused her heaviest rain along the VA Blue Ridge counties where 3 to 6 inches fell. All of these storms were associated with slow average speeds of 15 mph or less. Rainfall from Frances was enhanced by a combination of strong easterly upslope and an old frontal boundary. This produced over 12 inches of rain across the northwest NC Mountains, and on average 4 to 8 inches along the Blue Ridge in VA. Although the heaviest rain from Ivan fell to the northwest of the Appalachians, Ivan's interaction with an old frontal boundary coincided with a brief period of upslope from the southeast to bring areas of 4 to 6 inches along the Blue Ridge.

6.3 Outlier Storms

There were two storms, Jerry and Juan that tracked within the 500 km radius, but stalled and dissipated before reaching the Appalachians. They did not fall into any of the above categories, so were classified as outlier storms (Fig. 6). Jerry moved inland across Florida and stalled well south of the area before dissipating. Juan made landfall along the central Gulf coast and then slowly drifted north into the Tennessee Valley where it also dissipated. Moisture from these systems did however produce between 2 and 5 inches of rain across Northwest NC and parts of the VA Blue Ridge mountains. Jerry also produced extreme rainfall across parts of the southern Appalachians, particularly in western South Carolina.

7. FACTORS INFLUENCING HEAVY RAINFALL

Upslope flow associated with tropical cyclones appeared to be the most important factor in determining the distribution of maximum rainfall. This was especially true with low-level flow from the southeast since this is the most favorable upslope orientation for the Blue Ridge, where the highest rainfall totals were most often observed (Fig. 8). The heavier rainfall was due to the stronger prolonged upslope, especially from Carolina Coast land falling systems which focused the heavier rainfall along the Blue Ridge rather than the higher terrain of the Appalachians to the

west. In addition, higher peaks and locations along the Blue Ridge that jut out are also highly favored for heavier rain due to upslope from several directions.

Speed of movement and overall strength/intensity (within the 500 km radius) appeared to be very important in determining overall extreme amounts, due to duration of tropical moisture in any one location as well as duration of enhanced upslope flow. Stronger storms (i.e., hurricane strength) that made landfall along the Atlantic Coast were usually more intense as they passed through the region of study compared to Gulf Coast landfalls, simply due to the proximity of the Atlantic to the Appalachian region. In terms of speed of movement, a subjective stratification of the 32 events by their average speed through the region showed that storms moving at speeds of 20 mph or greater tended to produce maximum rainfall of 3 inches or less. The few exceptions to this were influenced by particularly strong upslope or interaction with a boundary, such as Camille. Slow moving storms (average speeds of 10 mph or less) generally resulted in rainfall amounts of at least 6 inches. Several other factors examined in this study, including overrunning and frontal boundary interaction across the Central Appalachians, were found to influence heavy rainfall distribution and amounts.

Atlantic land falling tropical cyclones that caused heavy rain were seen to be highly track, speed, and strength dependent, with nearly all exhibiting some enhancement by upslope flow. Storms that made landfall further south were better supported by prolonged east-southeast upslope, while Carolina coastal landfalls oriented heavy rain along the track (such as Isabel - Fig 9), with a shorter span of upslope, particularly in northwest NC and far southwest VA.

Gulf track systems were found to be highly dependent upon east-southeast upslope (Agnes, Opal, and Frederic) as well as enhanced by overrunning and interaction with residual frontal boundaries (Beryl, Juan, Eloise, Danny [97]). However, in the presence of upslope and overrunning, speed of movement proved critical as slow moving systems with average speeds of 10 mph or less, such as Agnes, Beryl, Danny (85), Eloise, and Juan produced significant widespread heavy rain, while fast movers with average speeds greater than 20 mph, such as Frederic, confined heavier rainfall to mainly the northwest NC mountains. Several systems were shown to exhibit combined factors with along-track heavy rain aided initially by upslope or overrunning, then enhanced by boundary interaction. This was especially true with Camille, Beryl, and Eloise, which tracked into the Appalachians as weakening tropical depressions.

8. CONCLUSION

Tropical cyclones that move inland and affect the Central Appalachians often produce heavy to excessive rainfall of 5 to 12 inches or occasionally much higher. These systems are most likely during the months of August, September, and early October with land falling tracks from both the Atlantic and Gulf of Mexico. The topography of the Appalachians plays an important role in focusing the heaviest rainfall in highly favored upslope regions. This includes the northwest NC Mountains, Blue Ridge mountains, Alleghany Highlands, and Shenandoah Valley of VA. Specifically, the higher terrain of the Blue Ridge on the eastern side of the Shenandoah Valley in Madison, Page, and Nelson counties in VA showed a high occurrence of heavy rainfall, especially in the extreme events. In addition, examination of rainfall analysis figures revealed that Floyd,

Franklin, and Patrick counties along the southern Blue Ridge mountains of VA, and Watauga and Ashe counties in the northwest NC mountains also had a relatively high frequency of rainfall maximum from tropical cyclones.

Several other factors including speed of storm movement, track relative to orientation of ridges, and boundary interaction also contributed to location and amount of rainfall. On average, the stronger tropical cyclones that affected the Appalachians were those making landfall on the southeast U.S. coast, particularly systems that moved inland across the Carolinas. With the exceptions of Camille and Opal, storms making landfall along the Gulf Coast were weaker, with most of minimal hurricane or tropical storm strength. However, storm intensity at the time of landfall was not a consistent factor, and not nearly as important as upslope flow and speed of movement as the systems encountered the Appalachian region.

The database containing electronic maps of the hurricane track, rainfall analysis, as well as surface and 500 hPa plots for each system, will serve as a baseline in assessing the potential effects of future tropical cyclones and their rainfall impact. This database of images of past tropical cyclone events will be made available soon on-line from the Blacksburg National Weather Service Forecast Office web site (<http://www.erh.noaa.gov/rnk/>), as well as internally to local forecasters, and will be organized to allow users to quickly search for a particular storm name, storm date, or view all storms within a particular category. The intention is to update the database as needed on a seasonal basis.

ACKNOWLEDGEMENTS

This study was supported by data provided by the Unisys (<http://weather.unisys.com>) and Plymouth State University (<http://cyclone.plymouth.edu>) web sites. Tracking software was supplied by Jincs Solutions (<http://www.jincsolution.com>). The use of commercial products and services does not constitute endorsement by the NWS. The authors wish to thank Brian Sutherland and Mike Gillen of WFO RNK for help with rainfall analysis, figure and text formatting.

REFERENCES

Hudgins, J. E., 2000: Tropical cyclones affecting North Carolina since 1586 – an historical perspective. *NOAA Tech Memo ER-92*, 83 pp. [Available from NWS Eastern Region Headquarters, Scientific Services Division, Bohemia, NY]

Jincs Solutions, cited 2004: Global Tracks. [Available on-line at: <http://www.jincsoptions.com>]

Neumann, C.J., B.R. Jarvinen, C.J. McAdie, and J.D. Elms, 1993: *Tropical Cyclones of the North Atlantic Ocean, 1871-1992*. Historical Climatology Series, Vol. 6, No. 2, National Climatic Data Center, 193 pp.

Schwarz, F.K. 1970: The unprecedented rains in Virginia associated with the remnants of Hurricane Camille. *Mon. Wea. Rev.*, **98**, p. 851–859.

Figures

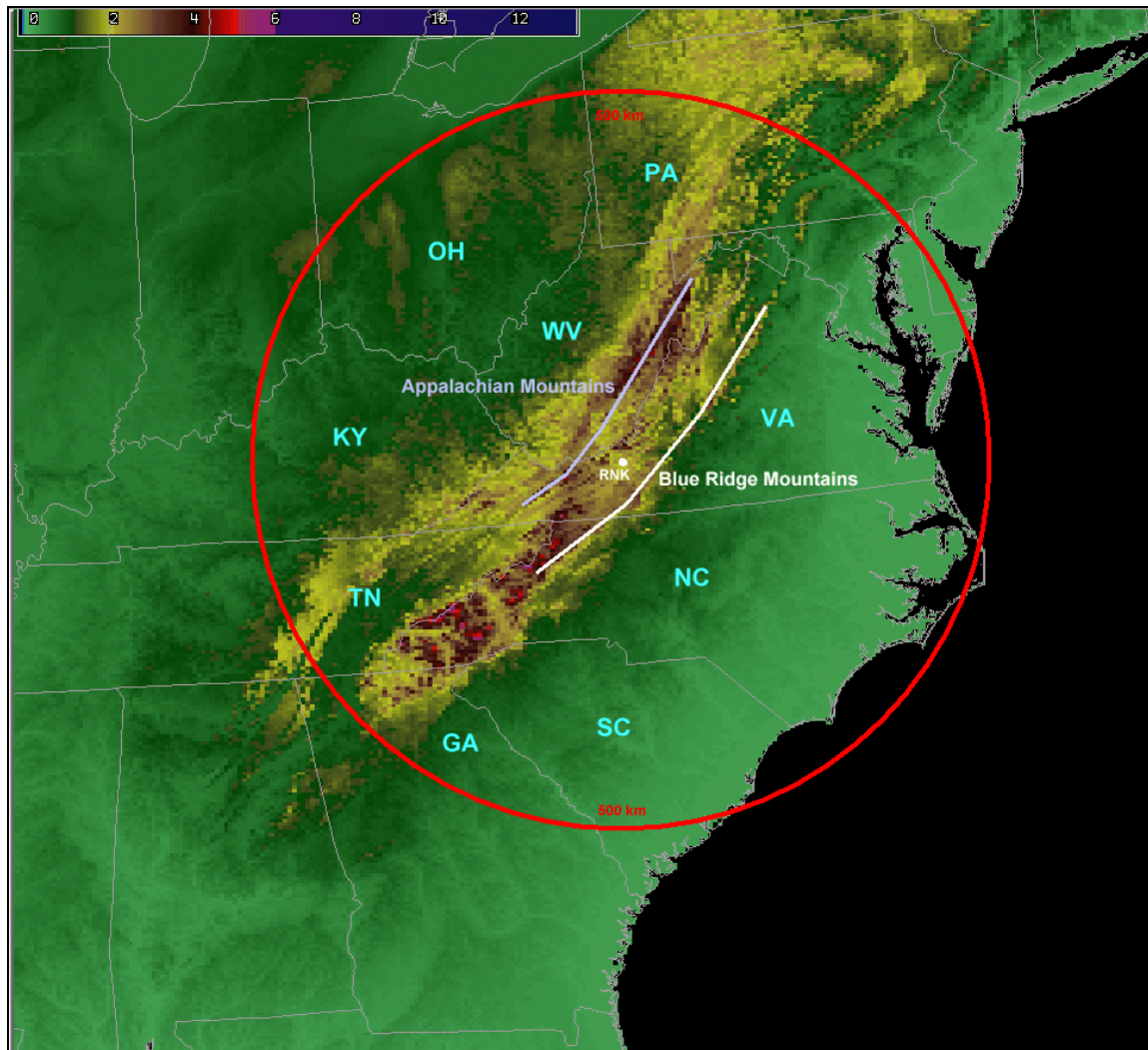


Figure 1. Color coded topographical map showing differences in elevation across the Blue Ridge Mountains (white line) and the Appalachians (gray line) as well as the 500 km range ring (red) depicting the area of interest around RNK. Color scale in upper left includes integers which are the elevations in thousands of feet (bright yellow being 2,000 ft for example).

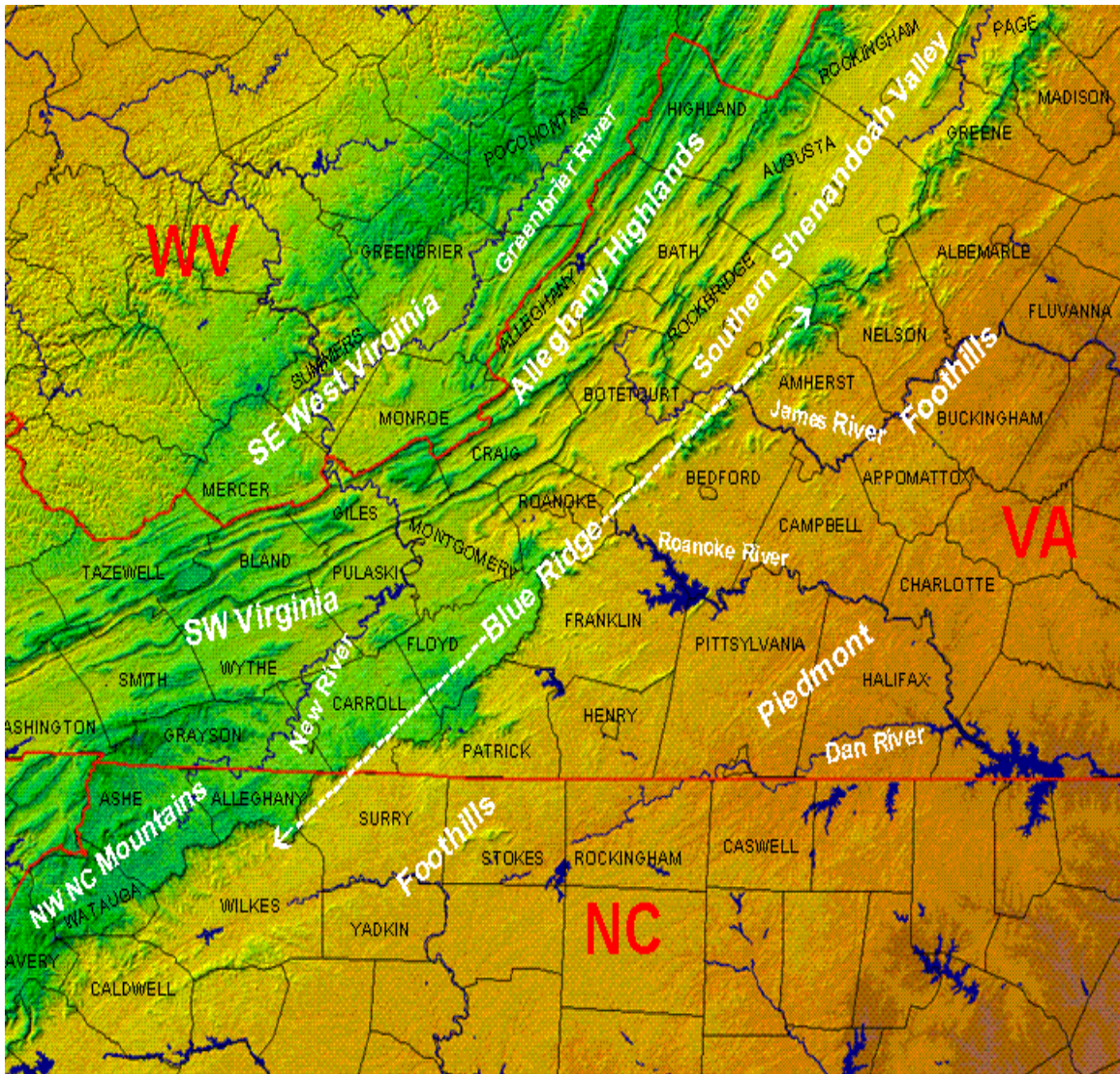


Figure 2. Map depicting geographical and political areas of interest including states, major river basins, and county names.

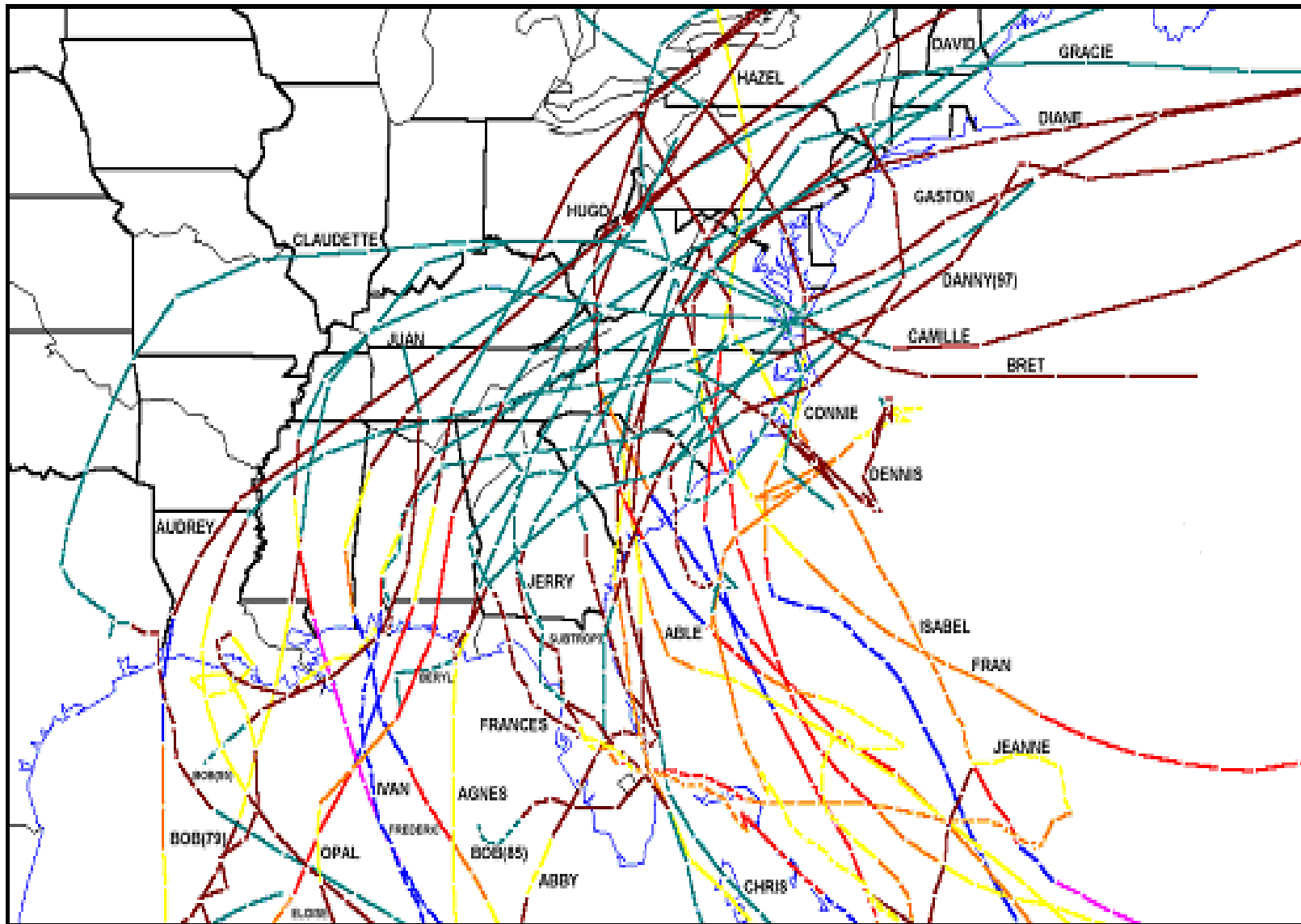


Figure 3. Tracks of the 32 storms studied (1950-2004). Each track is labeled with storm name.

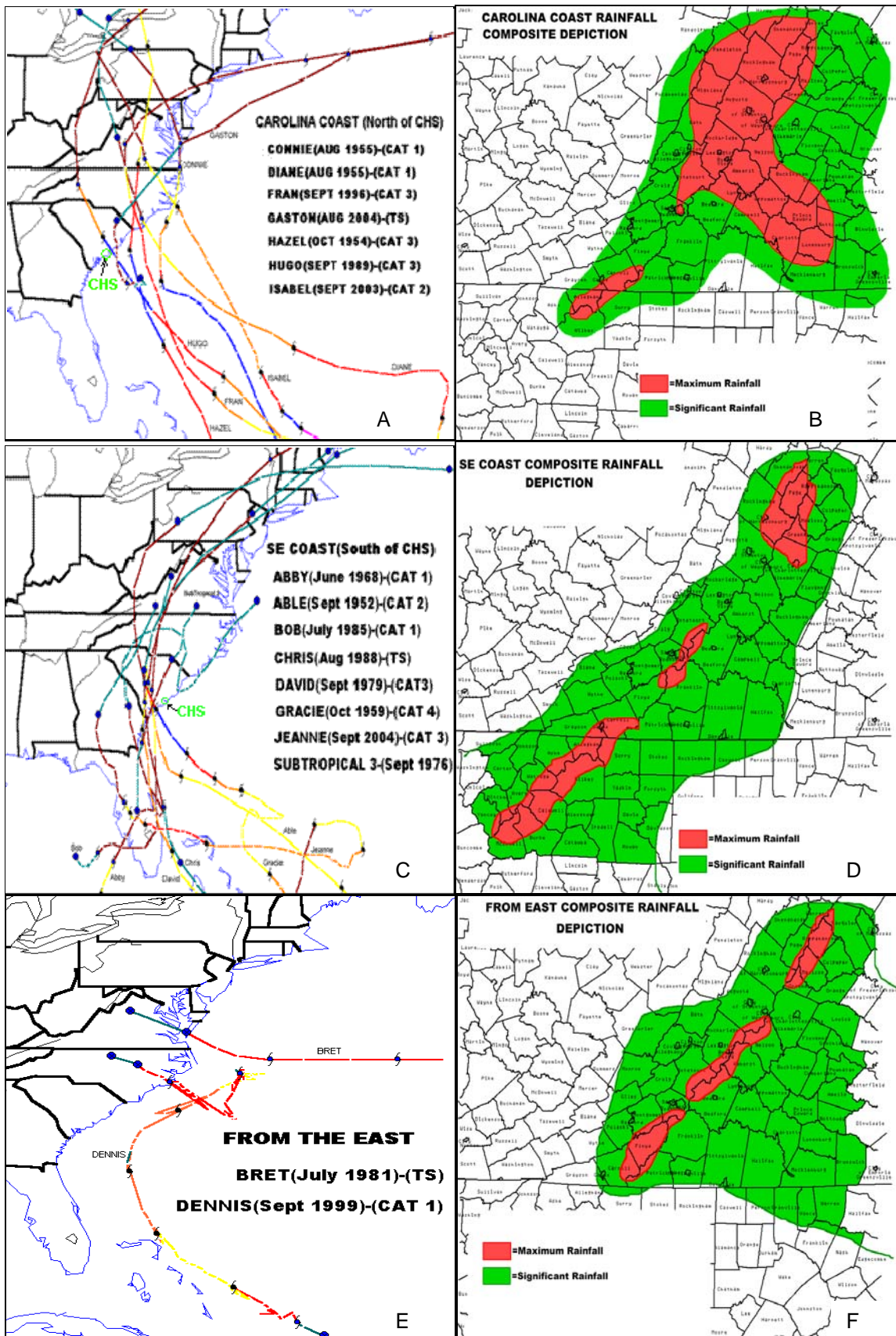


Figure 4(a-f). Tracks and rainfall composites of cyclones making landfall along the Atlantic Coast.

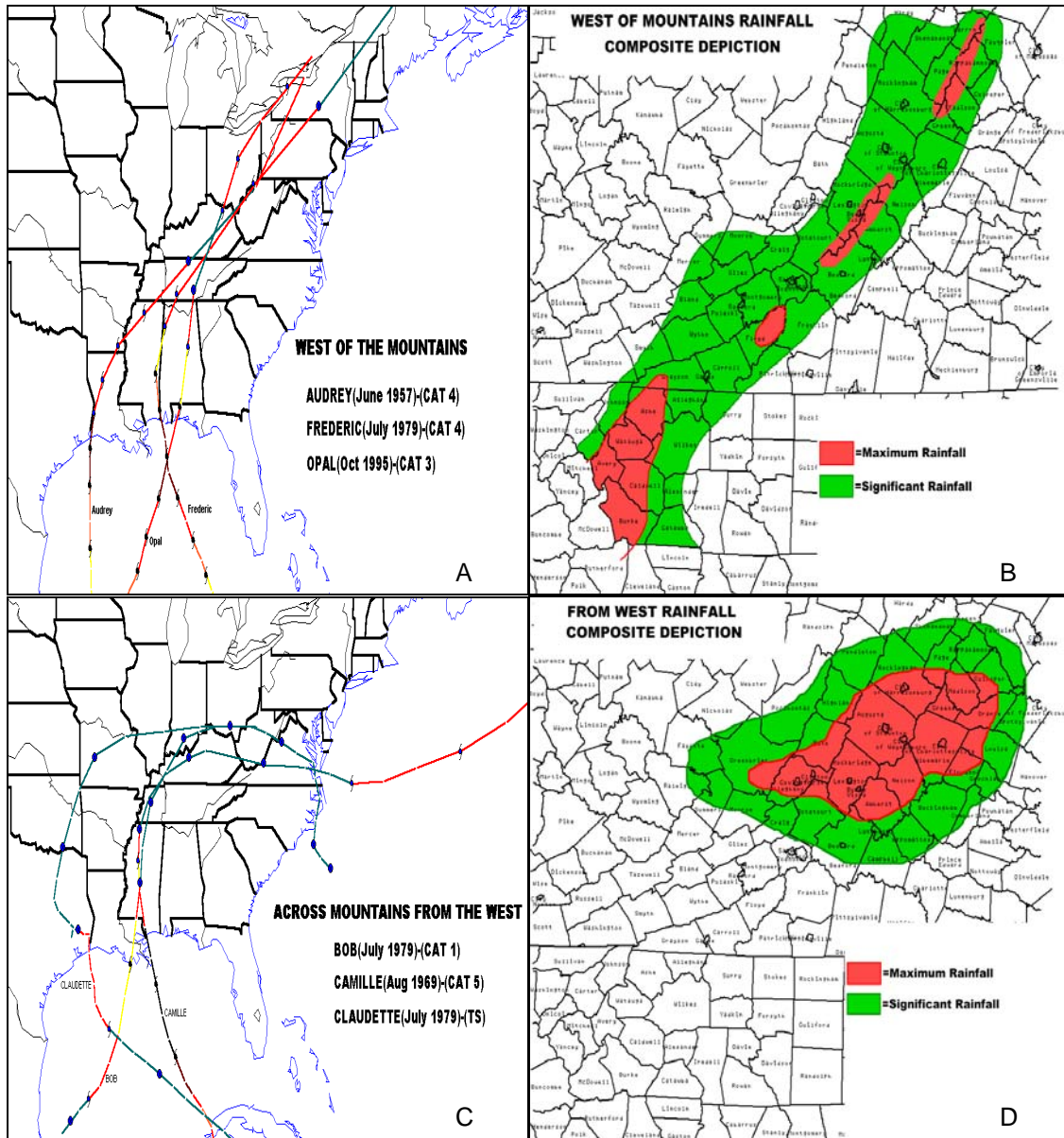


Figure 5 (a-d). Tracks and rainfall composites of cyclones making landfall along the Gulf Coast.

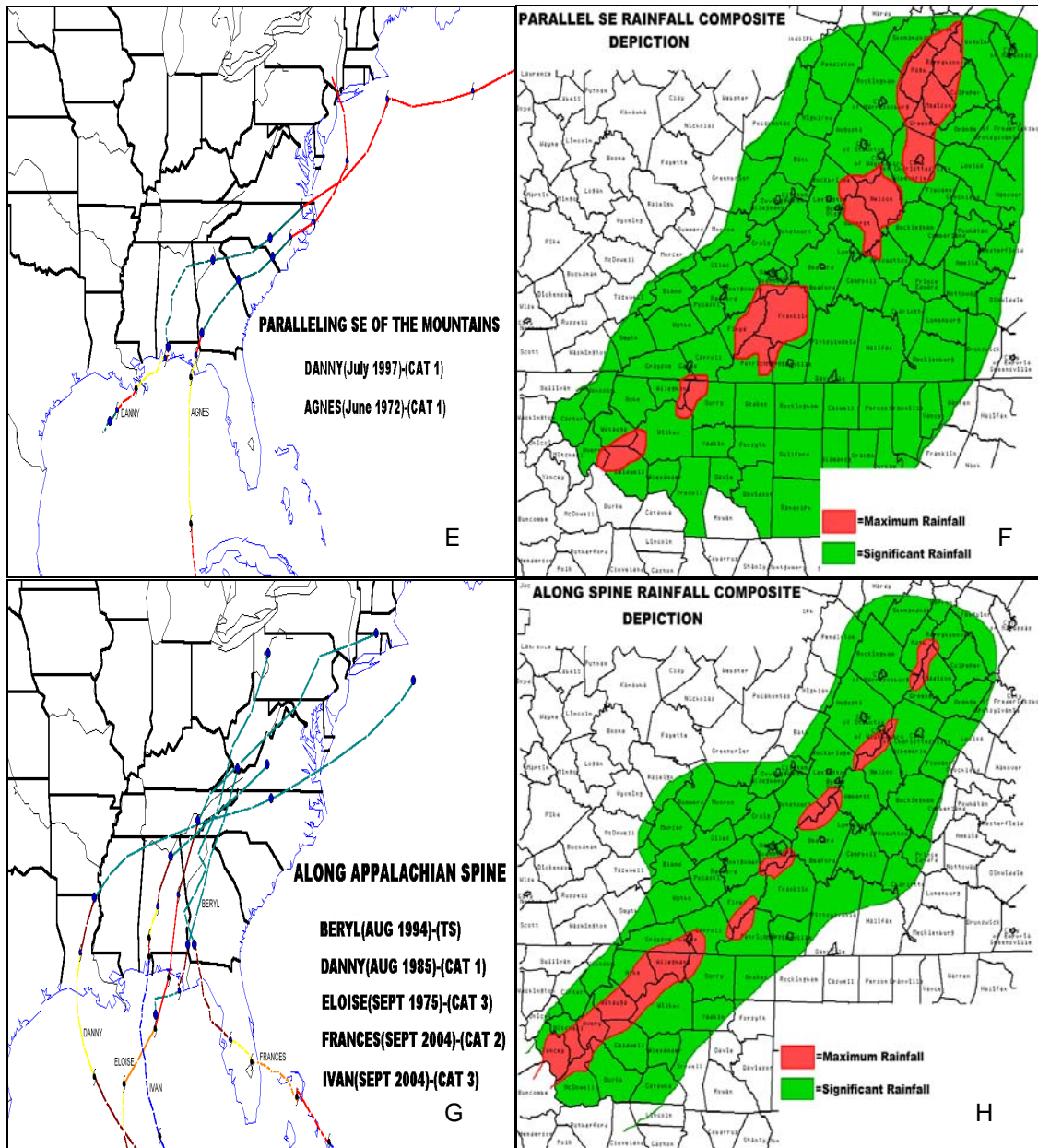


Figure 5 continued (e-h). Tracks and rainfall composites of cyclones making landfall along the Gulf Coast.

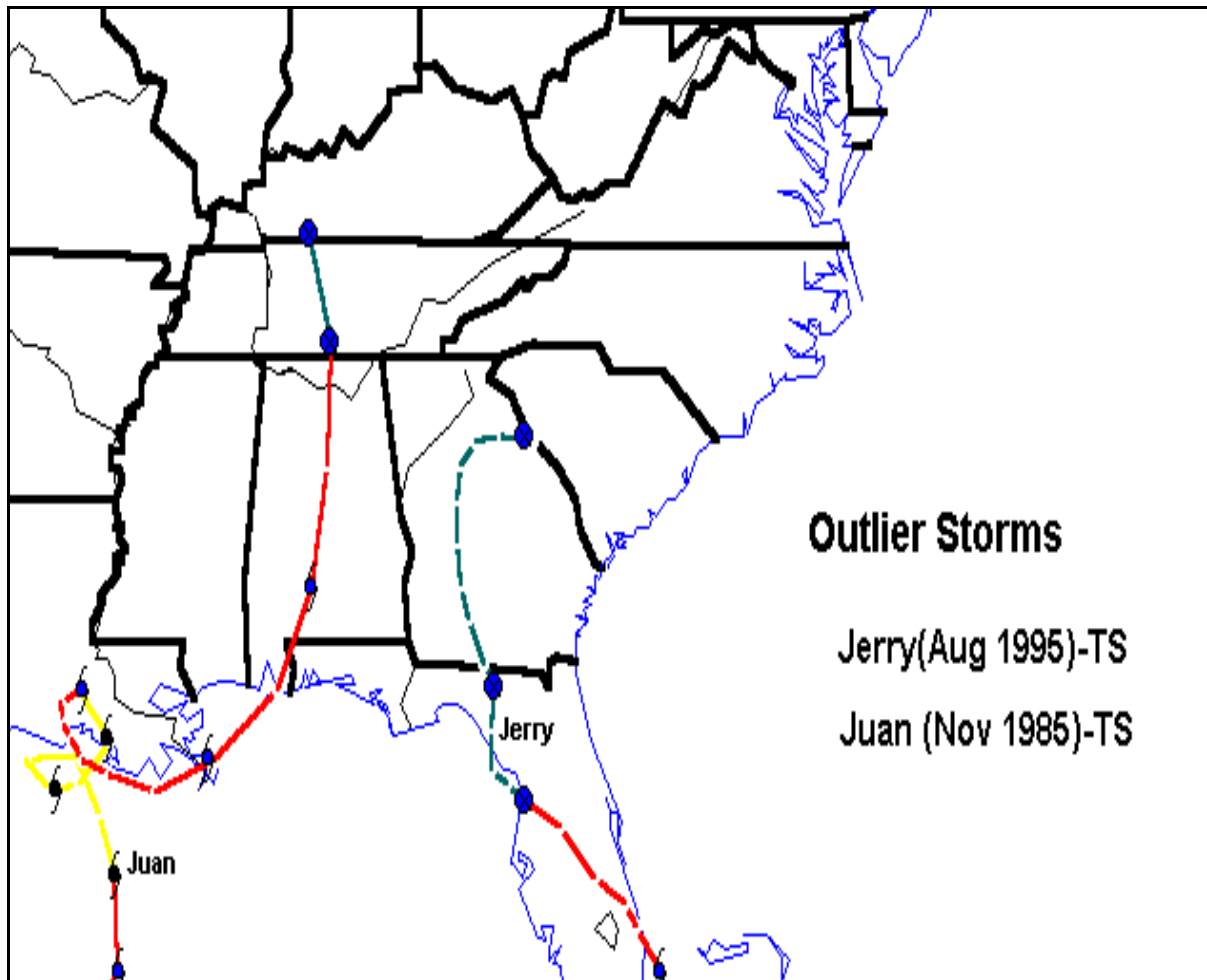


Figure 6. Tracks of outlier storms.

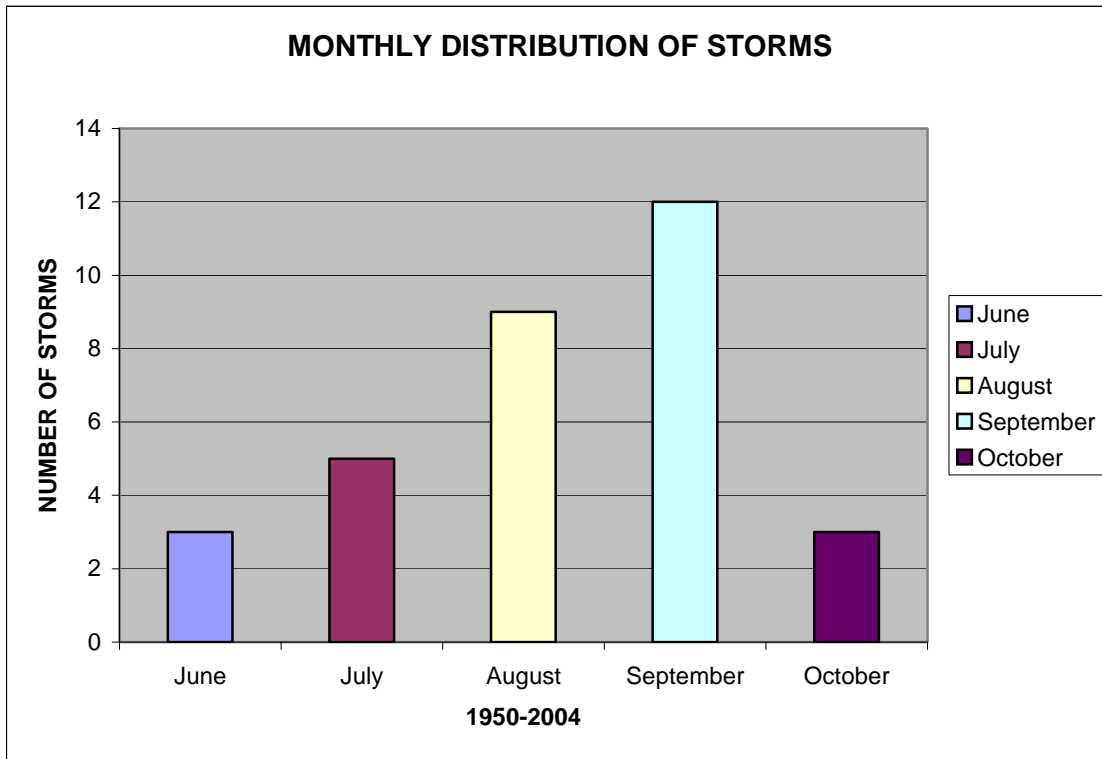


Figure 7. Monthly distribution of the tropical cyclones studied that passed within 500 km of the NWS WFO RNK between 1950 and 2004.

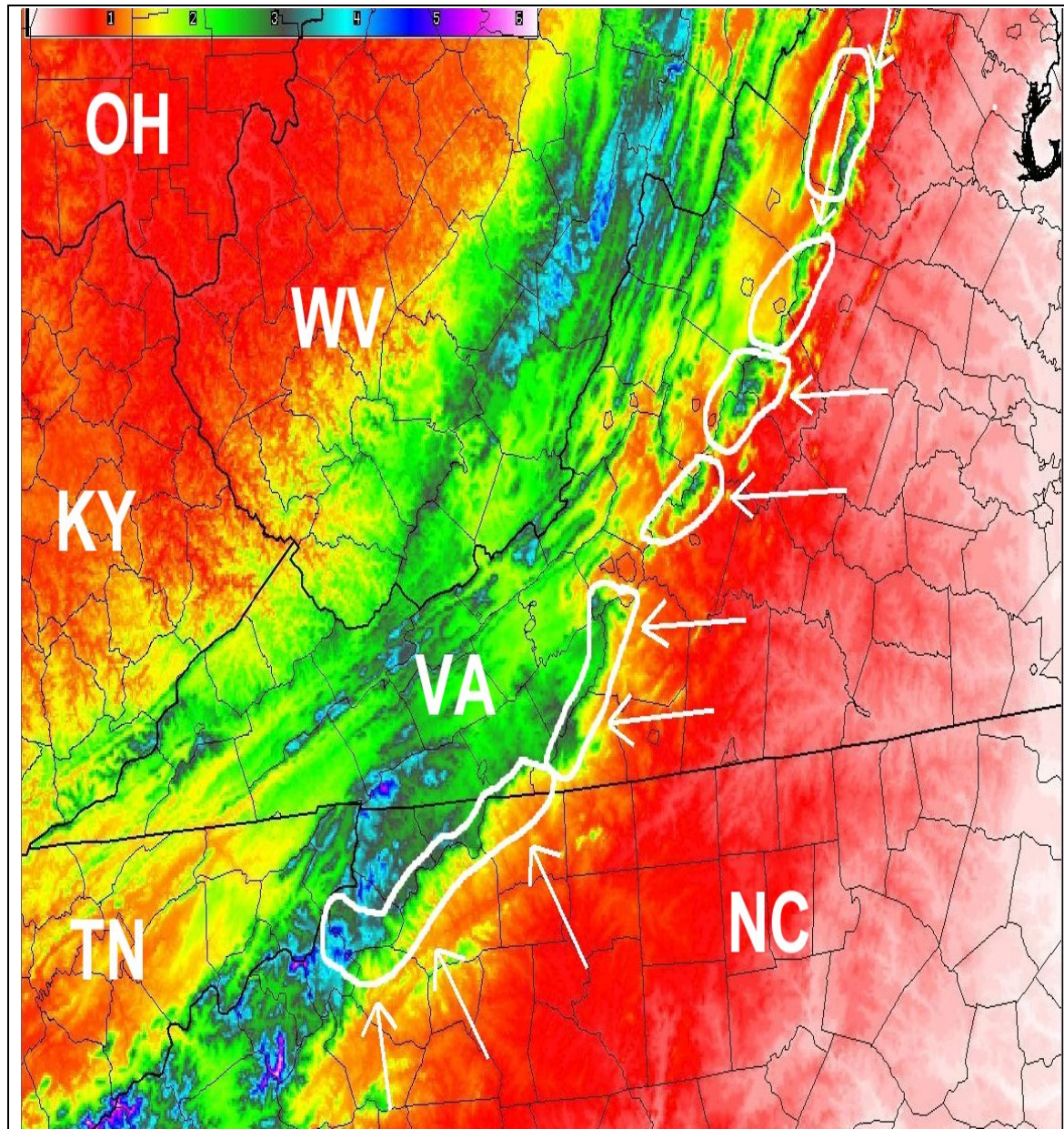


Figure 8. Favored upslope locations (white circles) and wind directions (white arrows) along the Blue Ridge. Terrain color coded with scale in upper left (thousands of feet).

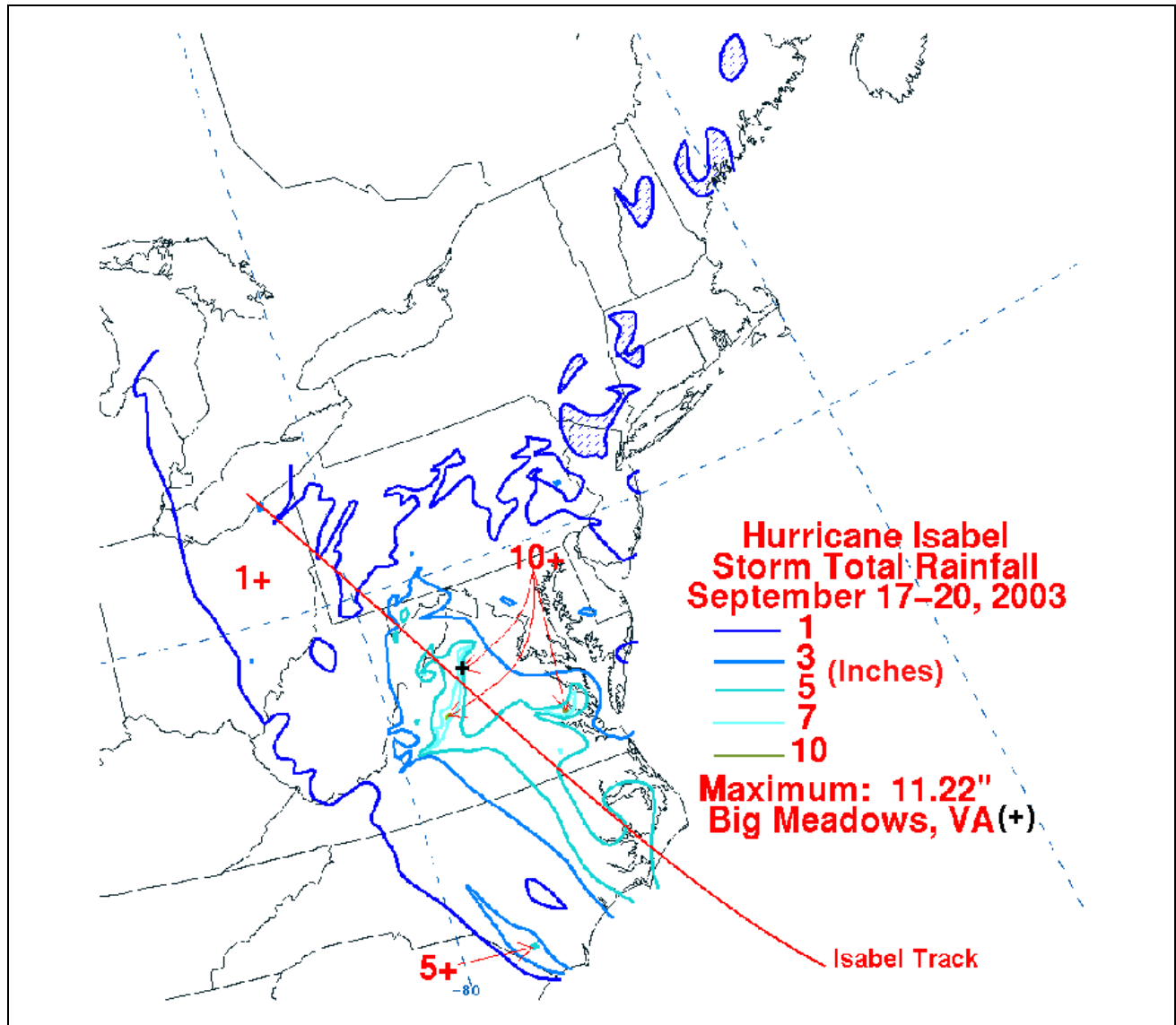


Figure 9. Rainfall associated with Hurricane Isabel (red line) showing axis of heavier upslope along the Blue Ridge.

Table 1. Summary of storms from 1950-2004 listing classification, strength, dates of influence, and the associated page numbers in Appendix A for each.

Classification	Storm(s)	Strength(At Landfall)	Dates of Influence	Pages
Carolina Coast (Atlantic)	Hazel Connie Diane Hugo Fran Isabel Gaston	Hurricane(Cat 3) Hurricane(Cat 1) Hurricane(Cat 1) Hurricane(Cat 4) Hurricane(Cat 3) Hurricane(Cat 2) Tropical Storm	October 15-16, 1954 August 12-13, 1955 August 17-18, 1955 Sept. 21-22, 1989 Sept. 5-6, 1996 Sept. 18, 2003 August 29-30, 2004	A4-5 A6-7 A8-9 A42-43 A50-51 A56-57 A58-59
SE Coast (Atlantic)	Able Gracie Abby Subtropical Storm 3 David Bob Chris Jeanne	Hurricane(Cat 2) Hurricane(Cat 4) Hurricane(Cat 1) Storm Hurricane(Cat 3) Hurricane(Cat 1) Tropical Storm Hurricane (Cat 3)	Sept. 1-2, 1952 Sept. 29-30, 1959 June 6-8, 1968 Sept. 14-16, 1976 Sept. 4-5, 1979 July 25, 1985 August 28-29, 1988 Sept. 27-28, 2004	A2-3 A12-13 A14-15 A22-23 A28-29 A34-35 A40-41 A64-65
From East (Atlantic)	Bret Dennis	Tropical Storm Hurricane(TS)	June 30-July 1, 1981 Sept. 5-6, 1999	A32-33 A54-55
West of Mountains (Gulf)	Audrey Frederic Opal	Hurricane(Cat 4) Hurricane(Cat 4) Hurricane(Cat 3)	June 28-29, 1957 August 13-14, 1979 October 4-6, 1995	A10-11 A30-31 A48-49
From West (Gulf)	Camille Bob Claudette	Hurricane(Cat 5) Hurricane(Cat 1) Tropical Storm	August 19-20, 1969 July 12-14, 1985 July 28-29, 1979	A16-17 A24-25 A26-27
Parallel SE (Gulf)	Agnes Danny	Hurricane(Cat 1) Hurricane(Cat 1)	June 21, 1972 July 23-24, 1997	A18-19 A52-53
Along Spine (Gulf)	Eloise Danny Beryl Frances Ivan	Hurricane(Cat 3) Hurricane(Cat 1) Tropical Storm Hurricane(Cat 2) Hurricane(Cat 3)	Sept. 23-24, 1975 August 18-19, 1985 August 17, 1994 Sept. 7-8, 2004 Sept. 16-17, 2004	A20-21 A36-37 A44-45 A60-61 A62-63
Outliers (Gulf)	Juan Jerry	Hurricane(Cat 1) Tropical Storm	November 1-2, 1985 August 26-27, 1995	A38-39 A46-47

APPENDIX A

INDIVIDUAL STORM ANALYSES

(All Image Data Provided by NOAA Central Library Data Imaging Project and JincSolutions)

The appendix contains a series of five figures on two pages for each storm in the study. The first page for each storm includes a map of the storm track and strength, along with the rainfall analysis overlaid on a terrain background image. The track map also includes short bullets indicating the most important features of the event, such as important contributing factors to heavy rainfall, or in some cases, lack thereof. These two figures together provide a relative sense for how the rainfall distribution was related to the path and intensity of the storm. The second page for each storm shows the observed surface station plot with frontal positions and precipitation at two different times as the storm moved across the area of study, as well as one representative observed 500 hPa chart with height contours and winds. These two figures provide the overall synoptic pattern, as well as an indication for potential boundary interaction.

The collection of charts for each event will serve as a quick reference for forecasters monitoring future tropical systems that are approaching with a similar expected tracks, strengths, and synoptic patterns.

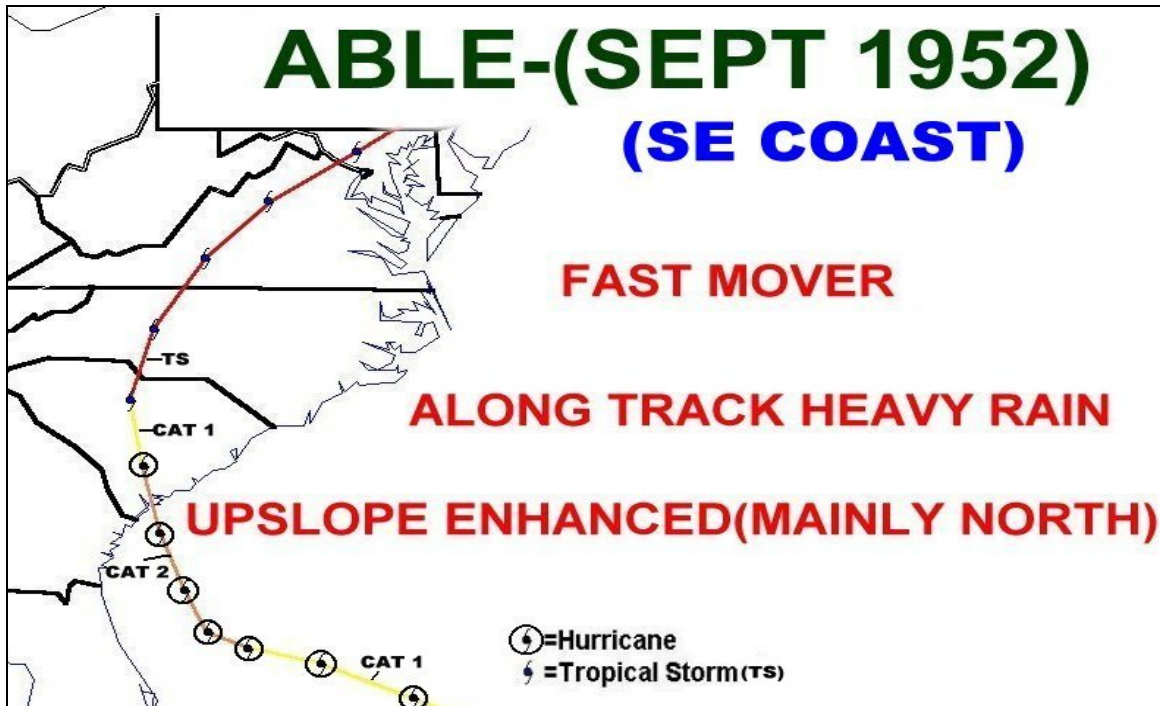


Fig. A-1: August 30 – September 2, 1952. *ABLE*.

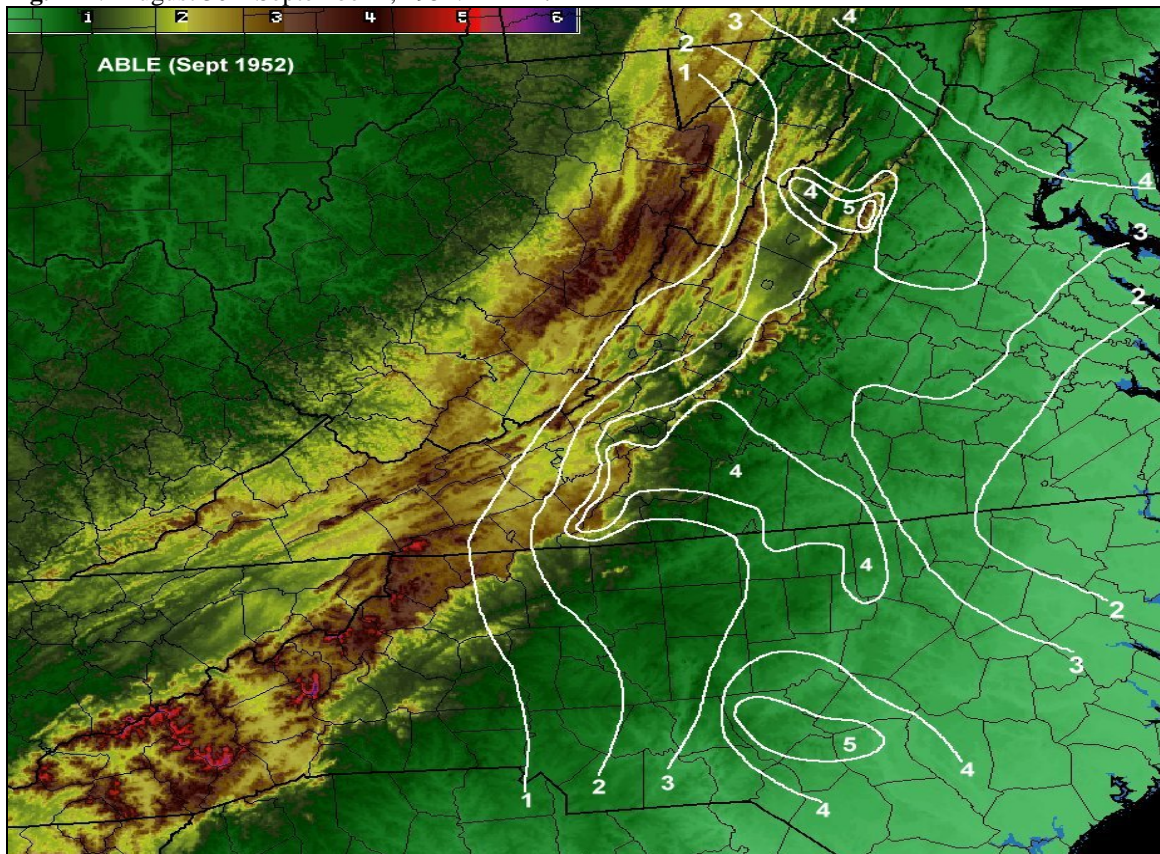


Fig. A-2: Able rainfall in inches (white contours), August 31-September 2, 1954, overlaid on terrain (k ft).

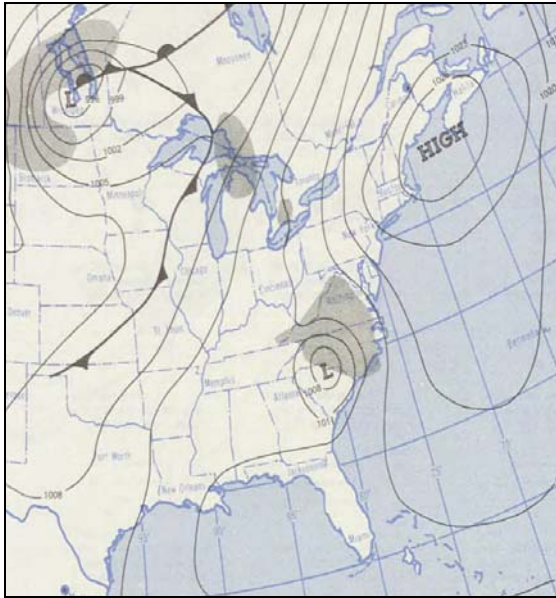


Fig. A-3: Observed standard station plot (4 mb contours), precipitation (shaded), 12 UTC, September 1, 1952.

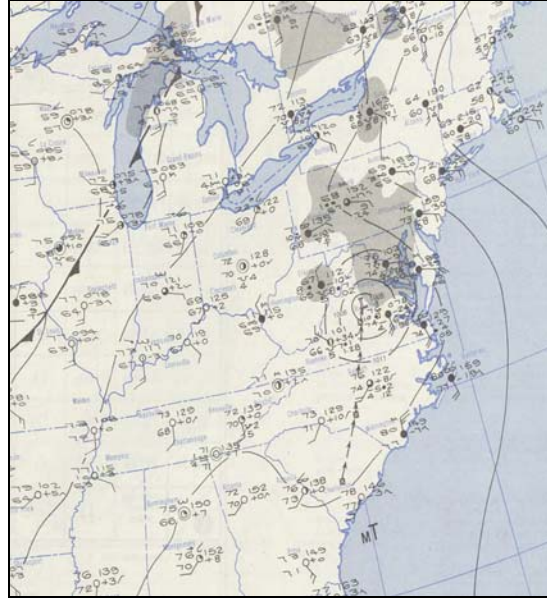


Fig. A-4: Observed standard station plot (4 mb contours), precipitation (shaded), 12 UTC, September 2, 1952.

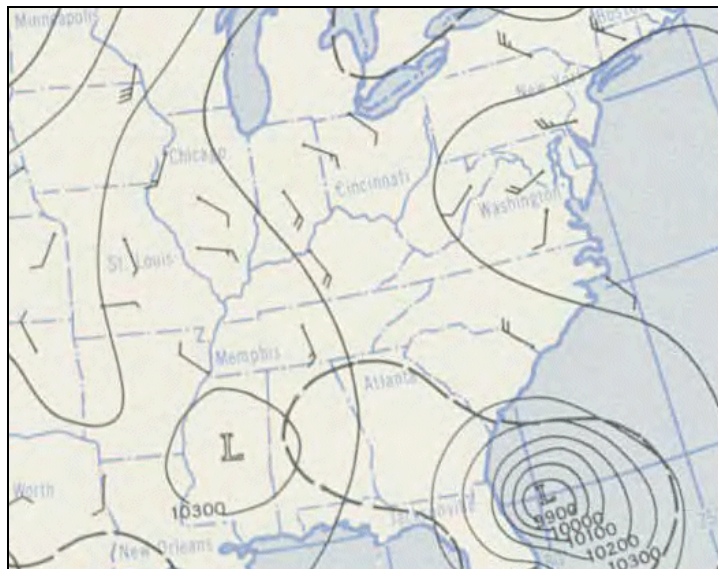


Fig. A-5: Observed 500 mb chart (100 ft contours), winds (kts), temperatures (C), 18 UTC, August 31, 1952.

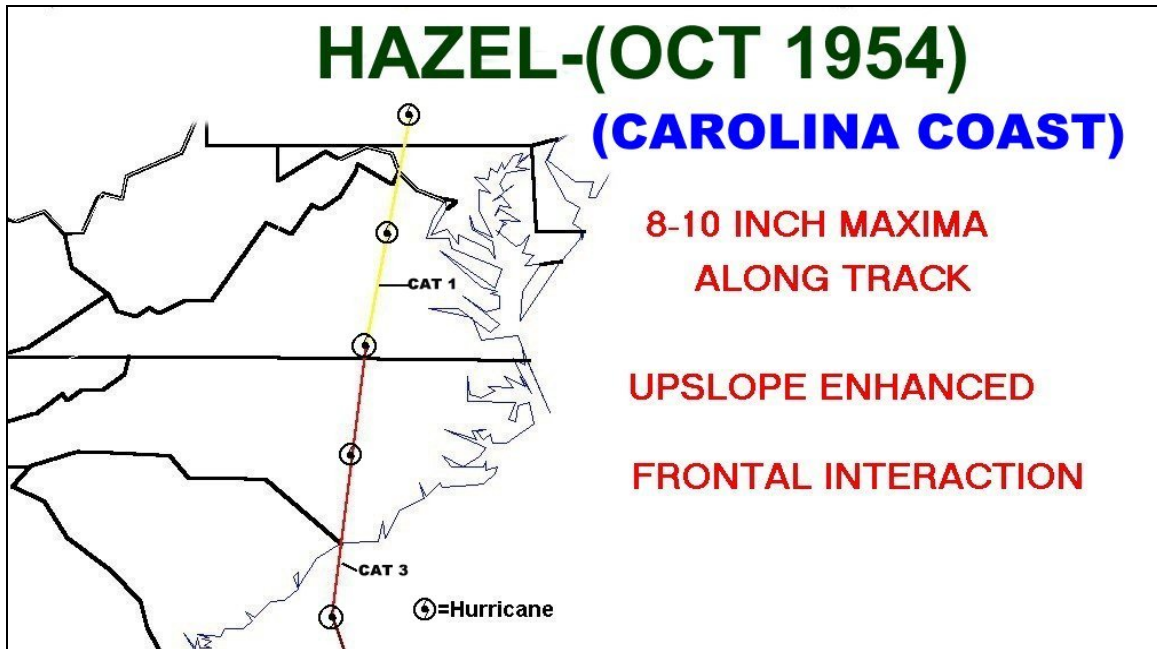


Fig. A-6: October 15-16, 1954. *HAZEL*.

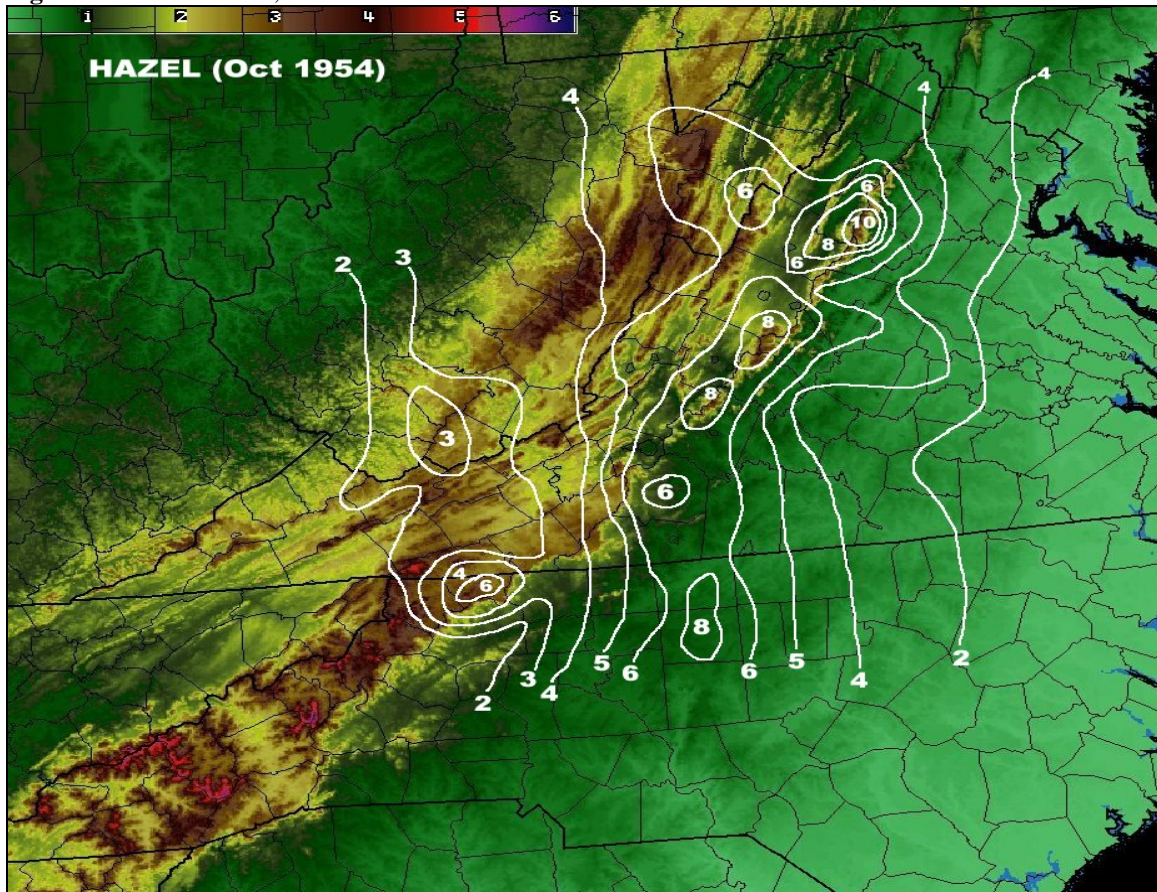


Fig. A-7: Hazel rainfall in inches (white contours), October 15-16, 1954, overlaid on terrain (k ft).

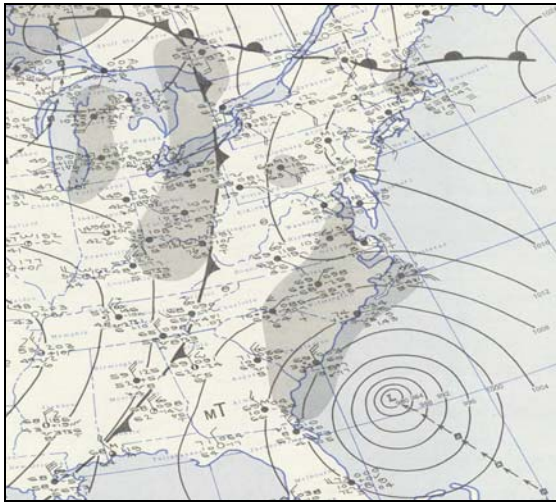


Fig. A-8: Observed standard station plot (4 mb contours), precipitation (shaded), 12 UTC, October 15, 1954.

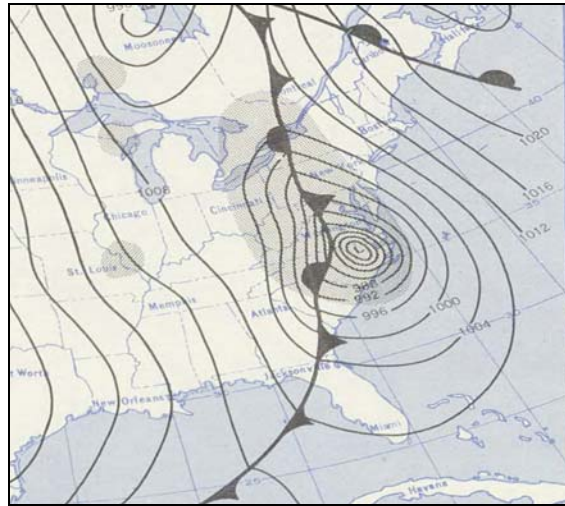


Fig. A-9: Observed standard station plot (4 mb contours), precipitation (shaded), 12 UTC, October 16, 1954.

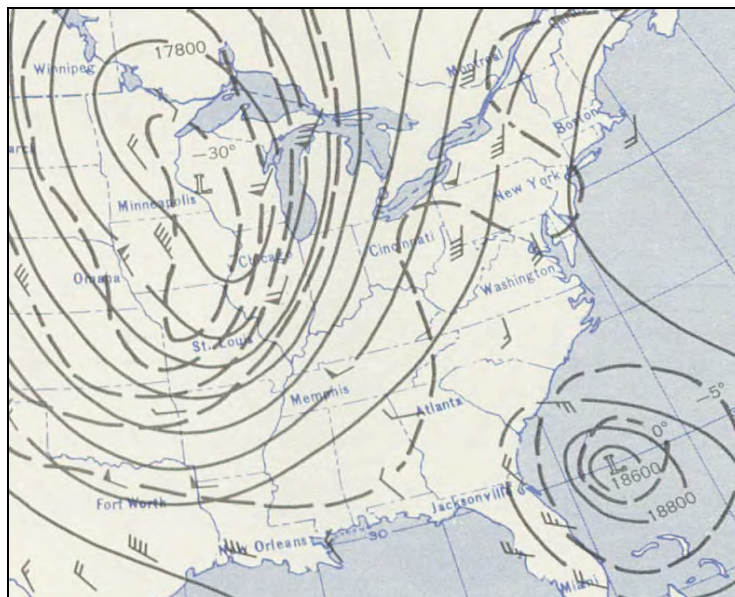


Fig. A-10: Observed 500 mb chart (200 ft contours), winds (kts), temperatures (C), 06 UTC, Oct. 15, 1954.

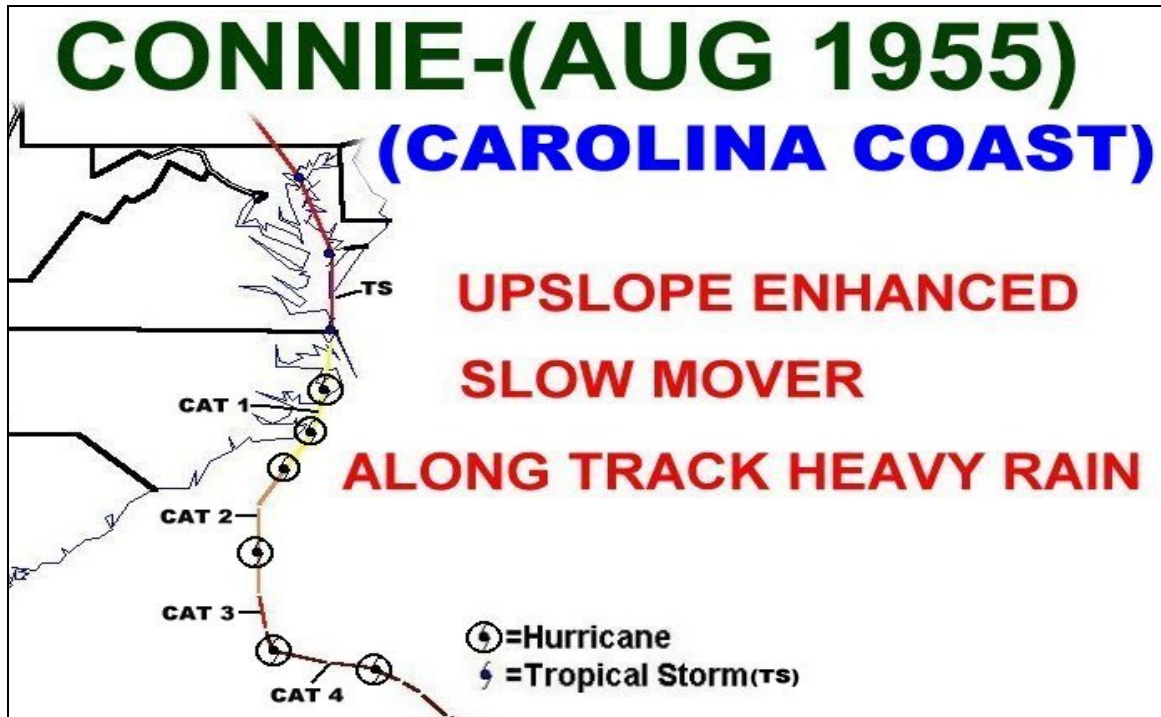


Fig. A-11: August 11-13, 1955. *CONNIE*.

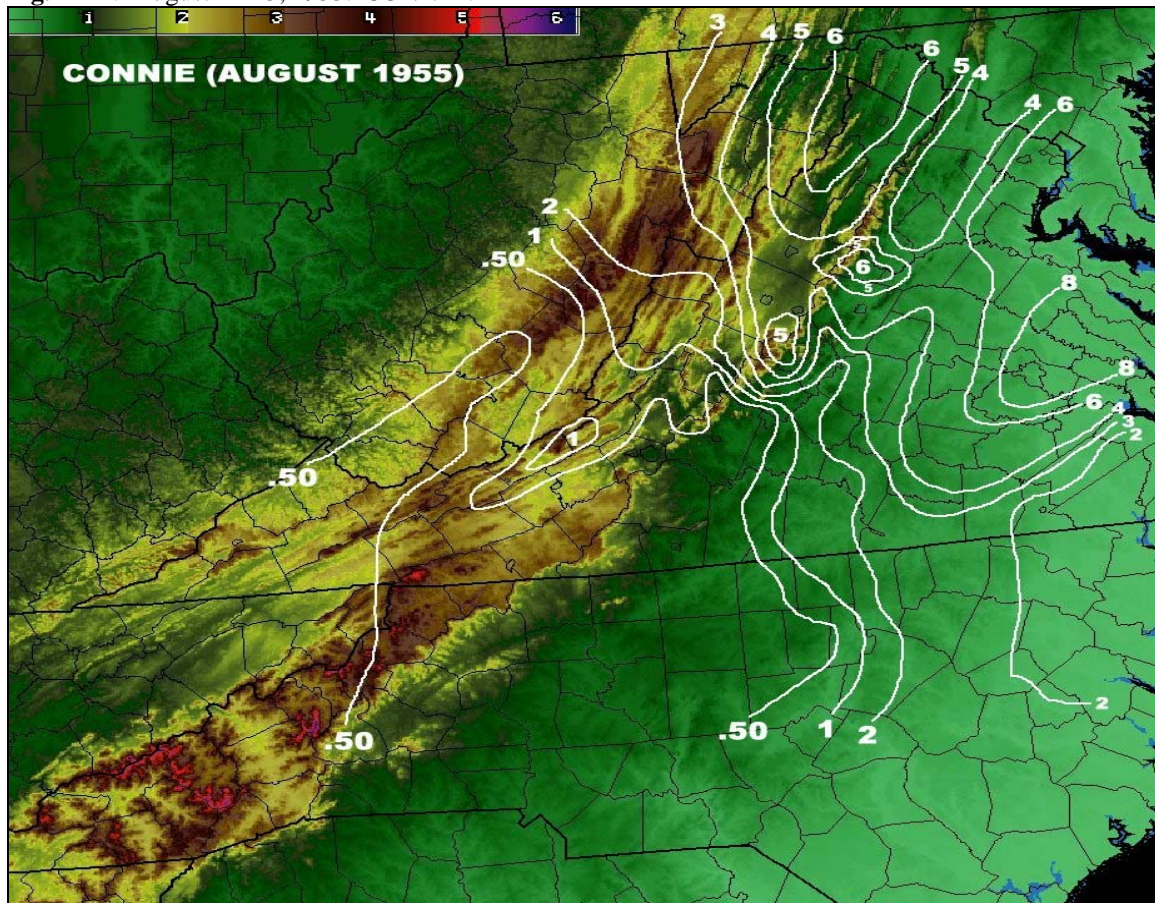


Fig. A-12: Connie rainfall in inches (white contours), August 12-13, 1955, overlaid on terrain (k ft).

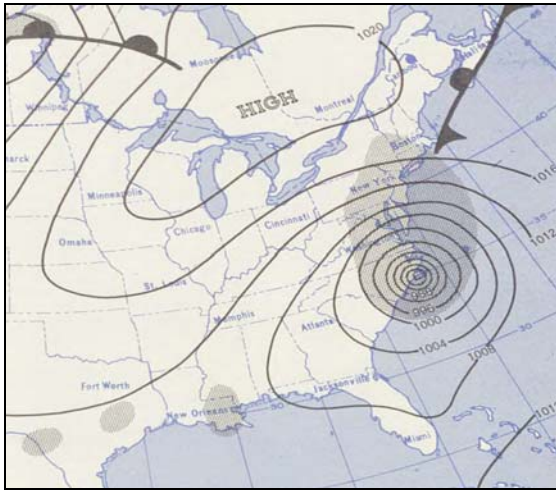


Fig. A-13: Observed standard station plot (4 mb contours), precipitation (shaded), 12 UTC, August 12, 1955.

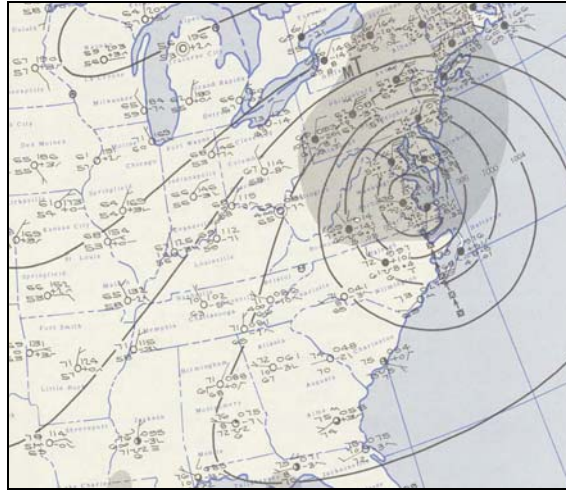


Fig. A-14: Observed standard station plot (4 mb contours), precipitation (shaded), 12 UTC, August 13, 1955.

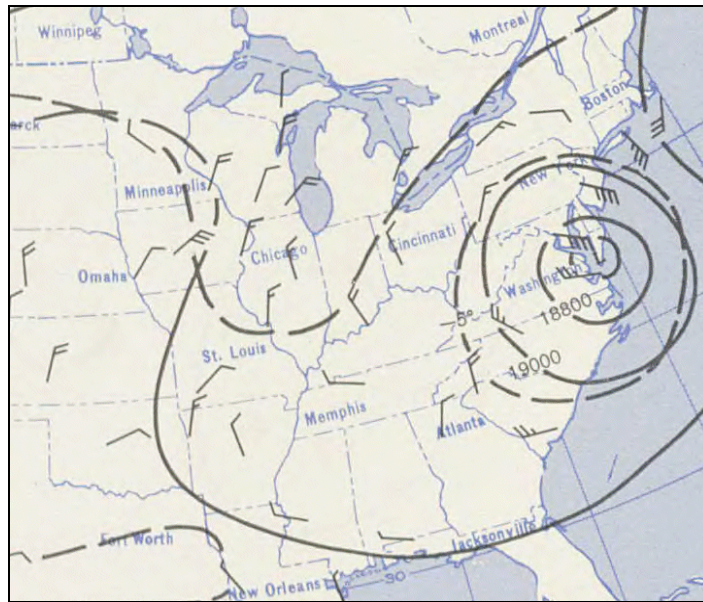


Fig. A-15: Observed 500 mb chart (200 ft contours), winds (kts), temperatures (deg C), 12 UTC, August 13, 1955.

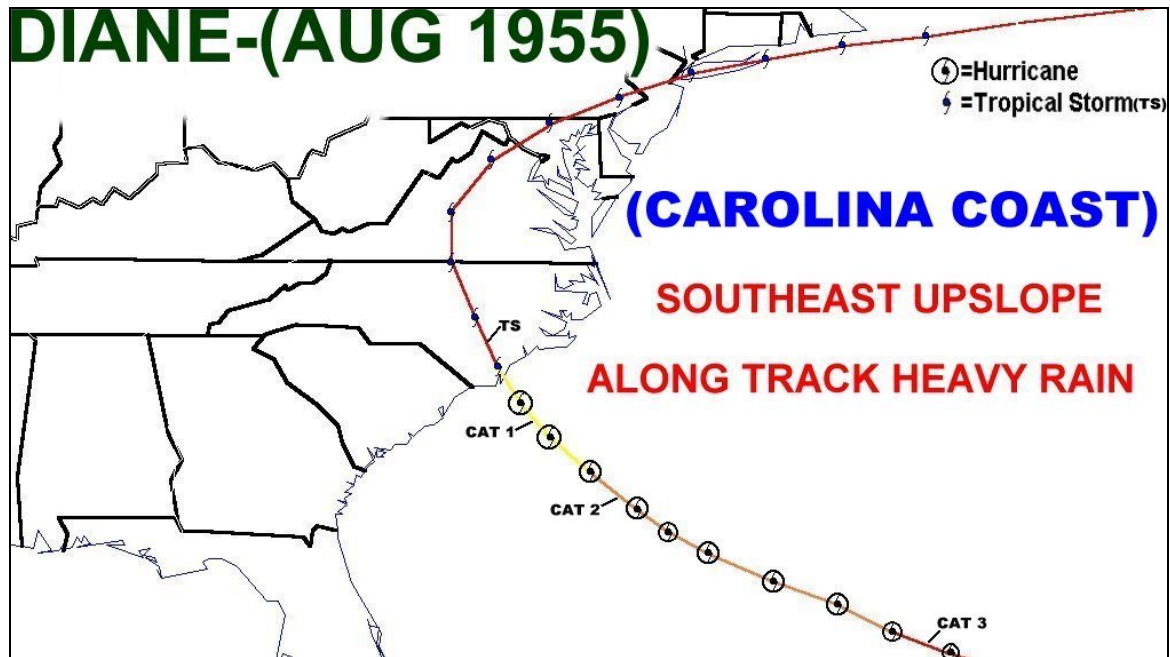


Fig. A-16: August 15-18, 1955. *DIANE*.

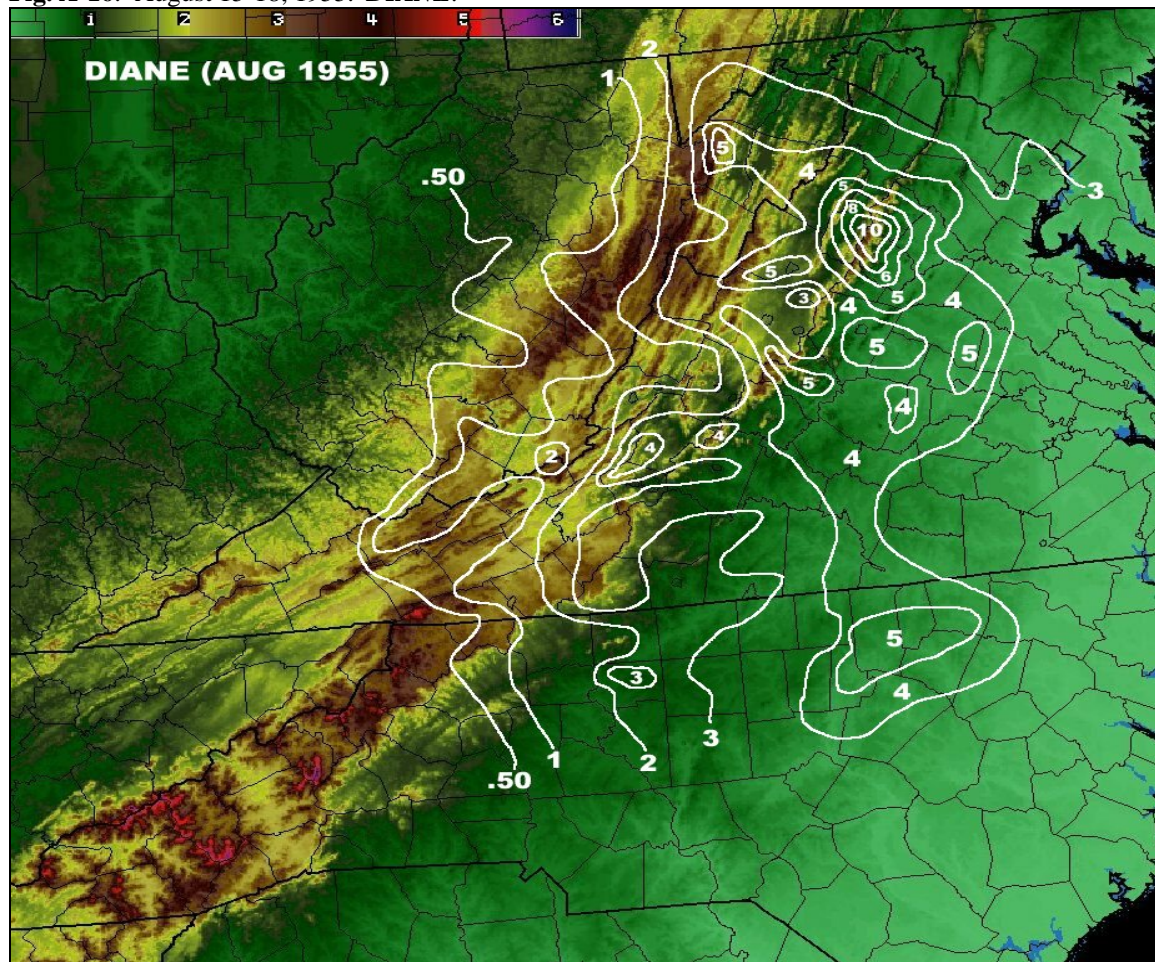


Fig. A-17: Diane rainfall in inches (white contours), August 17-18, 1955, overlaid on terrain (k ft).



Fig. A-18: Observed standard station plot, (4 mb contours), precipitation (shaded), 12 UTC, August 17, 1955.

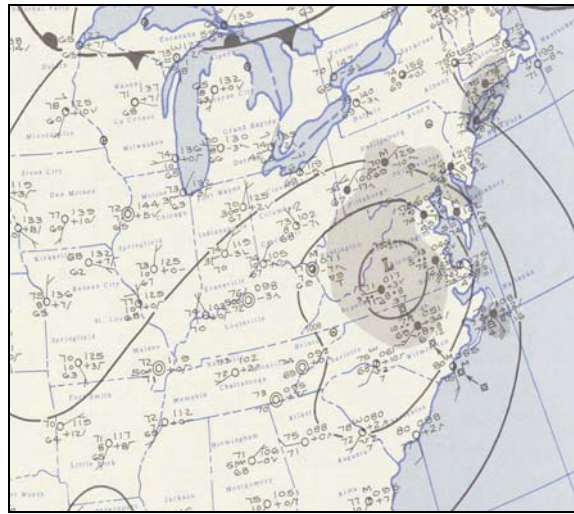


Fig. A-19: Observed standard station plot, (4 mb contours), precipitation (shaded), 12 UTC, August 18, 1955.

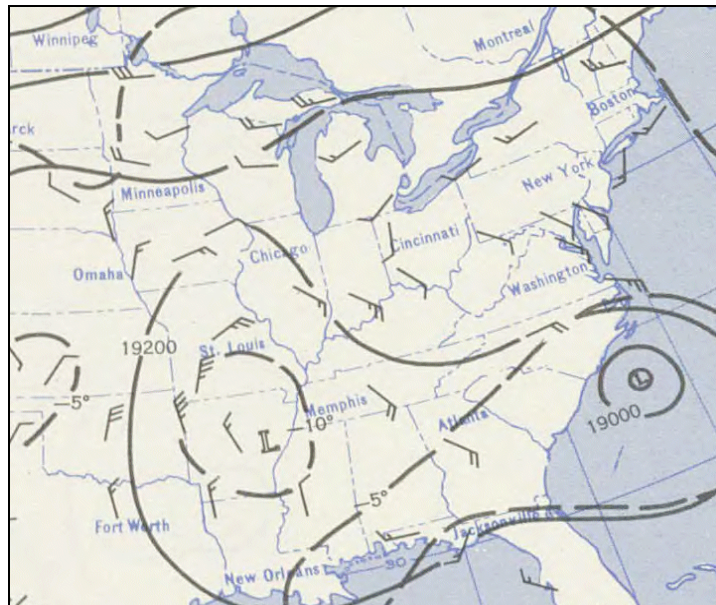


Fig. A-20: Observed 500 mb chart (200 ft contours), winds (kts), temperatures (deg C), 06 UTC, August 17, 1955

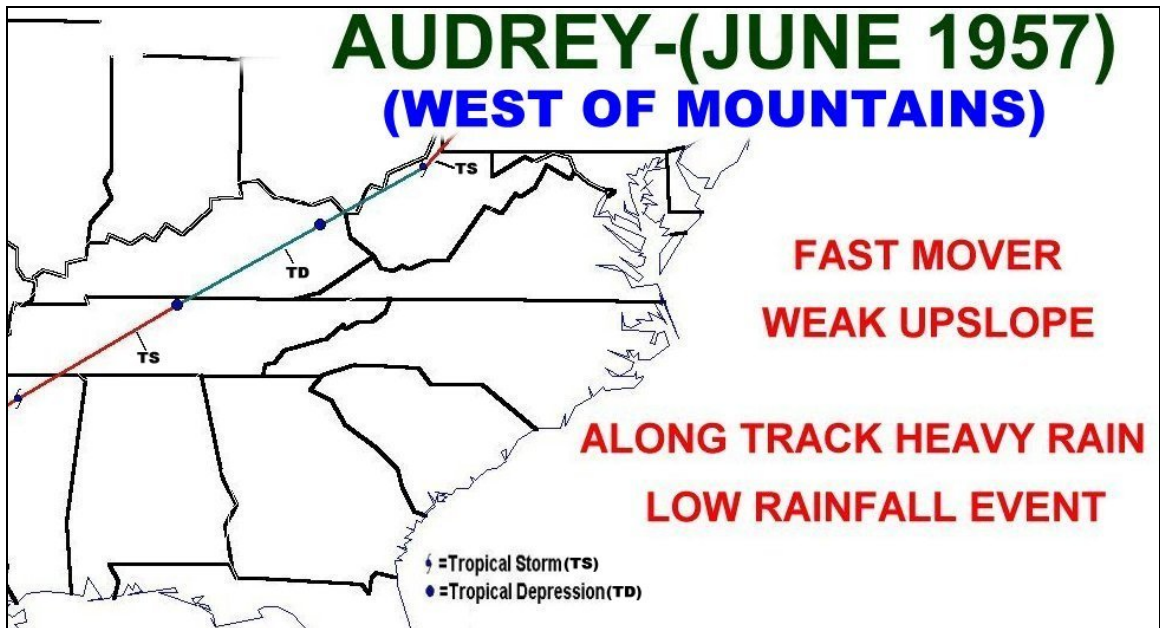


Fig. A-21: June 28-29, 1957. *AUDREY*.

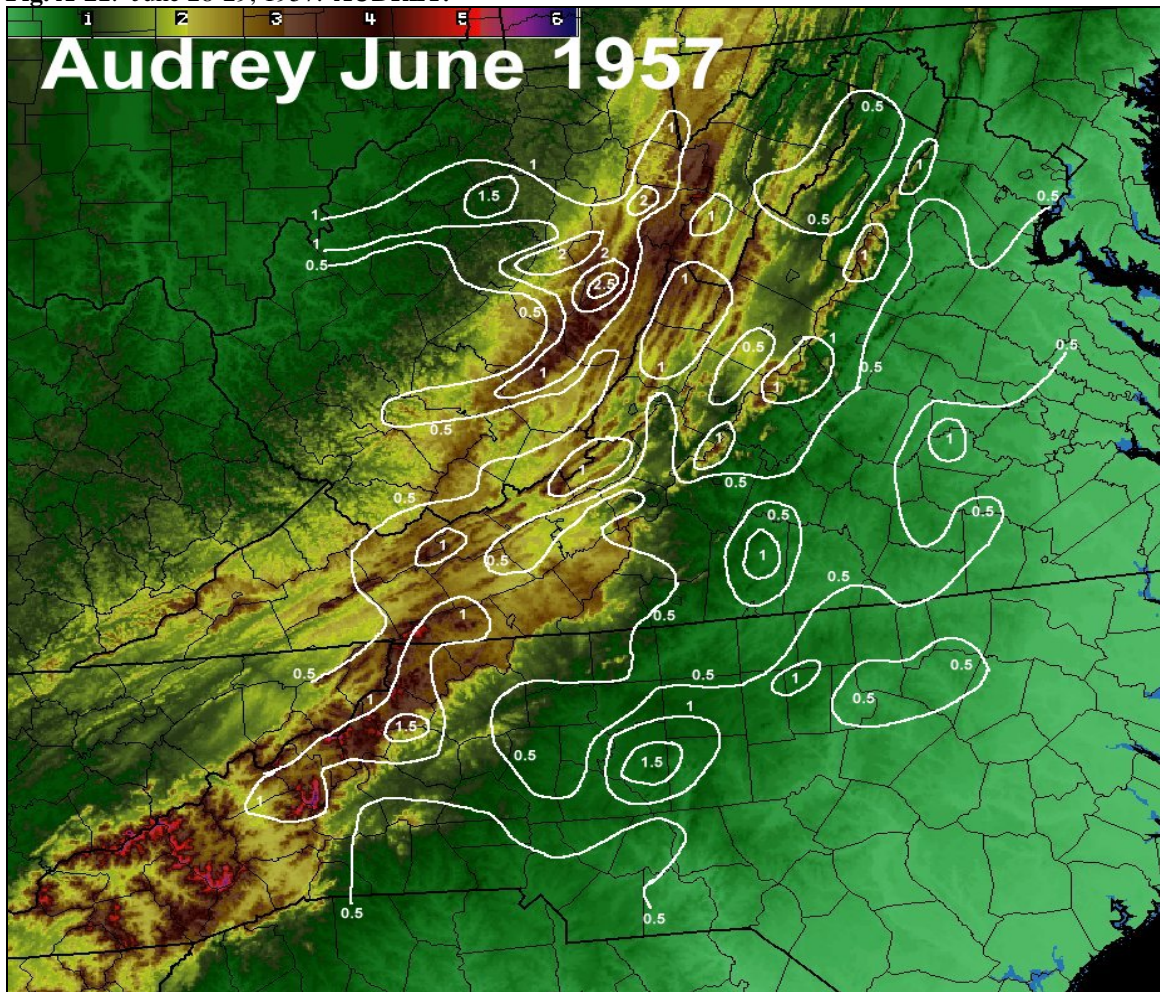


Fig. A-22: Audrey rainfall in inches, (white contours), June 28-29, 1957, overlaid on terrain (k ft).

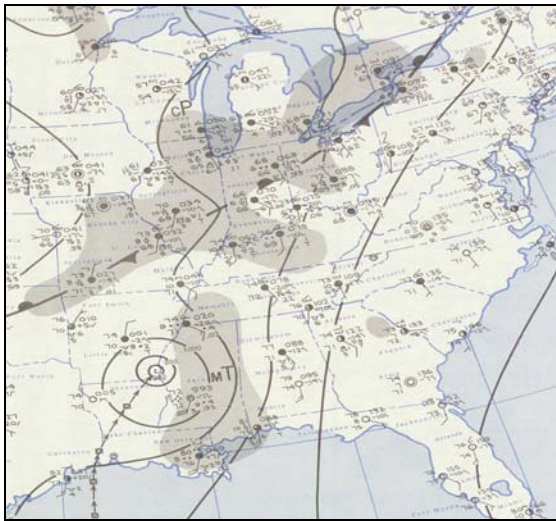


Fig. A-23: Observed standard station plot, (4 mb contours), precipitation (shaded), 12 UTC, June 28, 1957.

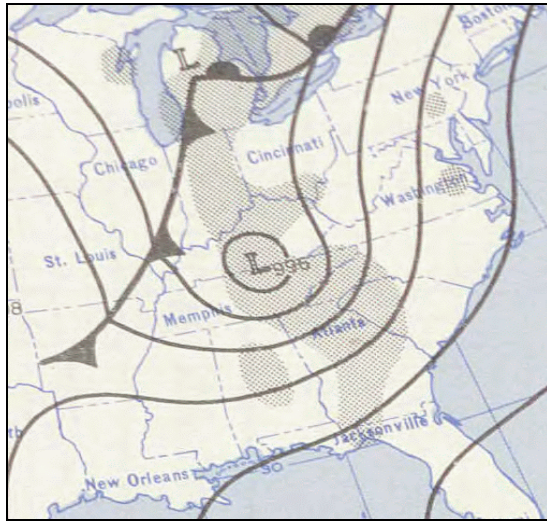


Fig. A-24: Observed standard station plot, 12 UTC, (4 mb contours), precipitation (shaded), 12 UTC, June 29, 1957.

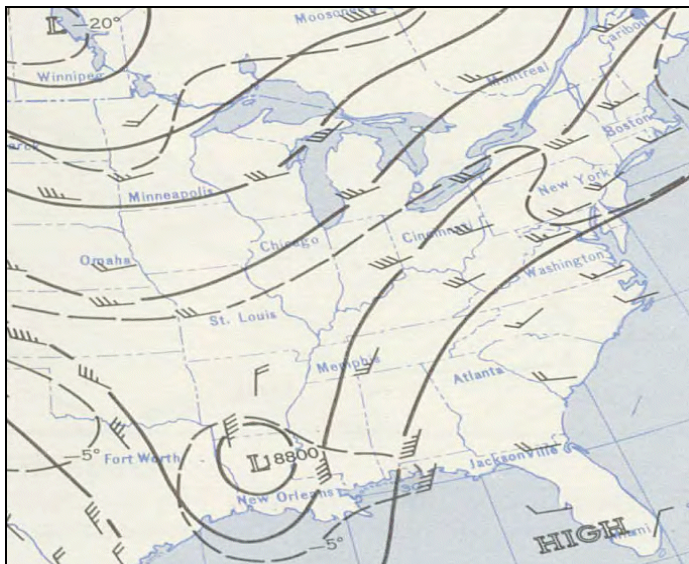


Fig. A-25: Observed 500mb chart (200 ft contours), winds (kts), temperatures (C), 12 UTC, June 28, 1957.

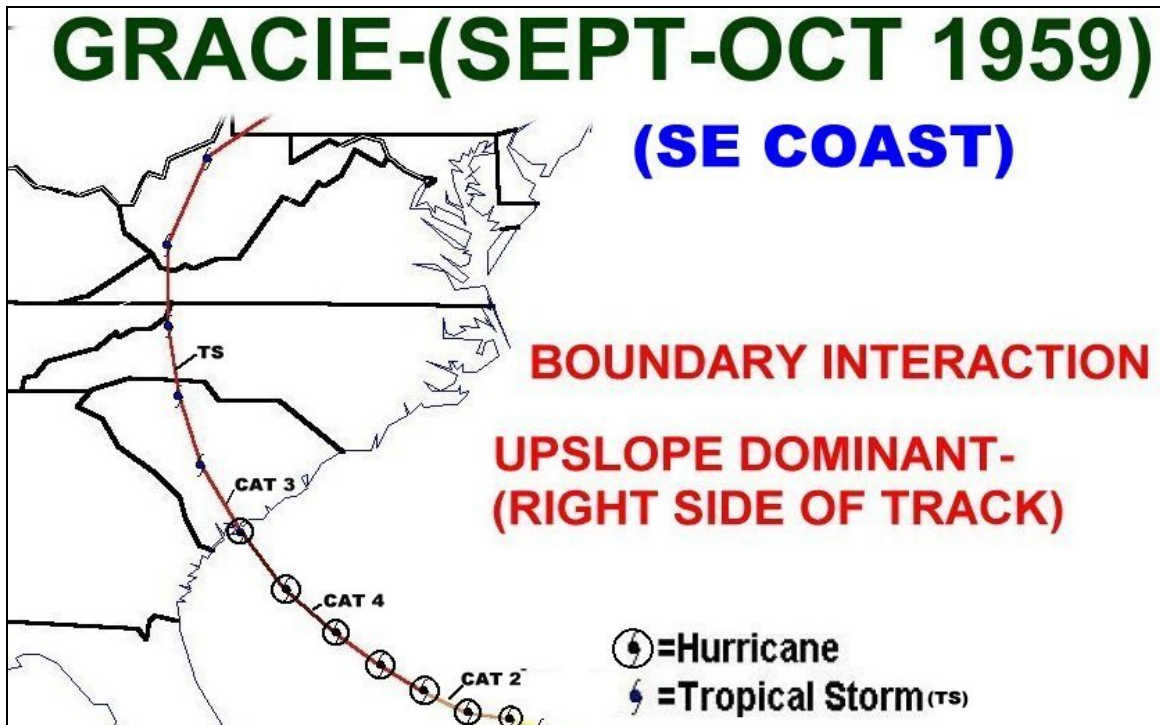


Fig. A-26: September 28-October 1, 1959. *GRACIE*.

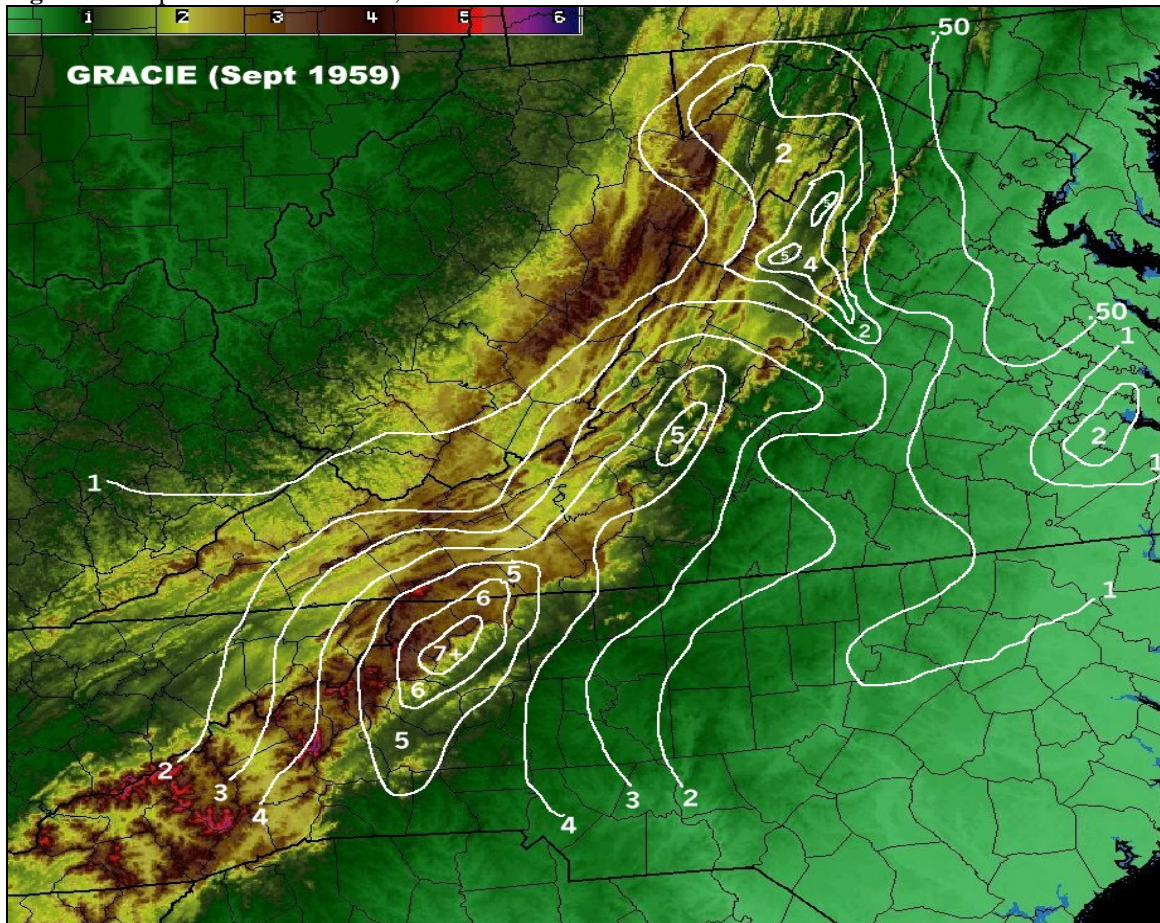


Fig. A-27: Gracie rainfall in inches (white contours), September 29-30, 1959, overlaid on terrain (k ft).

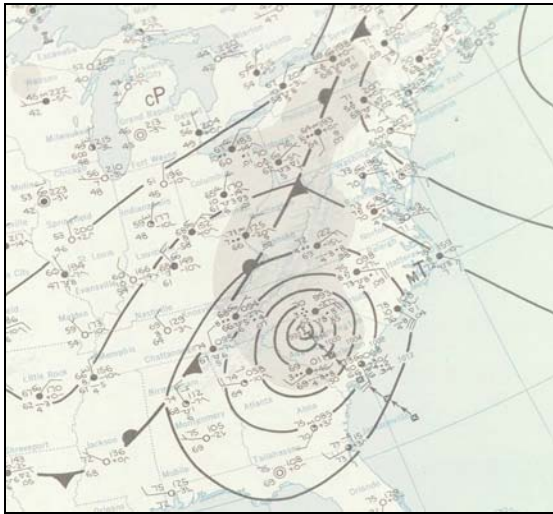


Fig. A-28: Observed standard station plot, (4 mb contours), precipitation (shaded), 12 UTC, September 29, 1959.

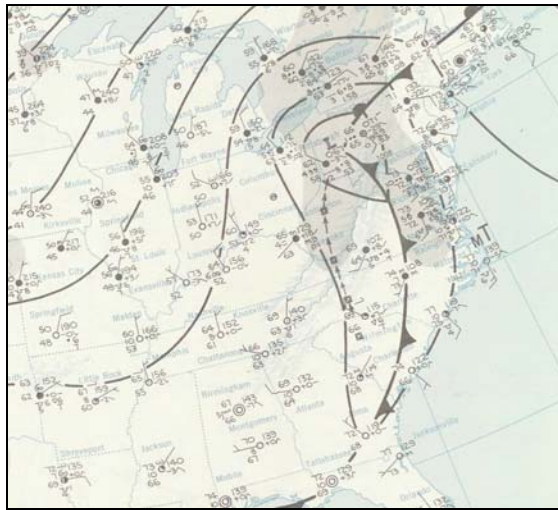


Fig. A-29: Observed standard station plot, (4 mb contours), precipitation (shaded), 12 UTC, September 30, 1959.

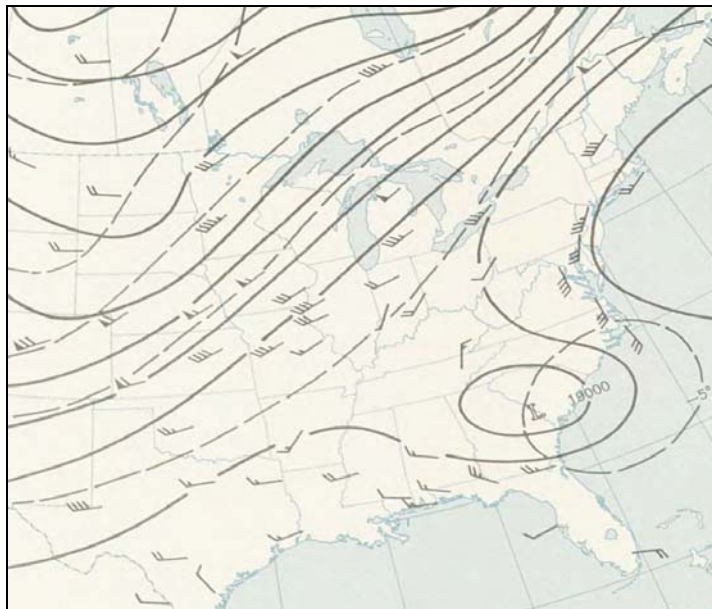


Fig. A-30: Observed Observed 500 mb chart (200 ft contours), winds (kts), temperatures (C) 00 UTC, Sept. 30, 1959.



Fig. A-31: June 8-10, 1968. *ABBY*.

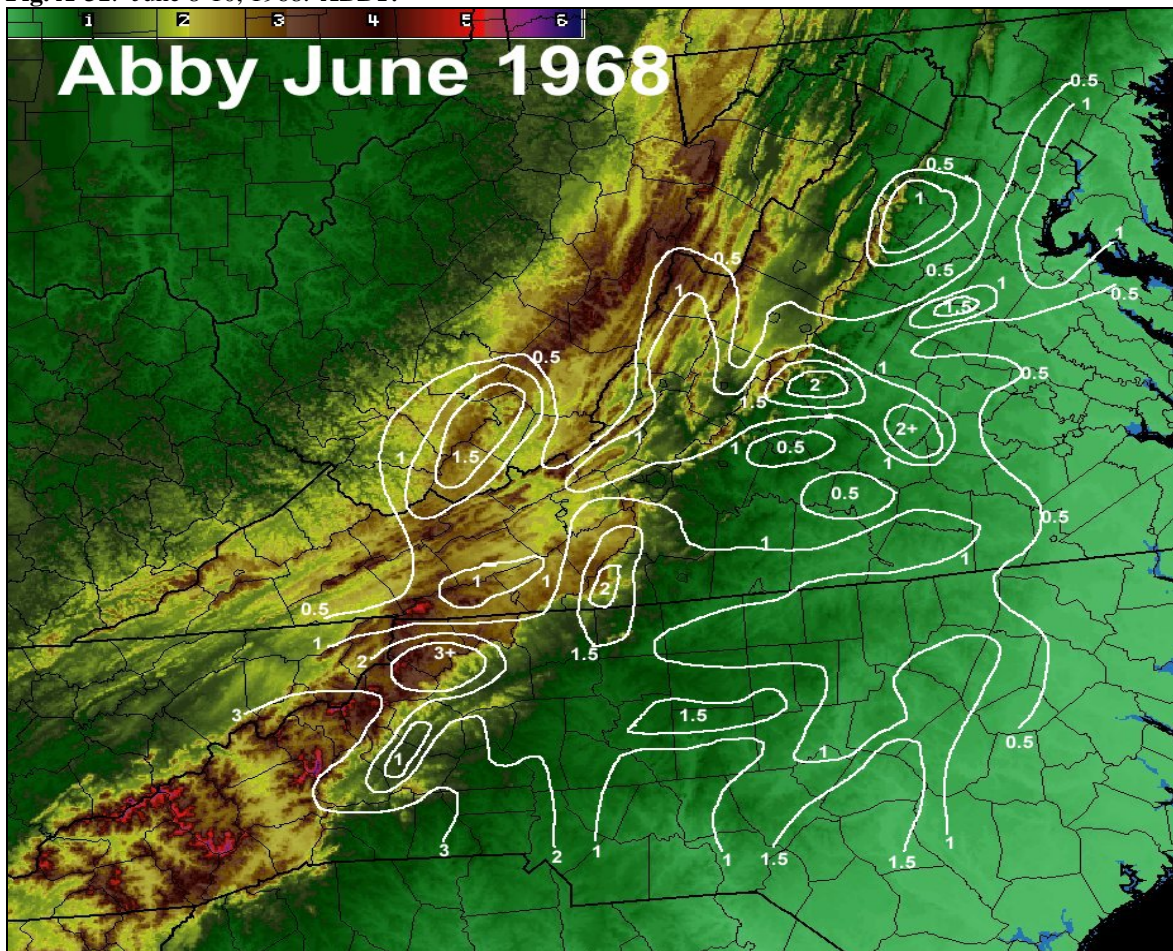


Fig. A-32: Abby rainfall in inches (white contours), June 8-10, 1968, overlaid on terrain (k ft).

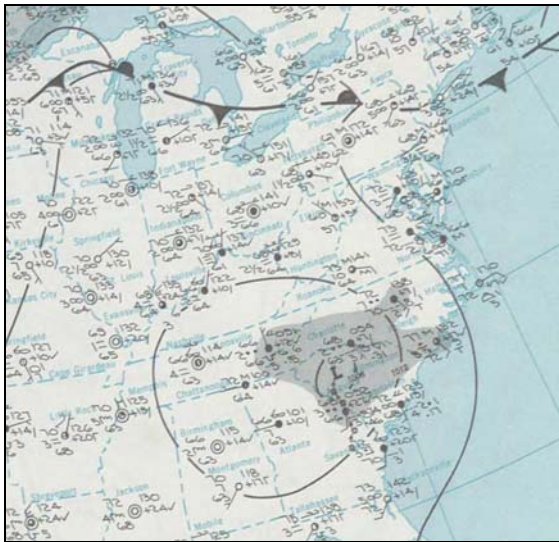


Fig. A-33: Observed standard station plot, (4 mb contours), precipitation (shaded), 12 UTC, June 8, 1968.



Fig. A-34: Observed standard station plot, (4 mb contours), precipitation (shaded), 12 UTC, June 9, 1968.

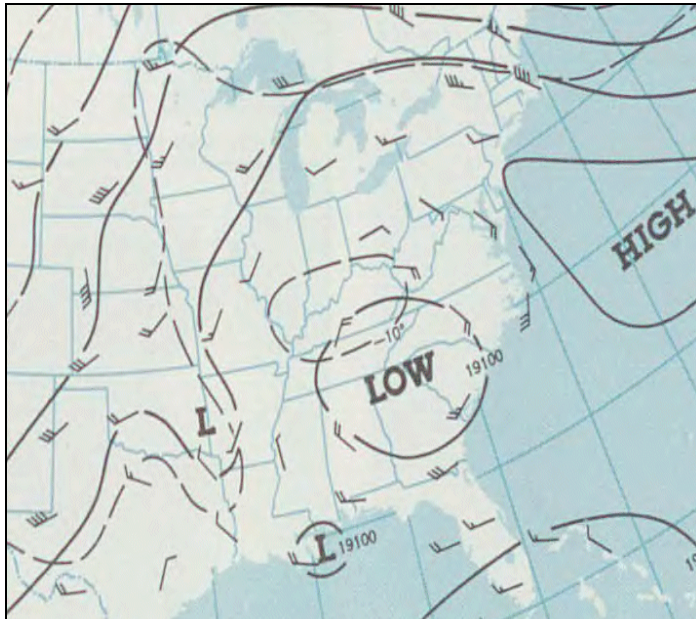


Fig. A-35: Observed Observed 500 mb chart (200 ft contours), winds (kts), temperatures (C), 06 UTC, June 9, 1968.

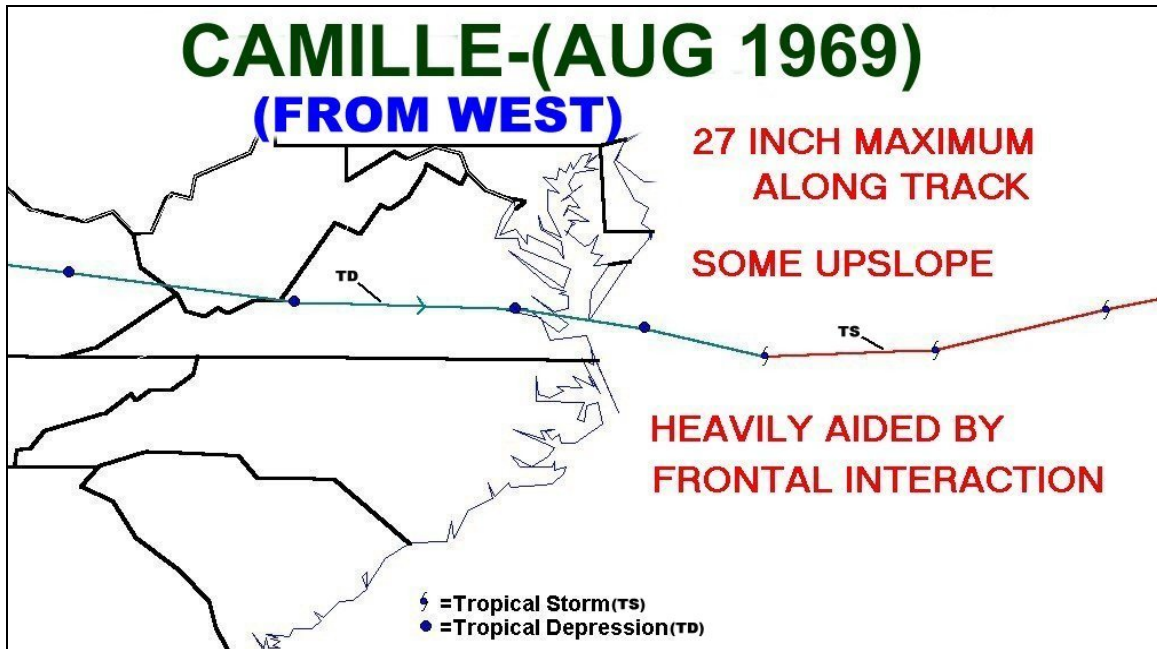


Fig. A-36: August 19-20, 1969. *CAMILLE*.

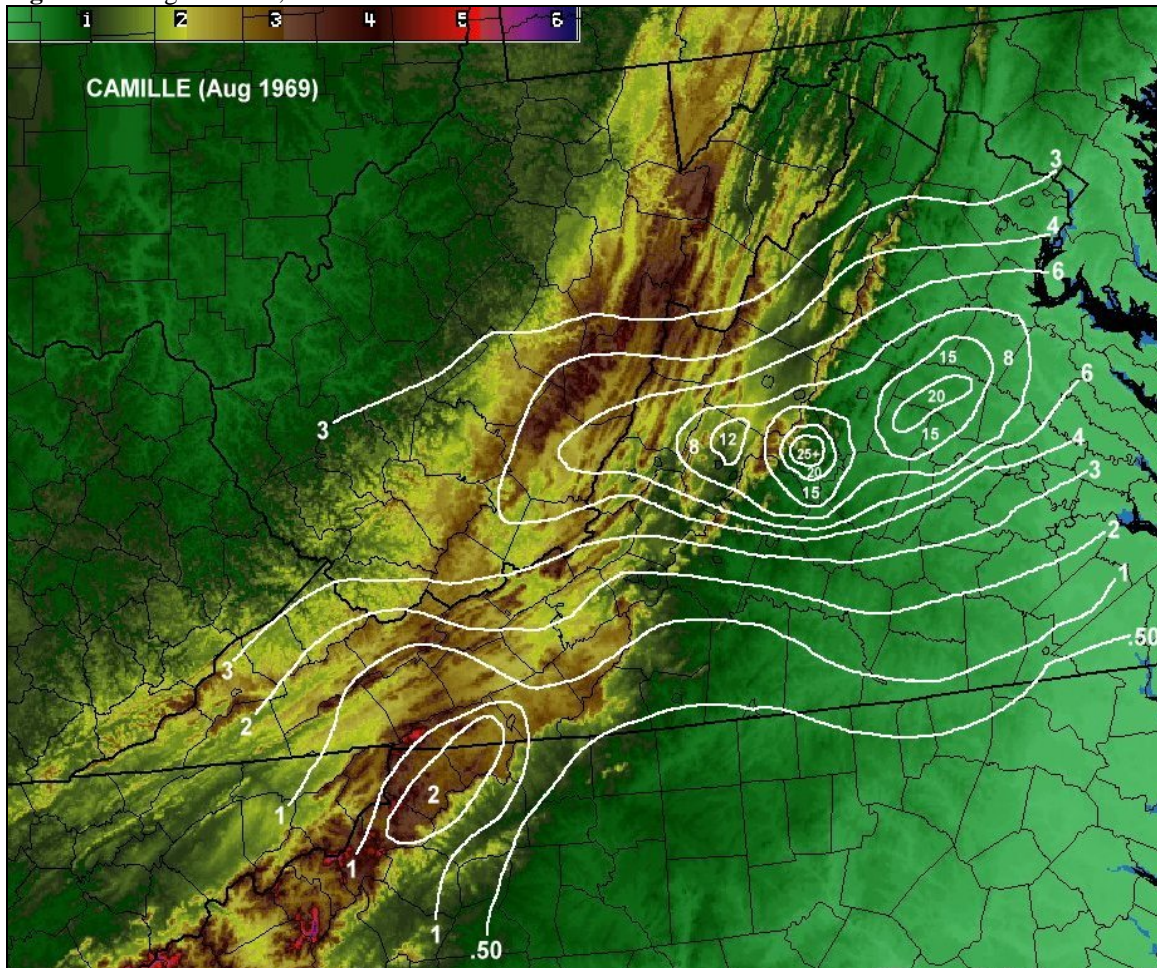


Fig. A-37: Camille rainfall in inches (white contours), August 19-20, 1969, overlaid on terrain (k ft).

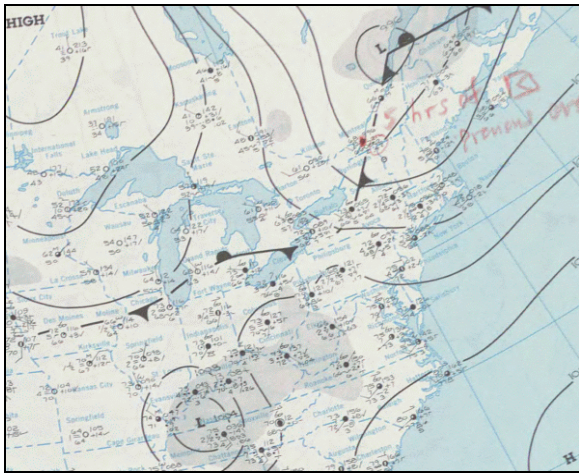


Fig. A-38: Observed standard station plot (4 mb contours), precipitation (shaded), 12 UTC, August 19, 1969.

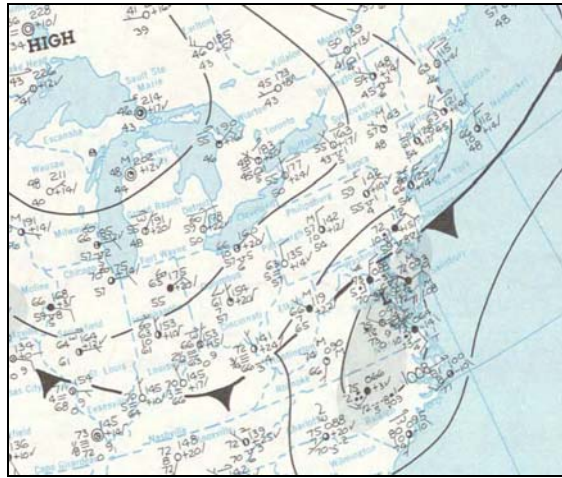


Fig. A-39: Observed standard station plot (4 mb contours), precipitation (shaded), 12 UTC, August 20, 1969.

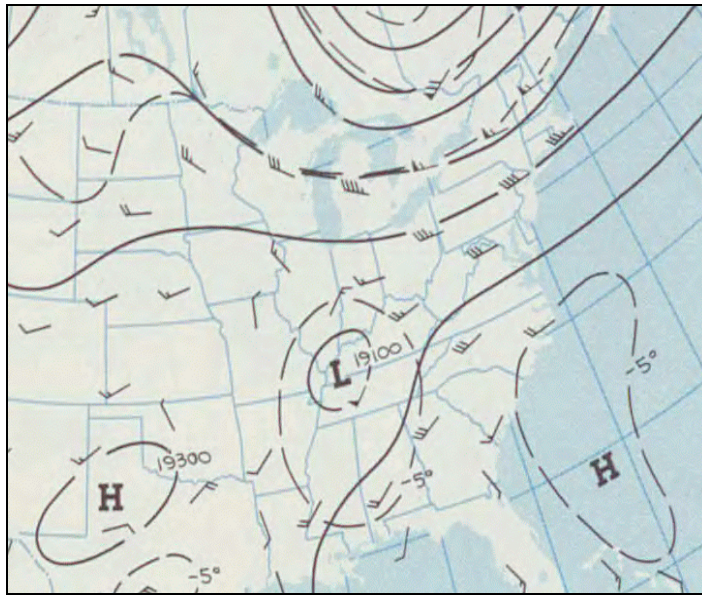


Fig. A-40: Observed 500 mb chart (200 ft contours), winds (kts), temperatures (C), 12 UTC, Aug. 19, 1969.

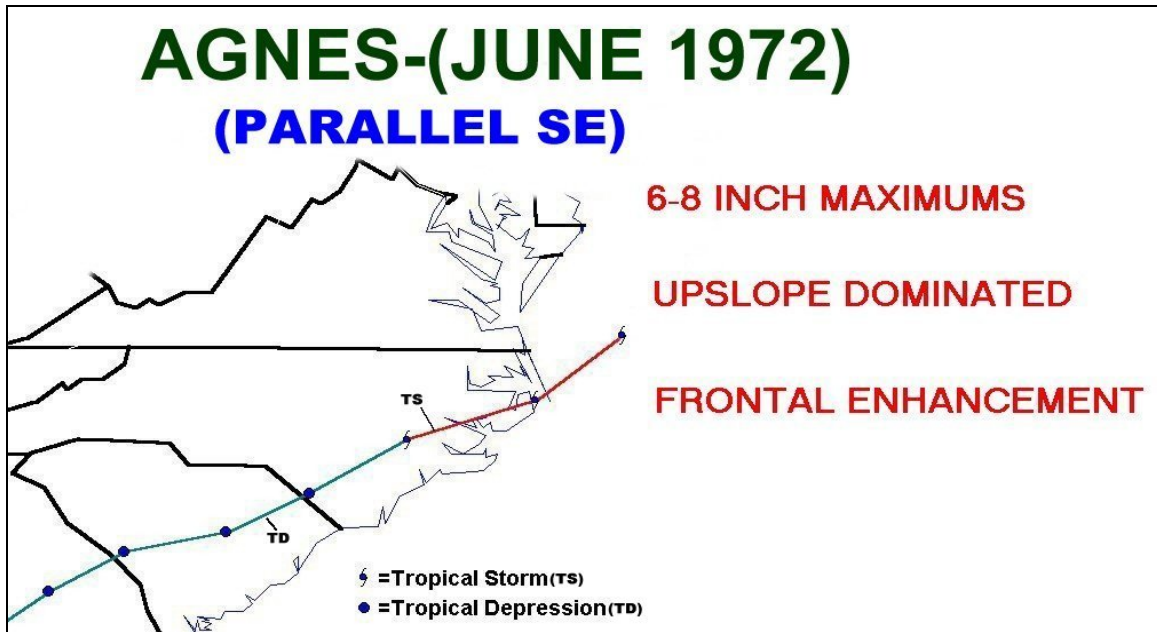


Fig. A-41: June 20-21, 1972. *AGNES*.

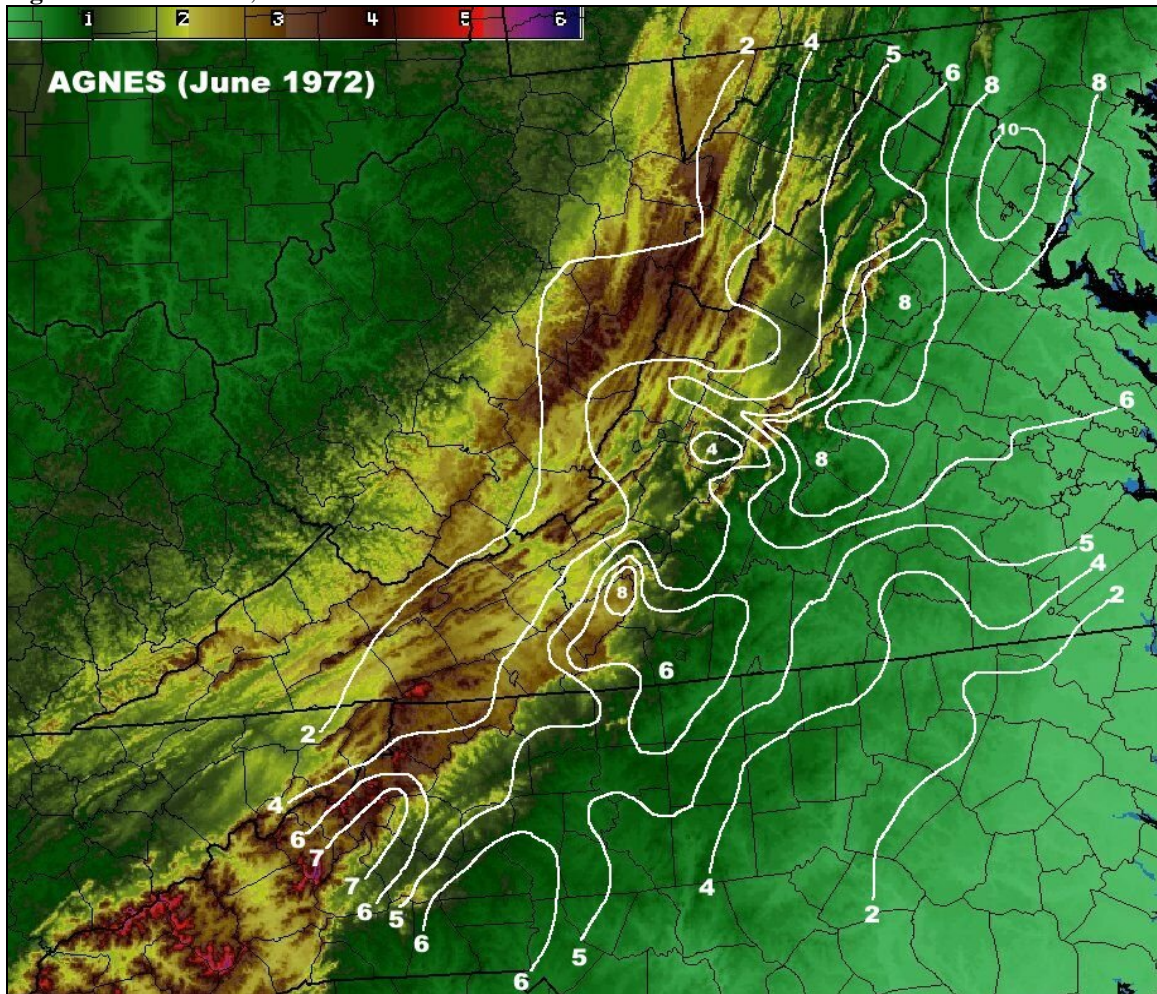


Fig. A-42: Agnes rainfall in inches (white contours), June 20-21, 1972, overlaid on terrain (k ft).



Fig. A-43: Observed standard station plot (4 mb contours), precipitation (shaded), 12 UTC, June 20, 1972.

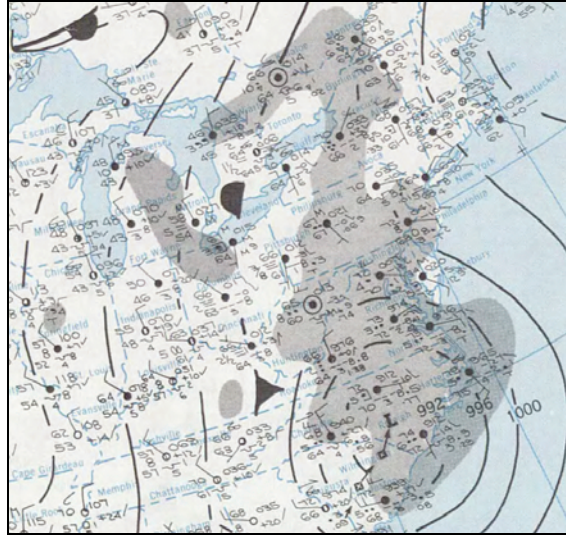


Fig. A-44: Observed standard station plot (4 mb contours), precipitation (shaded), 12 UTC, June 21, 1972.

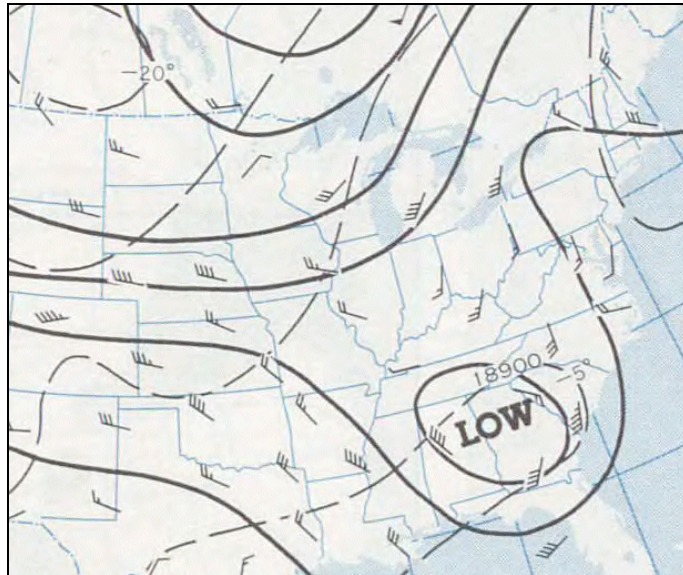


Fig. A-45: Observed 500 mb chart (200 ft contours), winds (kts), temperatures (C), 06 UTC, June 20, 1972.

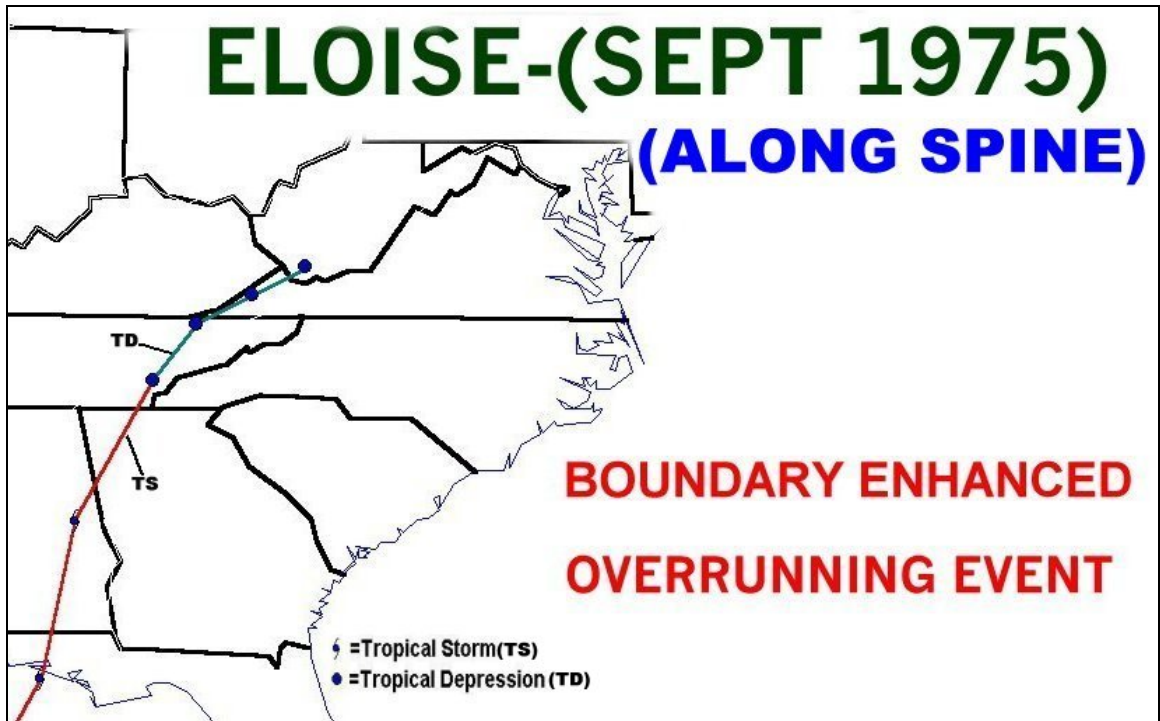


Fig. A-46: September 23-24, 1975. *ELOISE*.

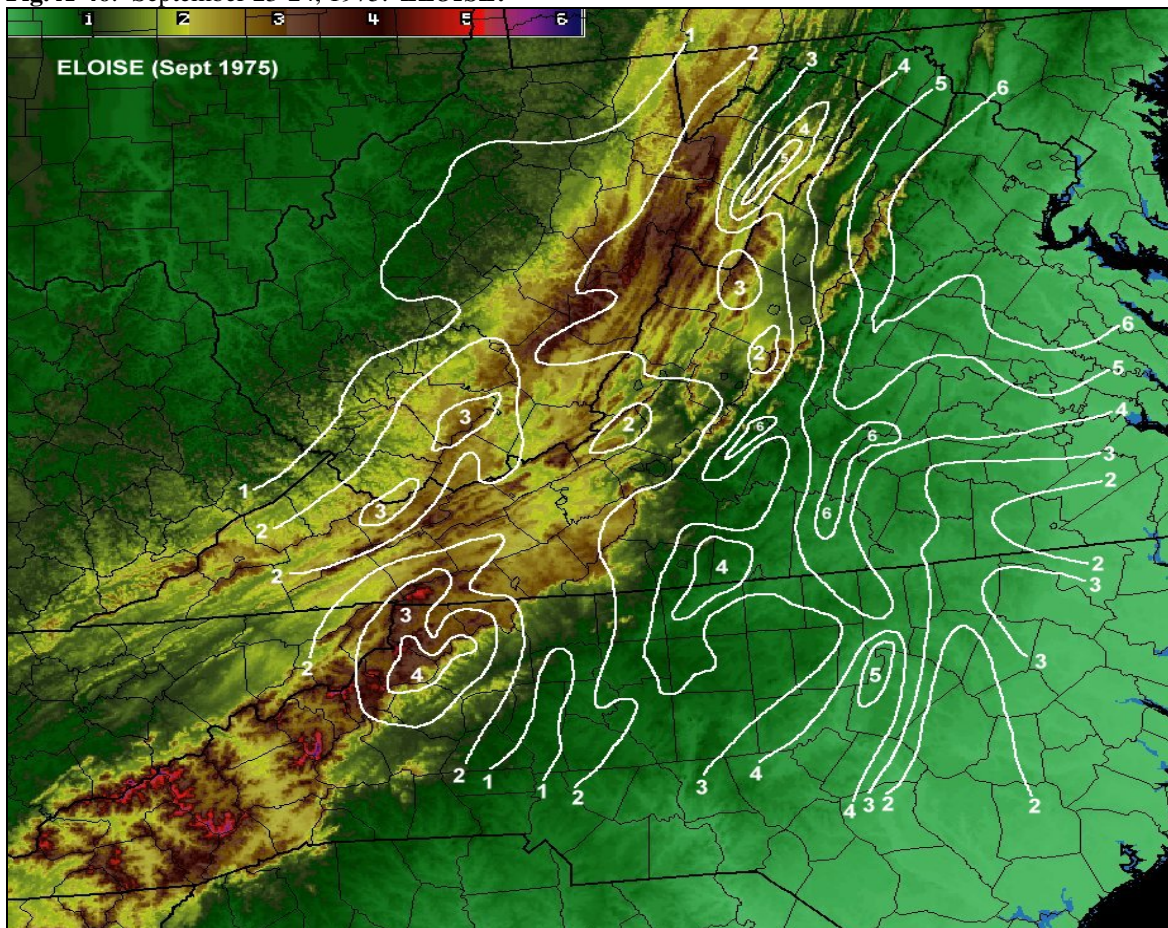


Fig. A-47: Eloise rainfall in inches (white contours), September 23-24, 1975, overlaid on terrain (k ft).

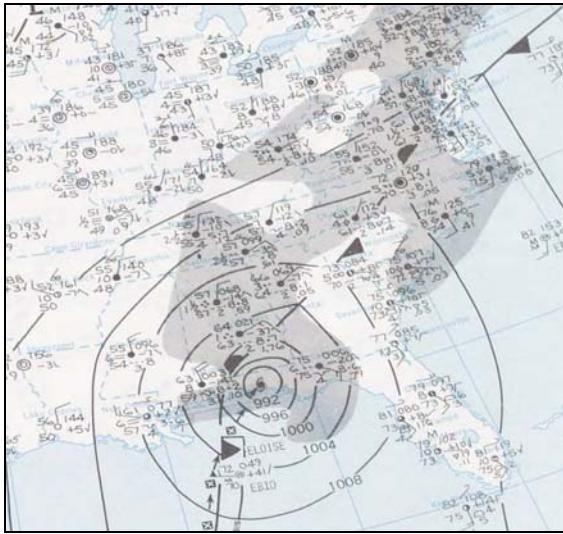


Fig. A-48: Observed standard station plot (4 mb contours), precipitation (shaded), 12 UTC, September 23, 1975.

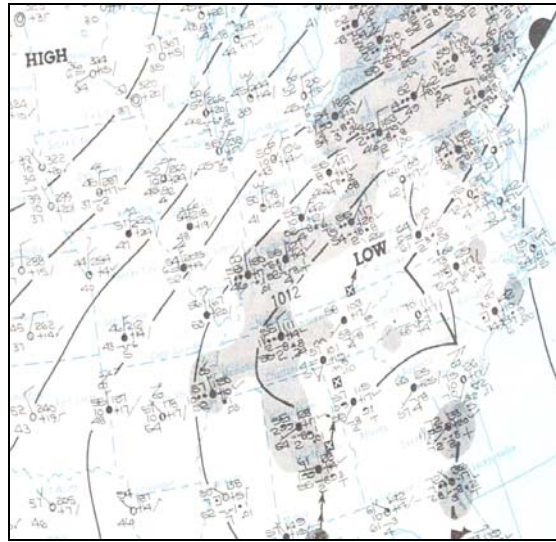


Fig. A-49: Observed standard station plot (4 mb contours), precipitation (shaded), 12 UTC, September 24, 1975.

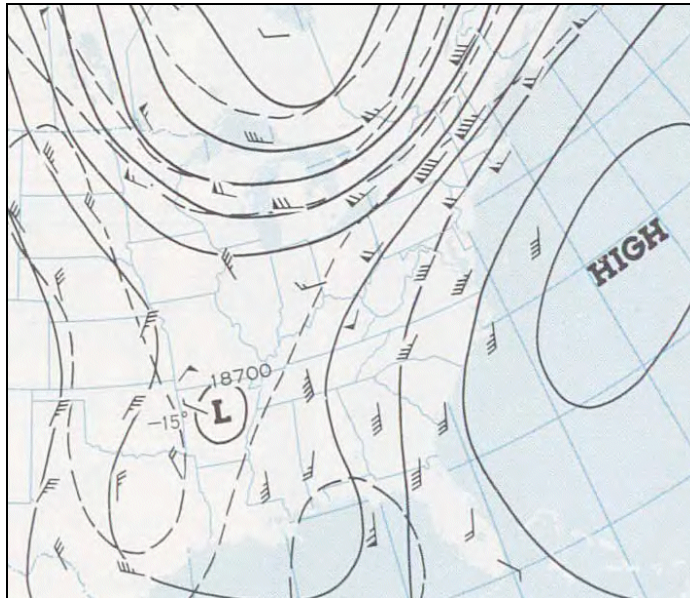


Fig. A-50: Observed 500 mb chart (200 ft contours), winds (kts), temperatures (C), 12 UTC, Sept. 23, 1975.

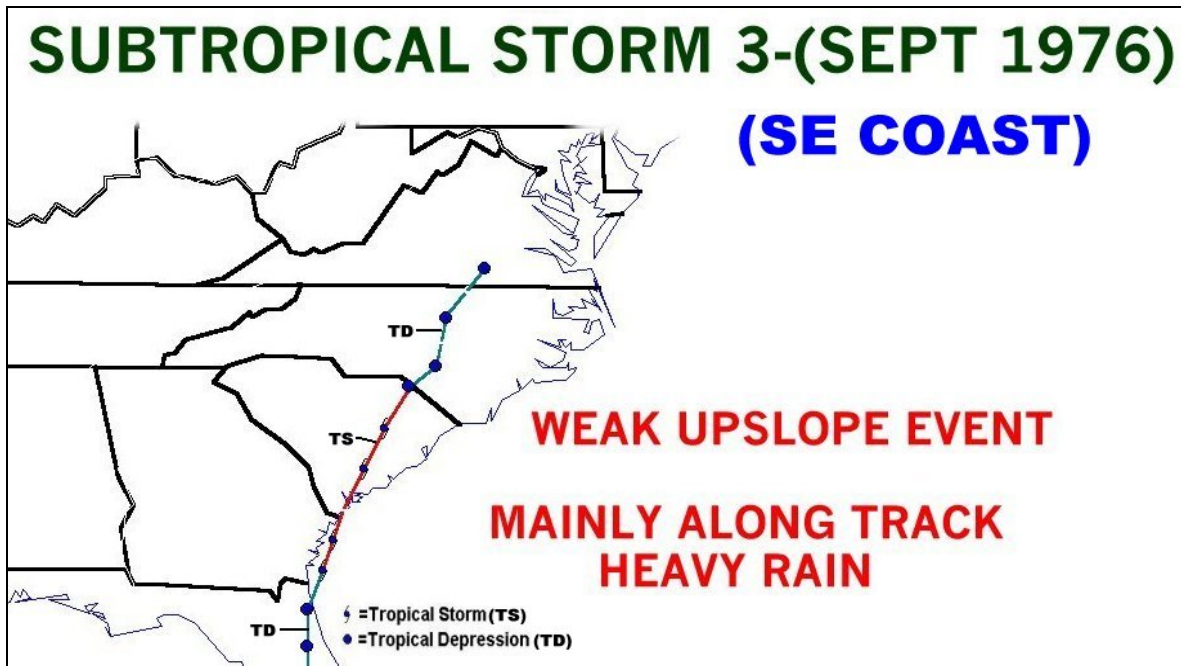


Fig. A-51: September 14-17, 1976. *SUBTROPICAL STORM 3*.

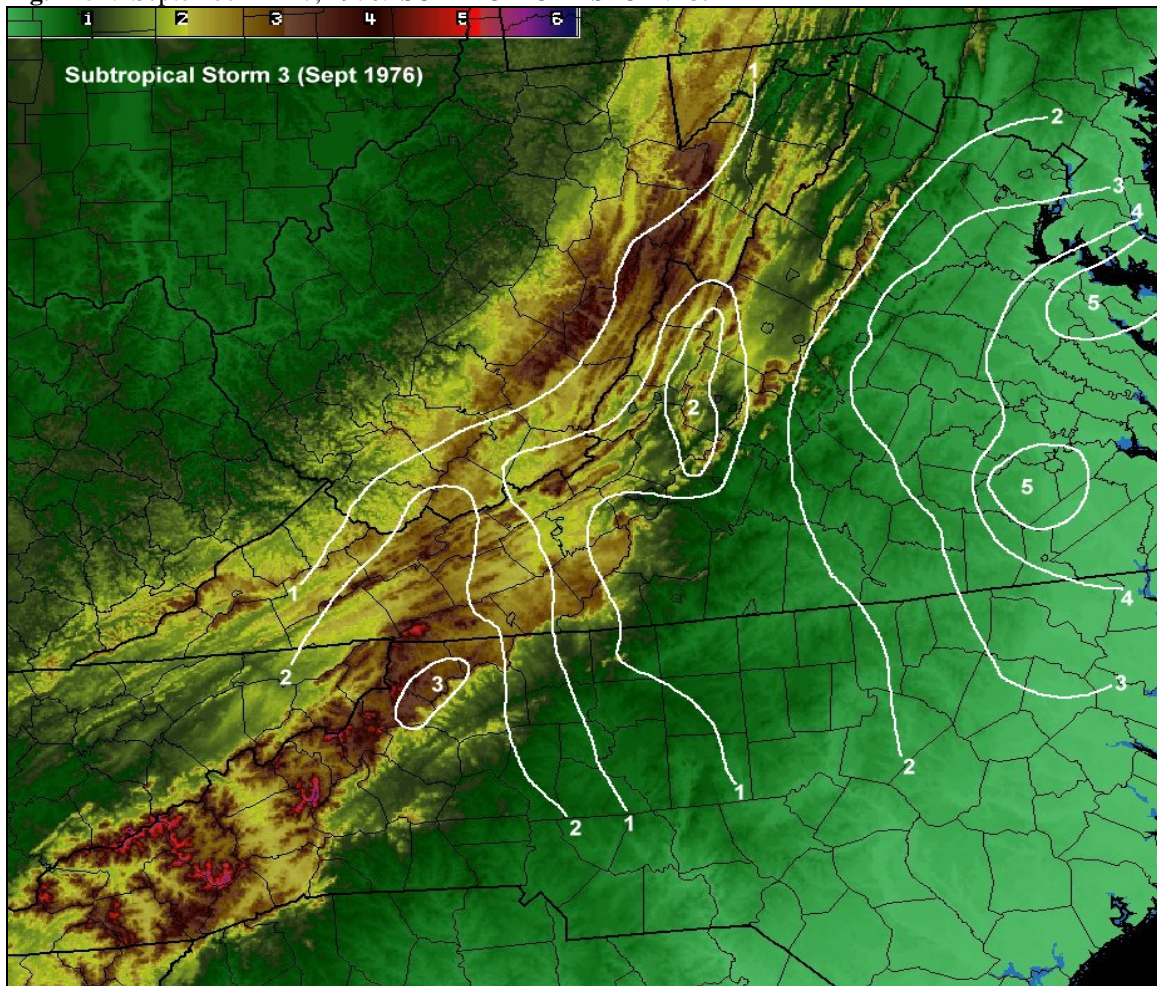


Fig. A-52: Storm 3 rainfall in inches (white contours), September 15-16, 1976, overlaid on terrain (k ft).

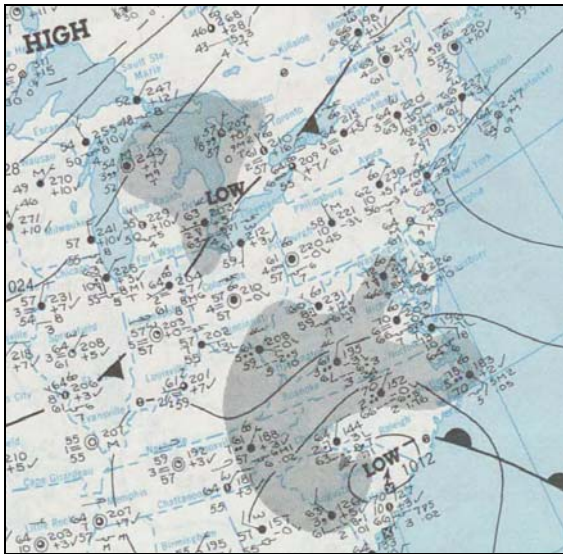


Fig. A-53: Observed standard station plot (4 mb contours), precipitation (shaded), 12 UTC, September 15, 1976.

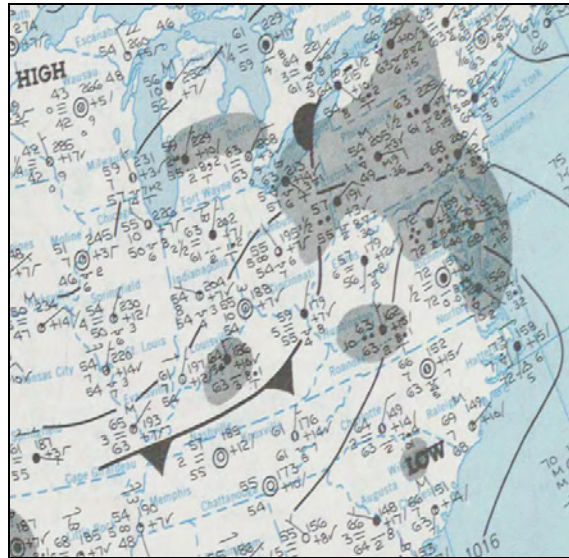


Fig. A-54: Observed standard station plot (4 mb contours), precipitation (shaded), 12 UTC, September 16, 1976.

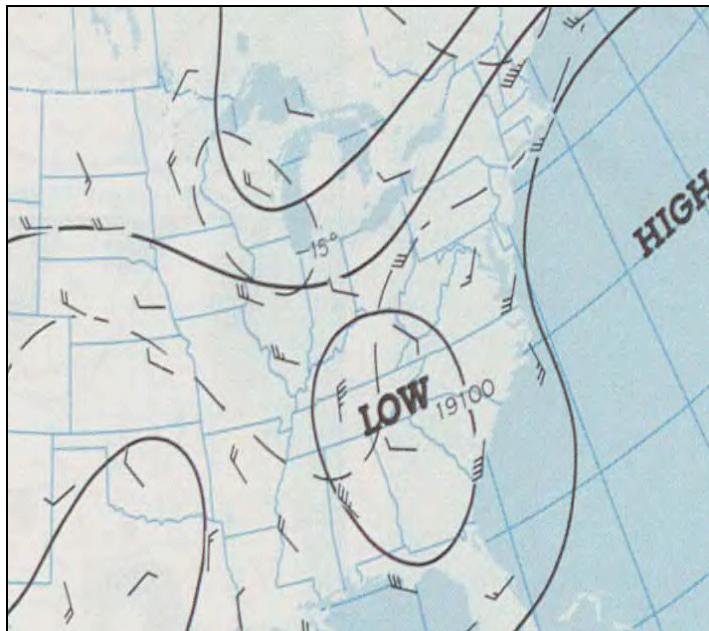


Fig. A-55: Observed 500 mb chart (200 ft contours), winds (kts), temperatures (C), 12 UTC, Sept. 15, 1976.

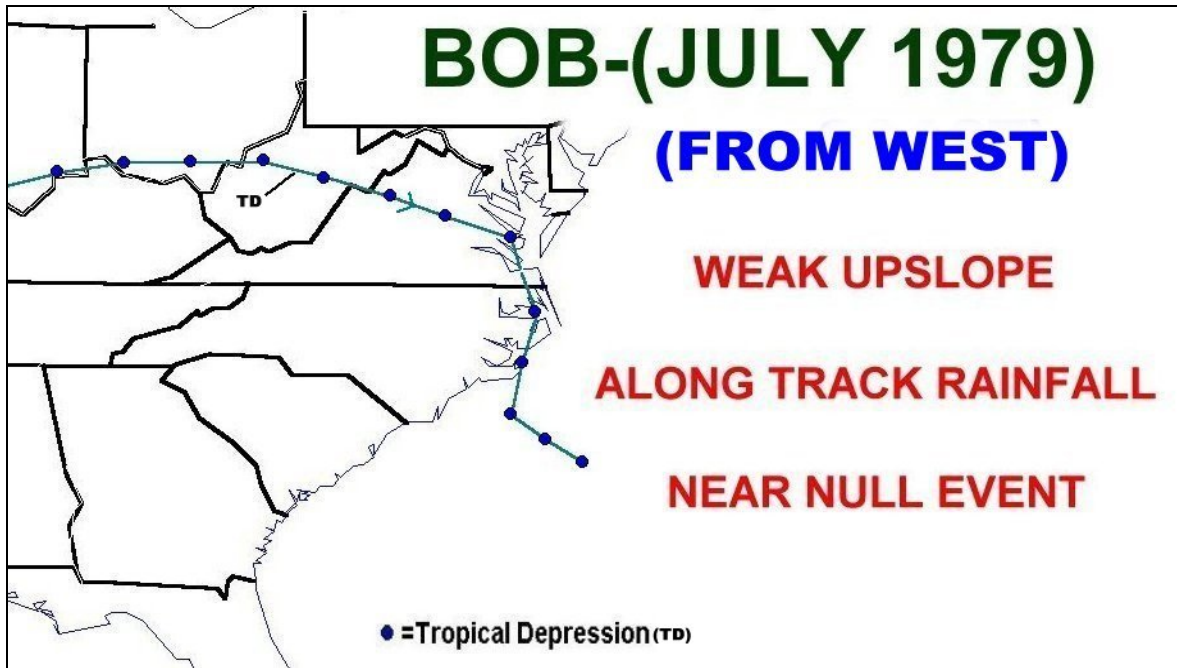


Fig. A-56: July 12-14, 1979. BOB.

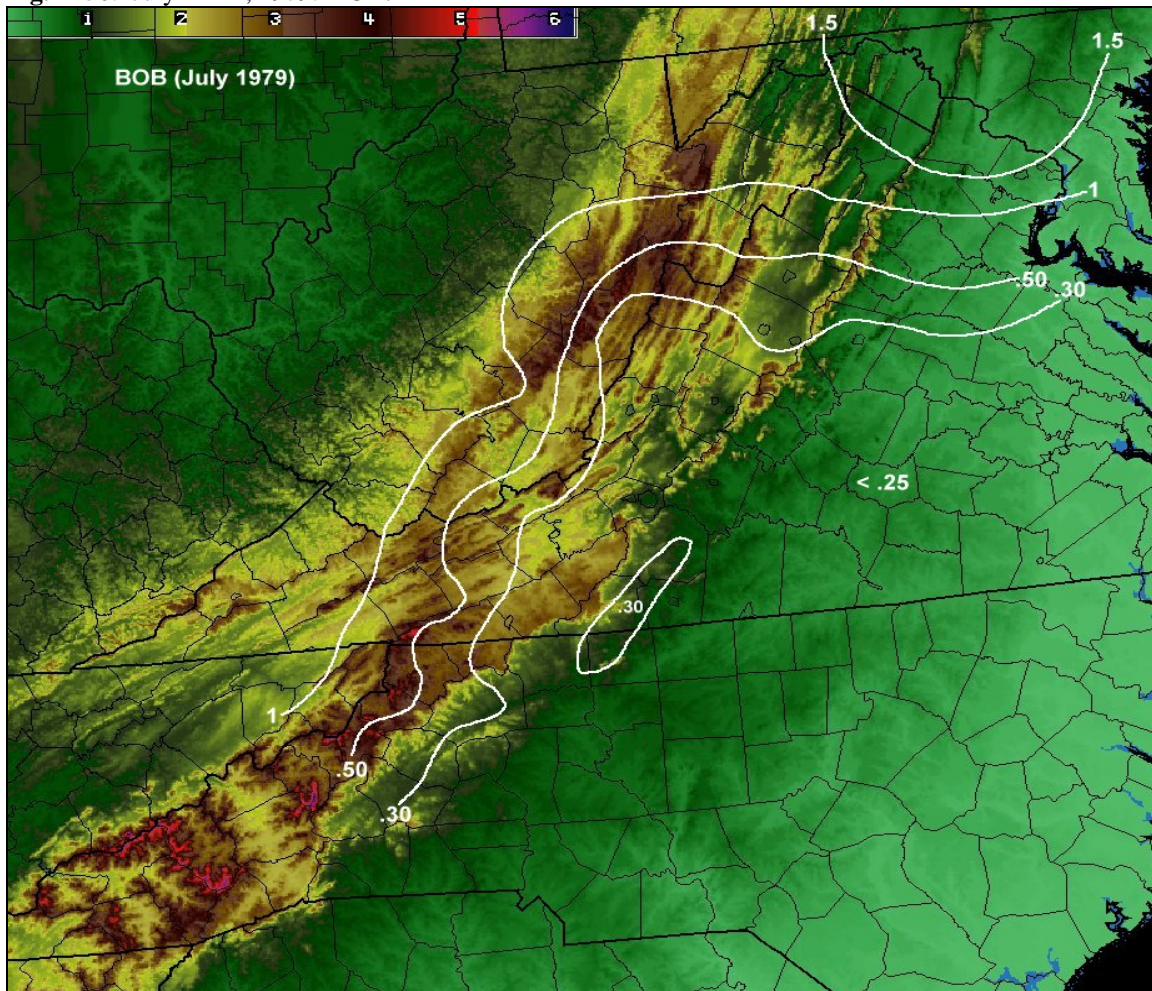


Fig. A-57: Bob rainfall in inches (white contours), July 12-14, 1979, overlaid on terrain (k ft).

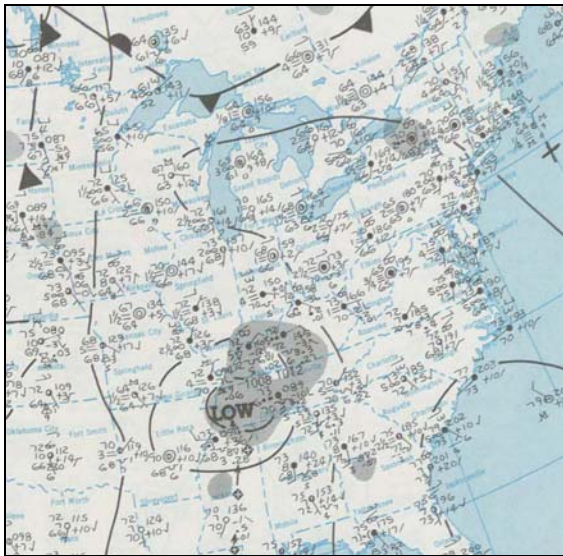


Fig. A-58: Observed standard station plot (4 mb contours), precipitation (shaded), 12 UTC, July 12, 1979.

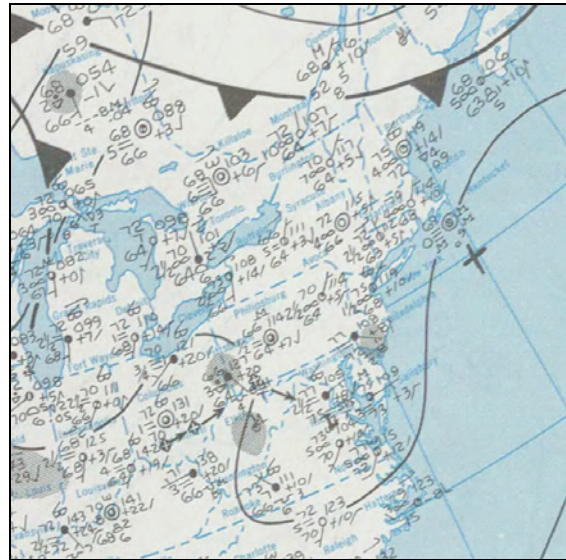


Fig. A-59: Observed standard station plot (4 mb contours), precipitation (shaded), 12 UTC, July 14, 1979.

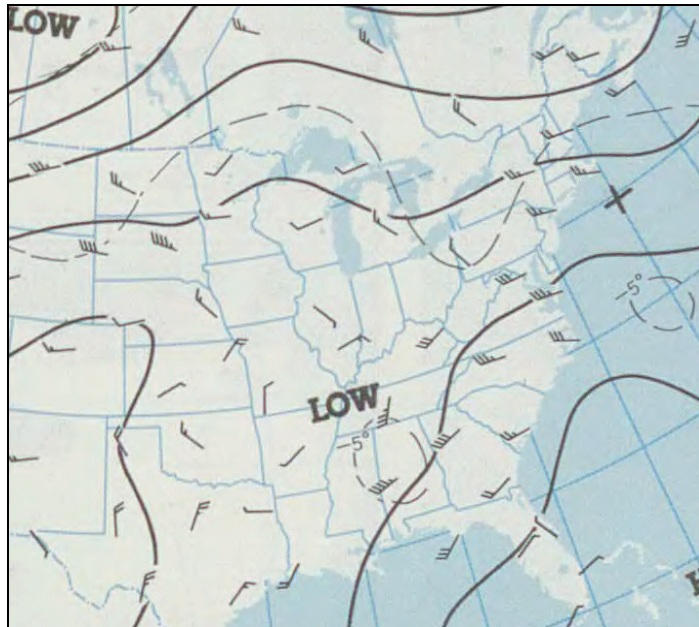


Fig. A-60: Observed 500 mb chart (200 ft contours), winds (kts), temperatures (C), 12 UTC, July 12, 1979.

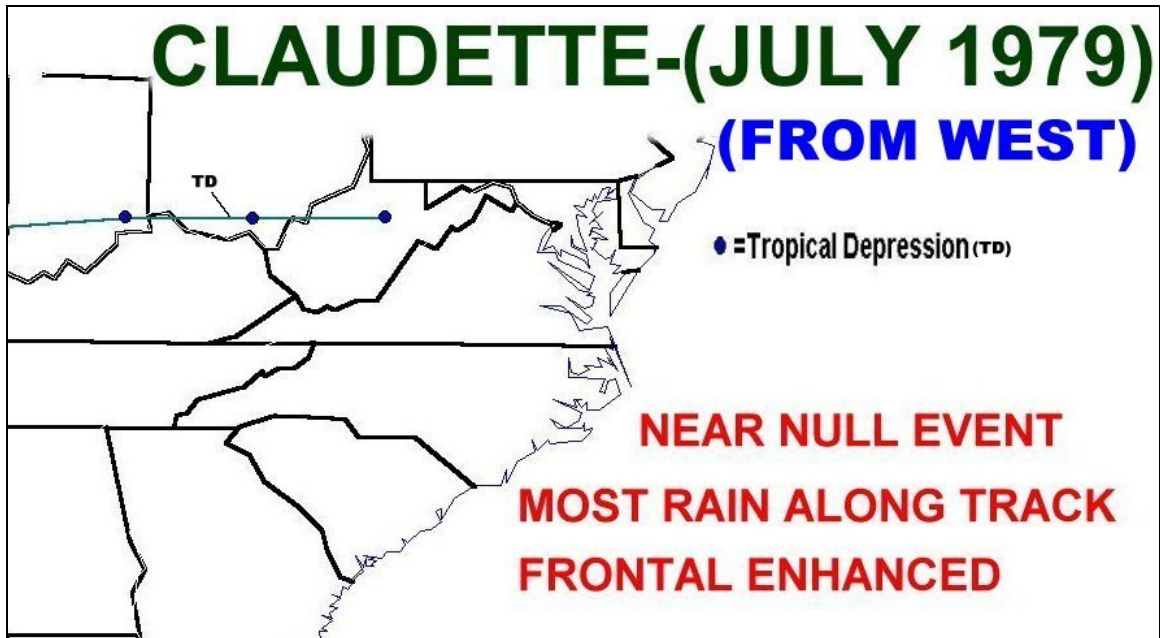


Fig. A-61: July 28-29, 1979. *CLAUDETTE*.

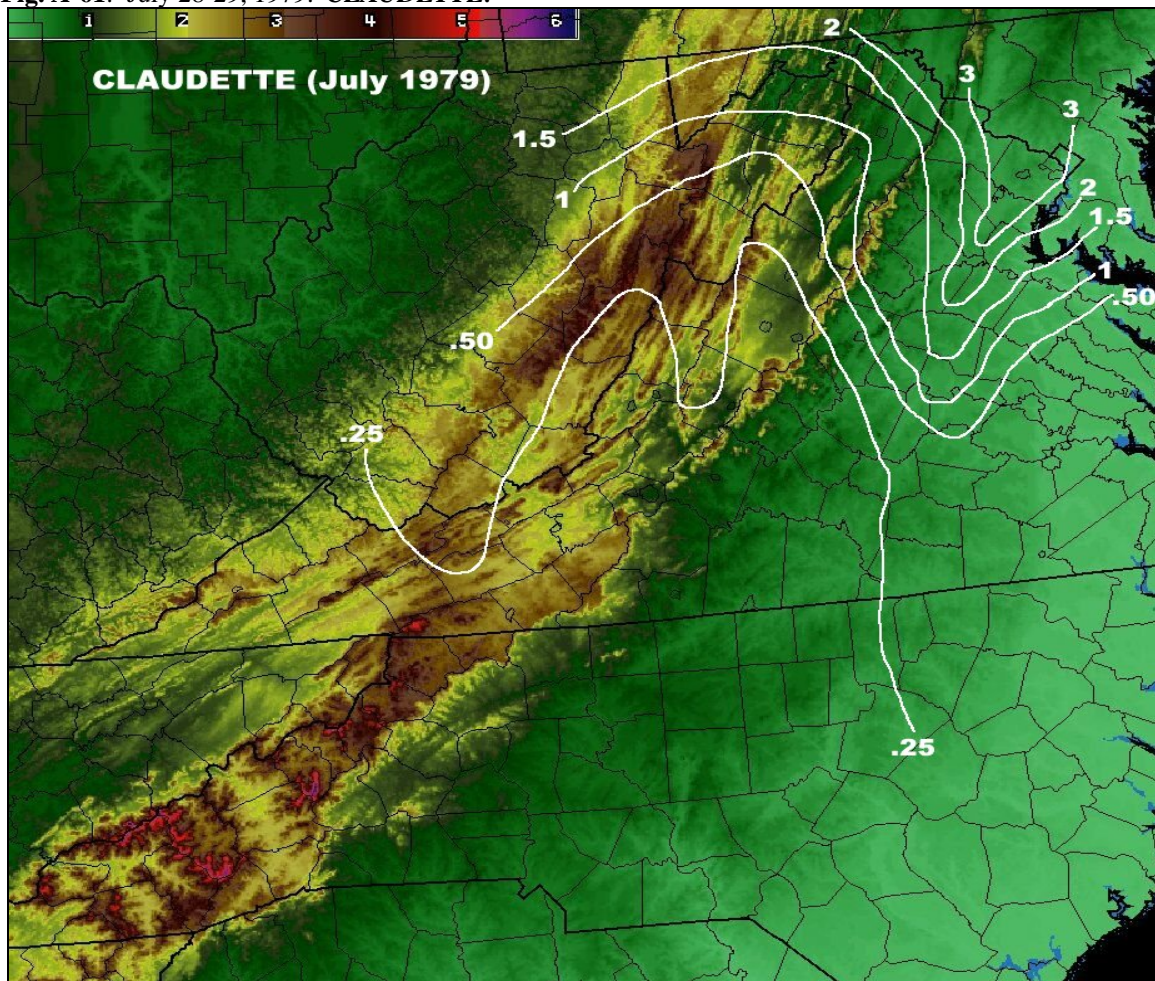


Fig. A-62: Claudette rainfall in inches (white contours), July 28-29, 1979, overlaid on terrain (k ft).

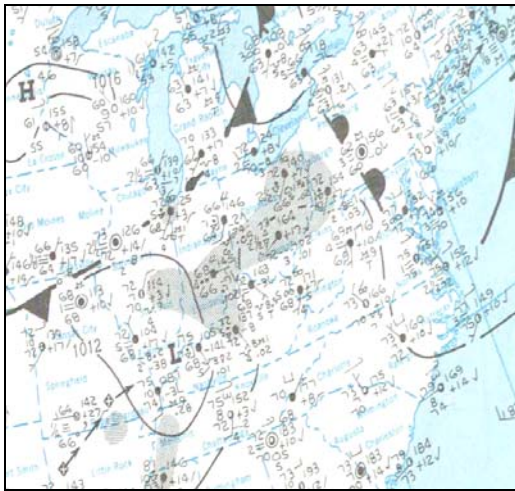


Fig. A-63: Observed standard station plot (4 mb contours), precip. (shaded), 12 UTC, July 28, 1979.

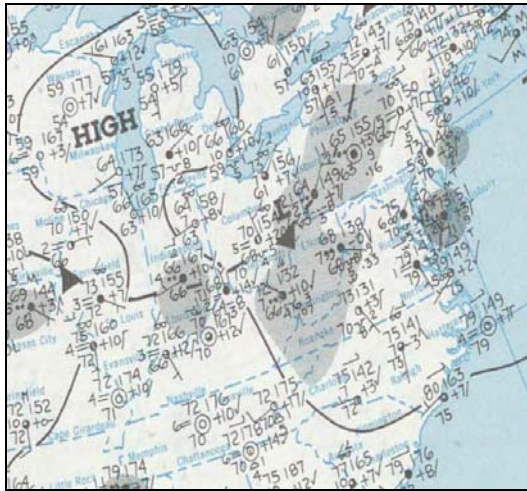


Fig. A-64: Observed standard station plot (4 mb contours), precip. (shaded), 12 UTC, July 29, 1979.

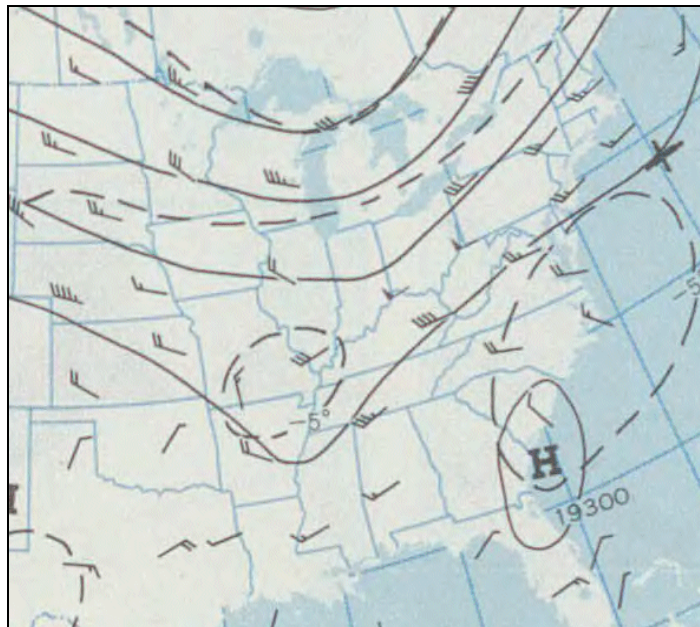


Fig. A-65: Observed 500 mb chart (200 ft contours), winds (kts), temperatures (C), 12 UTC, July 28, 1979.

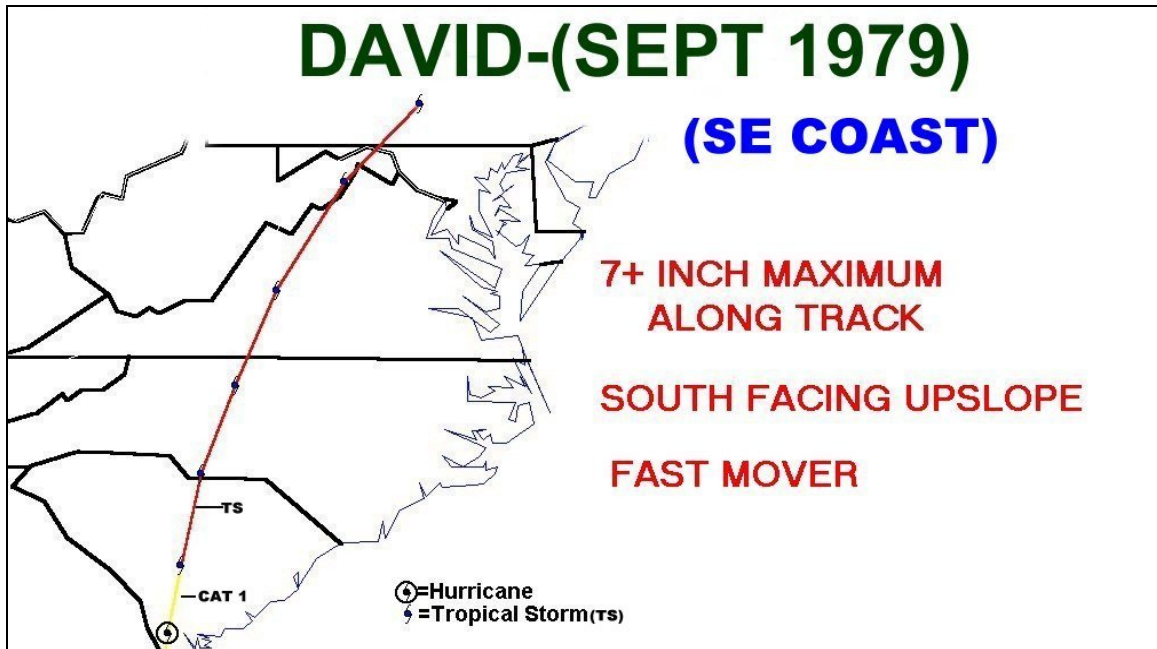


Fig. A-66: September 4-6, 1979. *DAVID*.

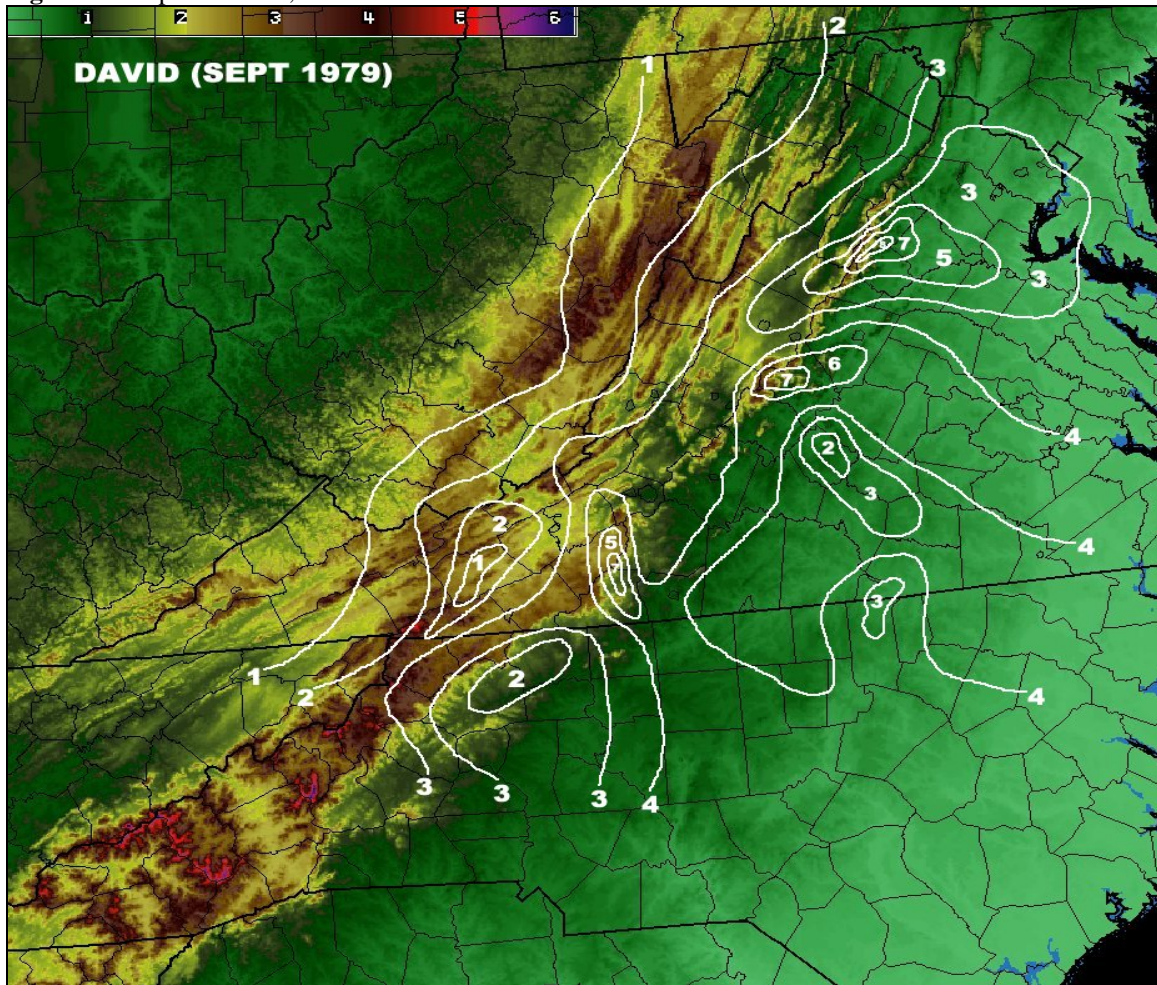


Fig. A-67: David rainfall in inches (white contours), September 4-5, 1979, overlaid on terrain (k ft).



Fig. A-68: Observed standard station plot (4 mb contours), precip. (shaded), 12 UTC, September 4, 1979.

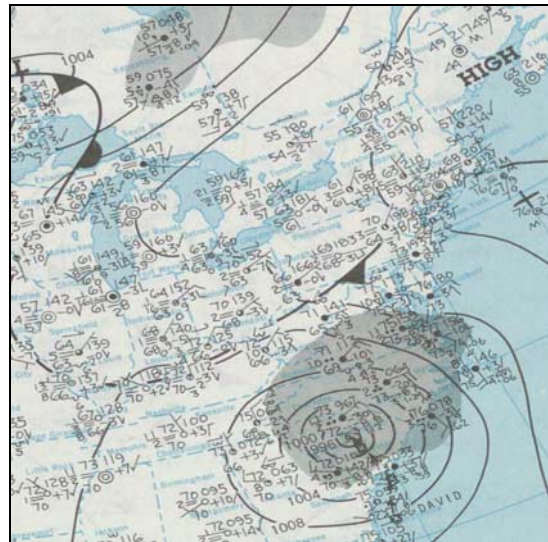


Fig. A-69: Observed standard station plot (4 mb contours), precip. (shaded), 12 UTC, September 5, 1979.

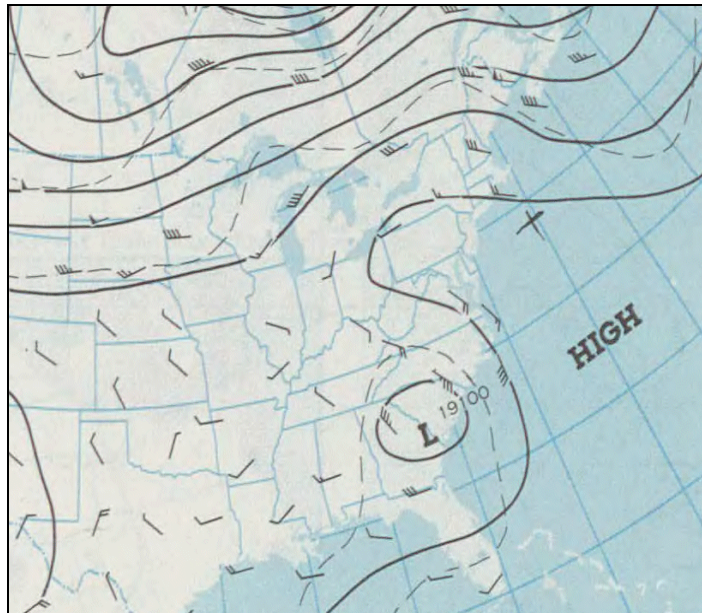


Fig. A-70: Observed 500 mb chart (200 ft contours), winds (kts), temperatures (C), 12 UTC, Sept 5, 1979.

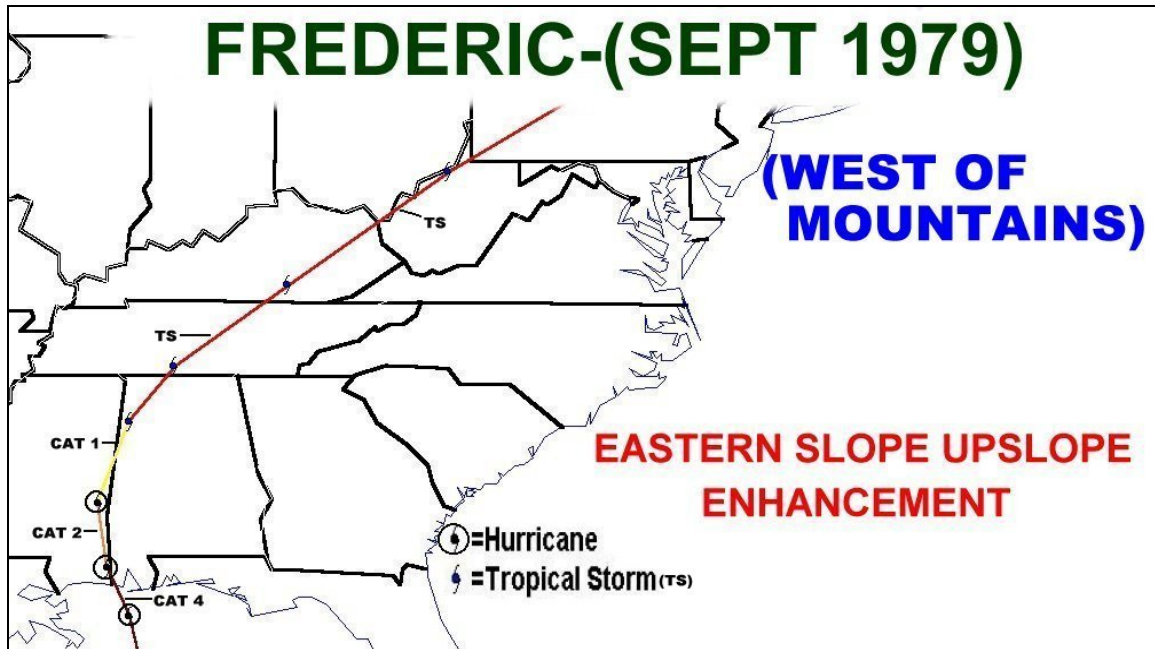


Fig. A-71: September 12-14, 1979. *FREDERIC*.

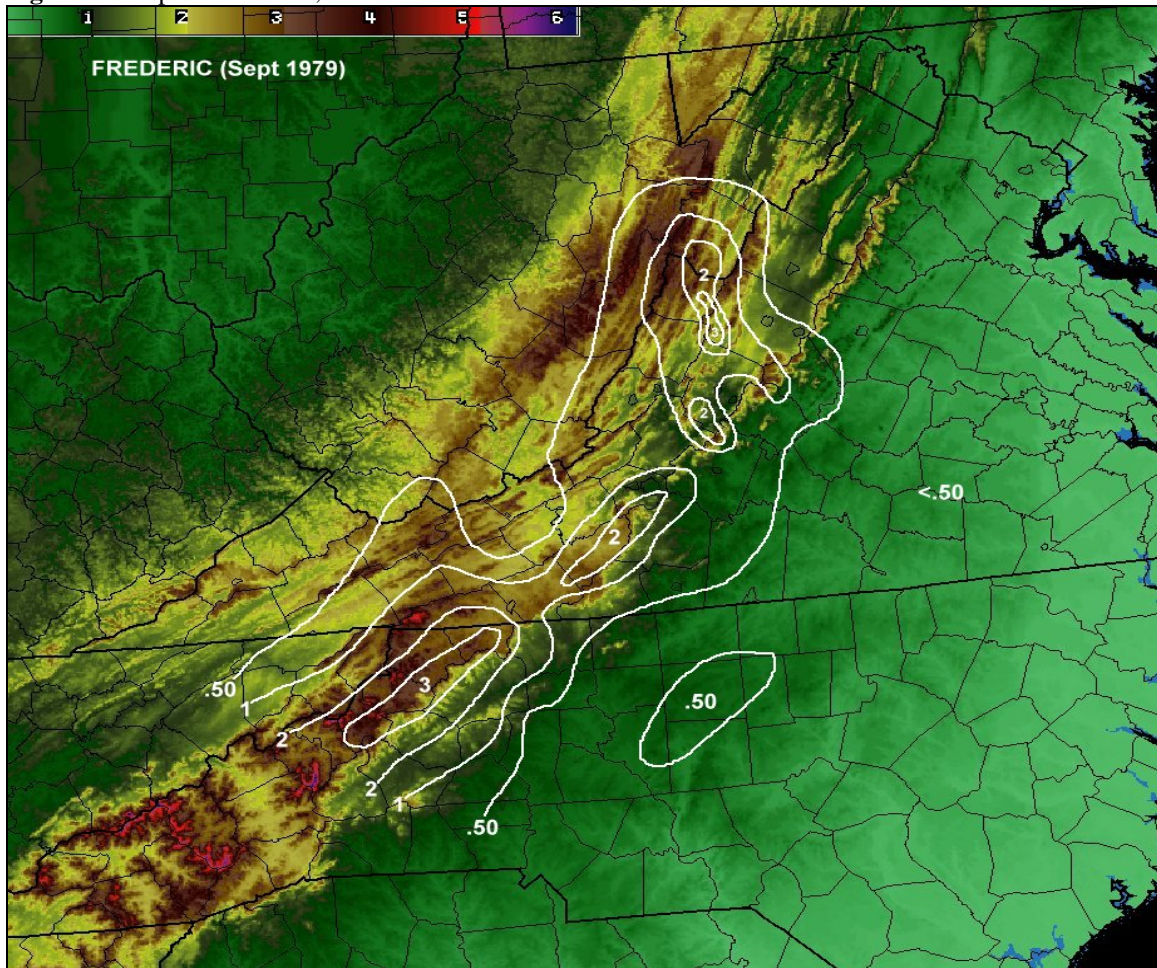


Fig. A-72: Frederic rainfall in inches (white contours), September 13-14, 1979, overlaid on terrain (k ft).

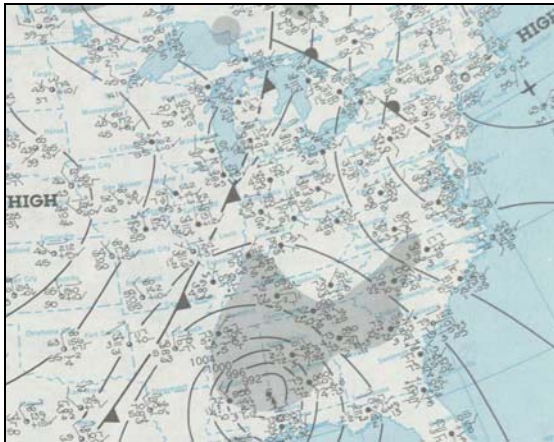


Fig. A-73: Observed standard station plot (4 mb contours), precip. (shaded), 12 UTC, September 13, 1979.

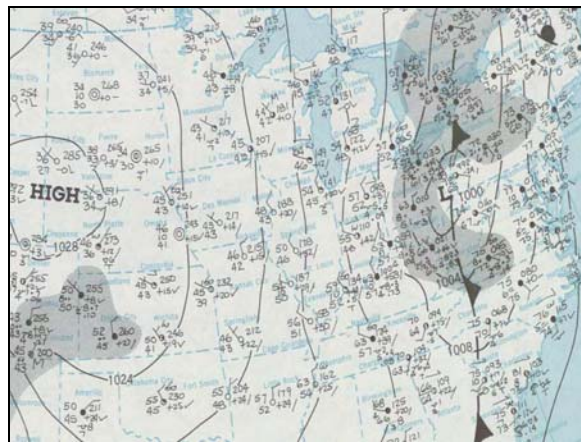


Fig. A-74: Observed standard station plot, (4 mb contours), precip. (shaded), 12 UTC, September 14, 1979.

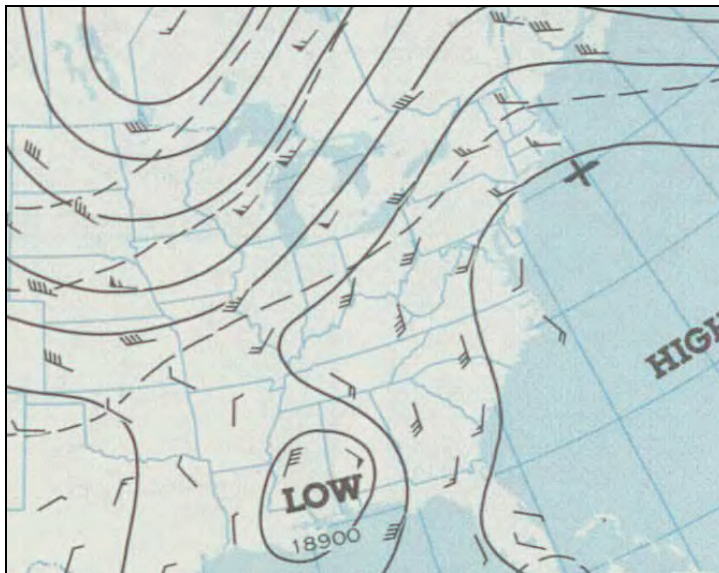


Fig. A-75: Observed 500 mb chart (200 ft contours), winds (kts), temperatures (C), 12 UTC, Sept 13, 1979.

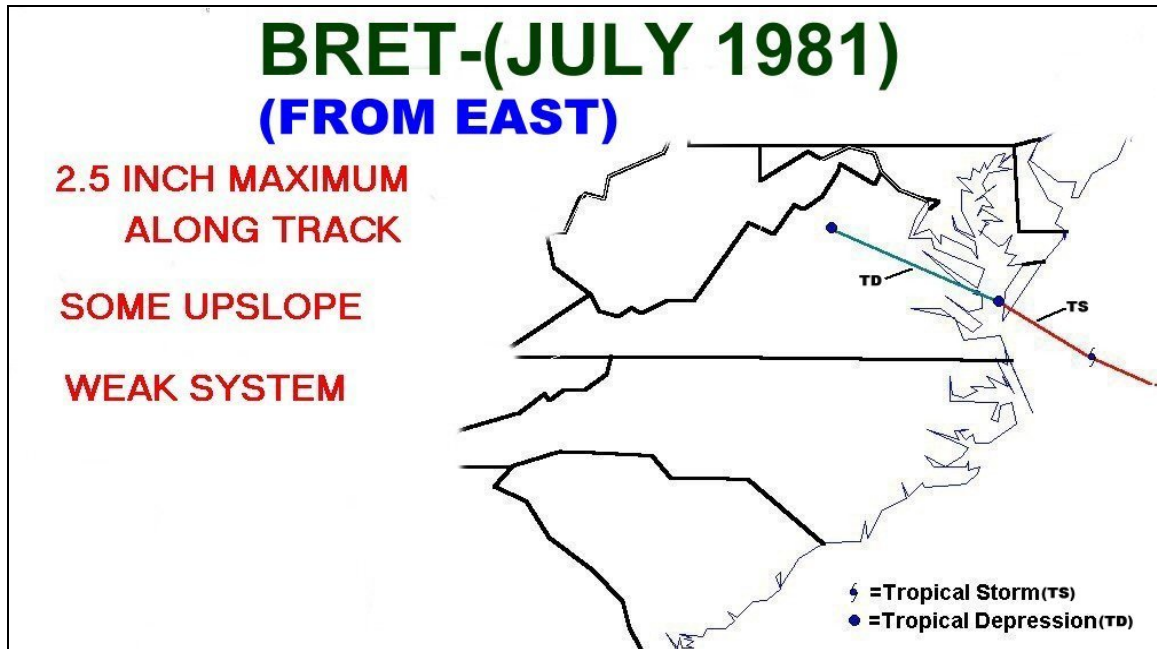


Fig. A-76: June 29-July 1, 1981. *BRET*.

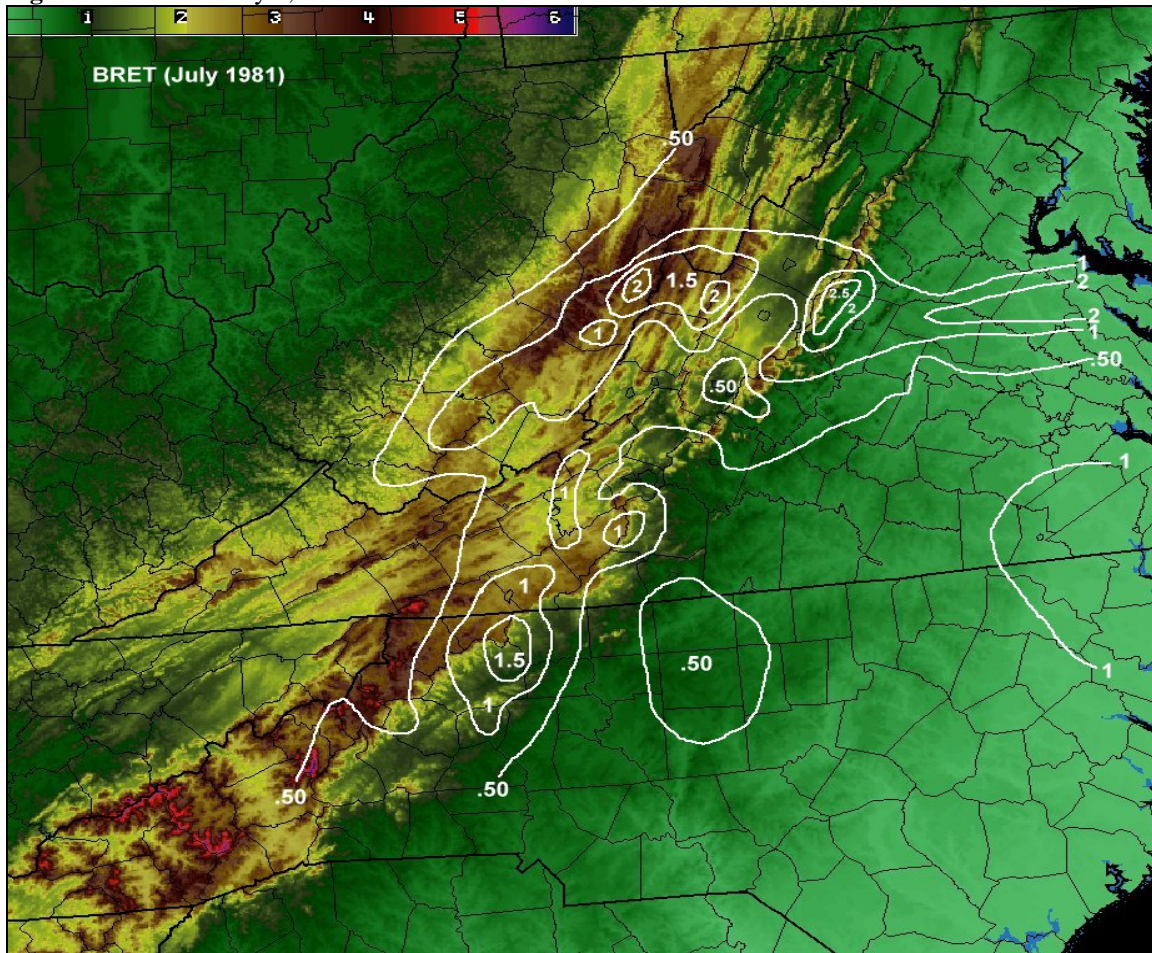


Fig. A-77: Bret rainfall in inches (white contours), June 30-July 1, 1981, overlaid on terrain (k ft).

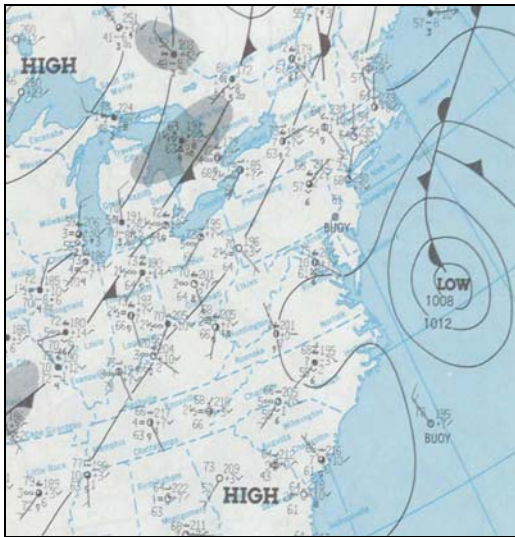


Fig. A-78: Observed standard station plot (4 mb contours), precip. (shaded), 12 UTC, June 30, 1981.

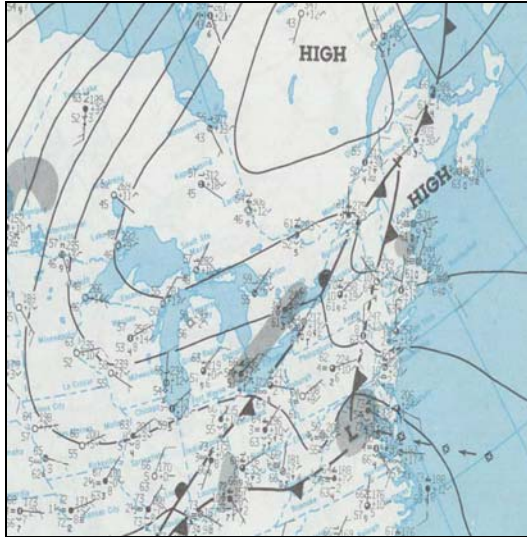


Fig. A-79: Observed standard station plot (4 mb contours), precip. (shaded), 12 UTC, July 1, 1981.

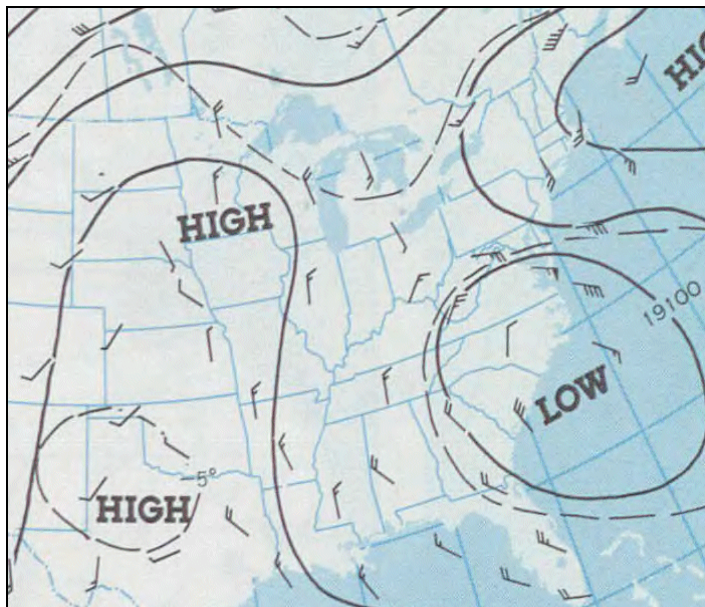


Fig. A-80: Observed 500 mb chart (200 ft contours), winds (kts), temperatures (C), 12 UTC, July 1, 1981.

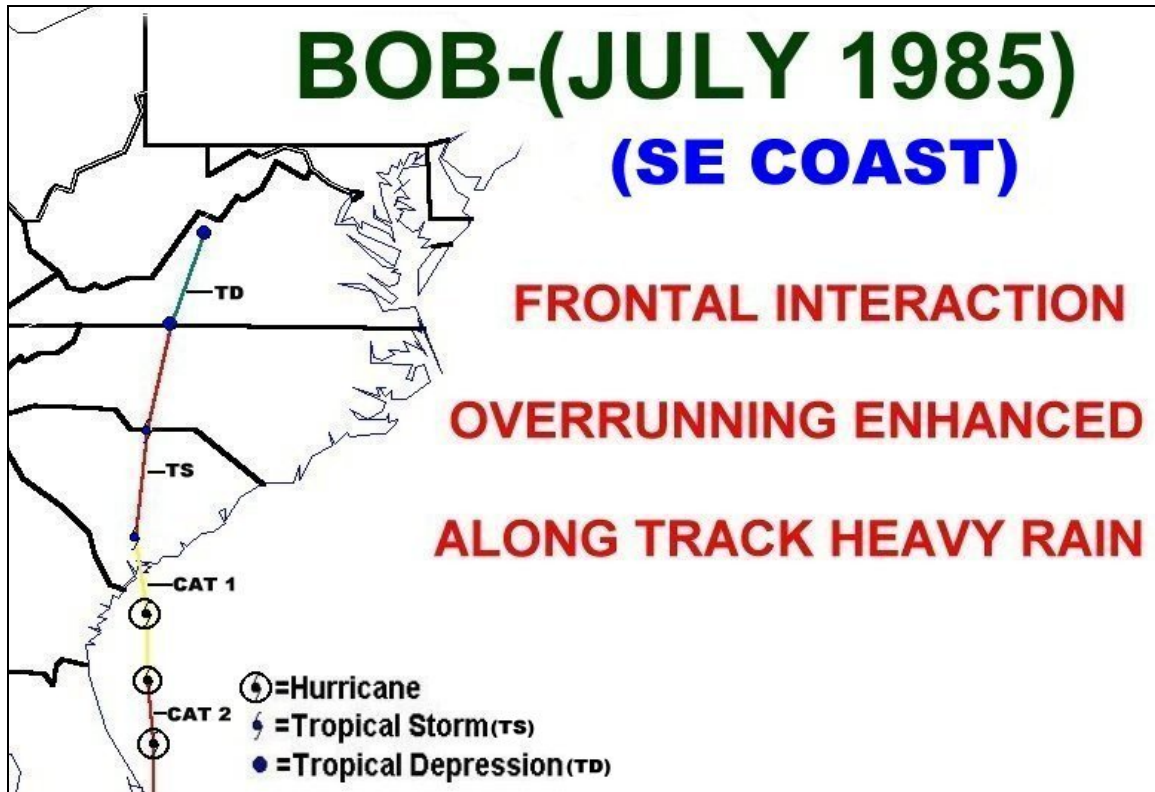


Fig. A-81: July 24-26, 1985. *BOB*.

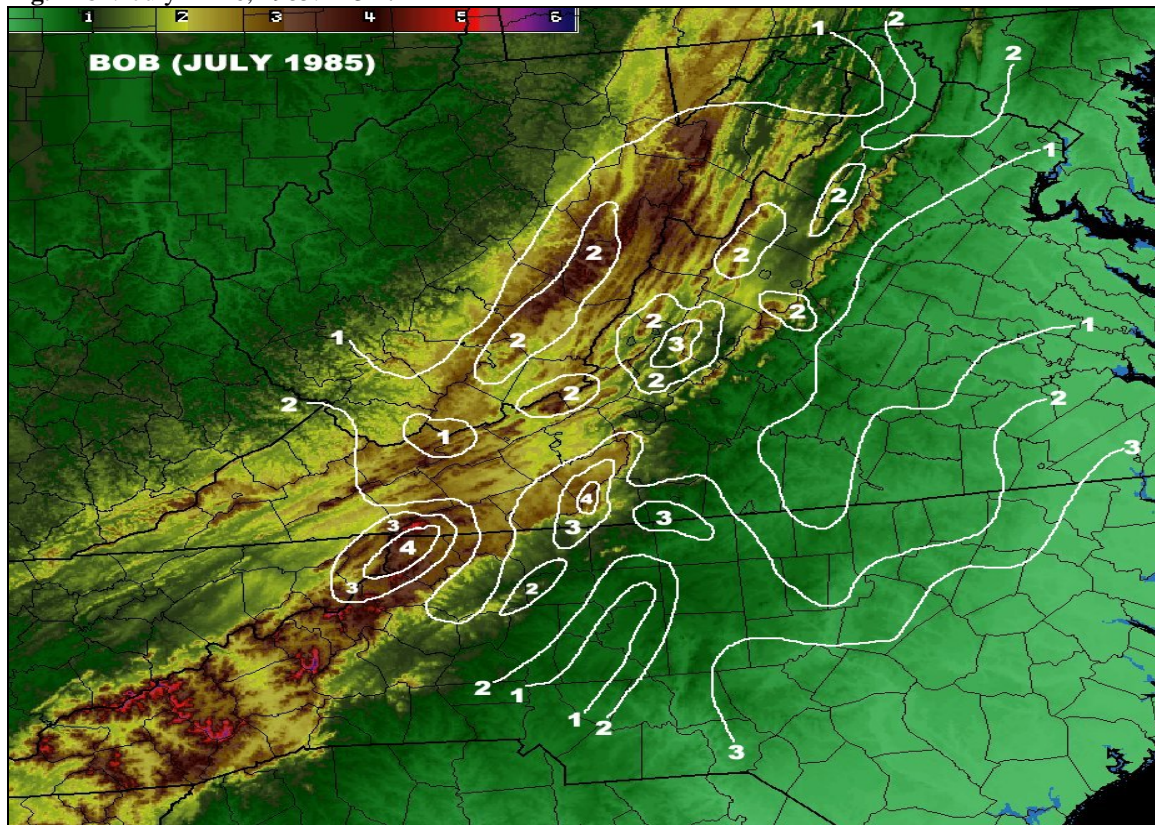


Fig. A-82: Bob rainfall in inches (white contours), July 25-26, 1985, overlaid on terrain (k ft).

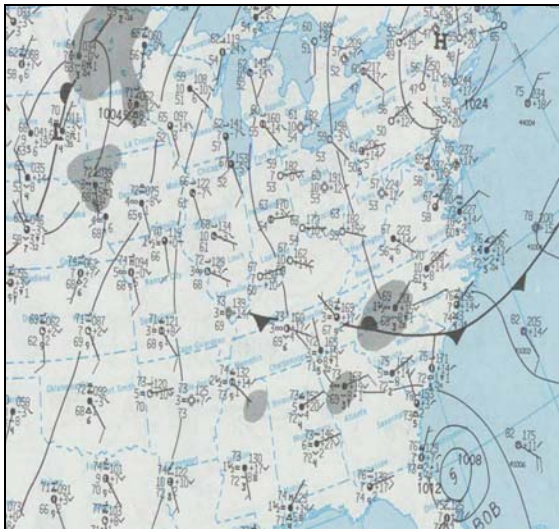


Fig. A-83: Observed standard station plot (4 mb contours), precip. (shaded), 12 UTC, July 24, 1985.

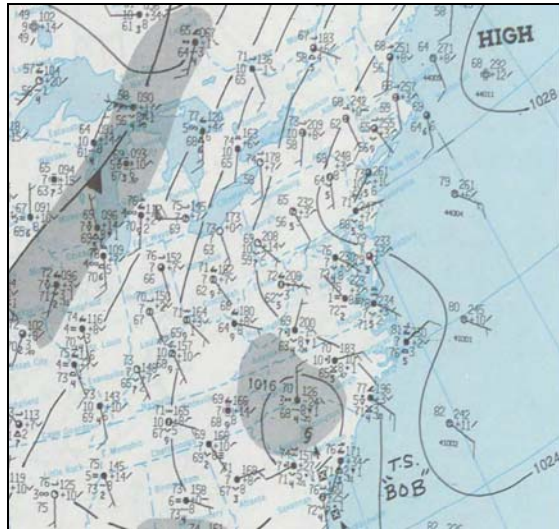


Fig. A-84: Observed standard station plot (4 mb contours), precip. (shaded), 12 UTC, July 25, 1985.

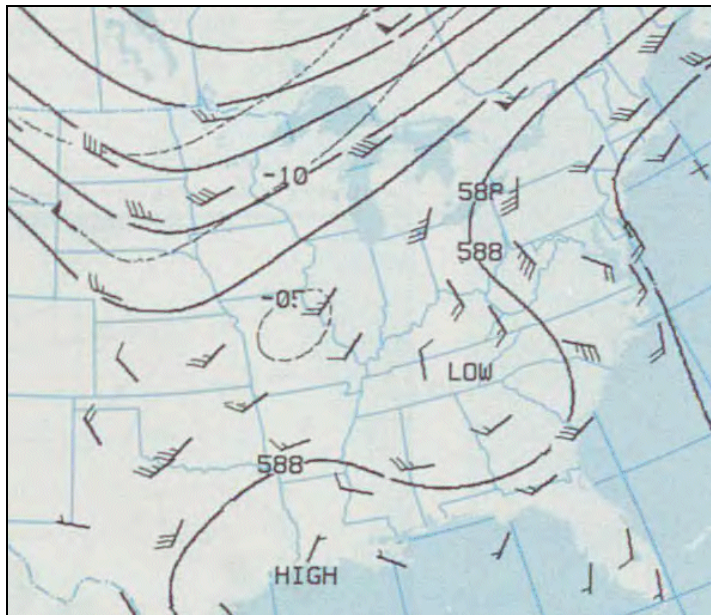


Fig. A-85: Observed 500 mb chart (60 m contours), winds (kts), temperatures (C), 12 UTC, July 25, 1985.

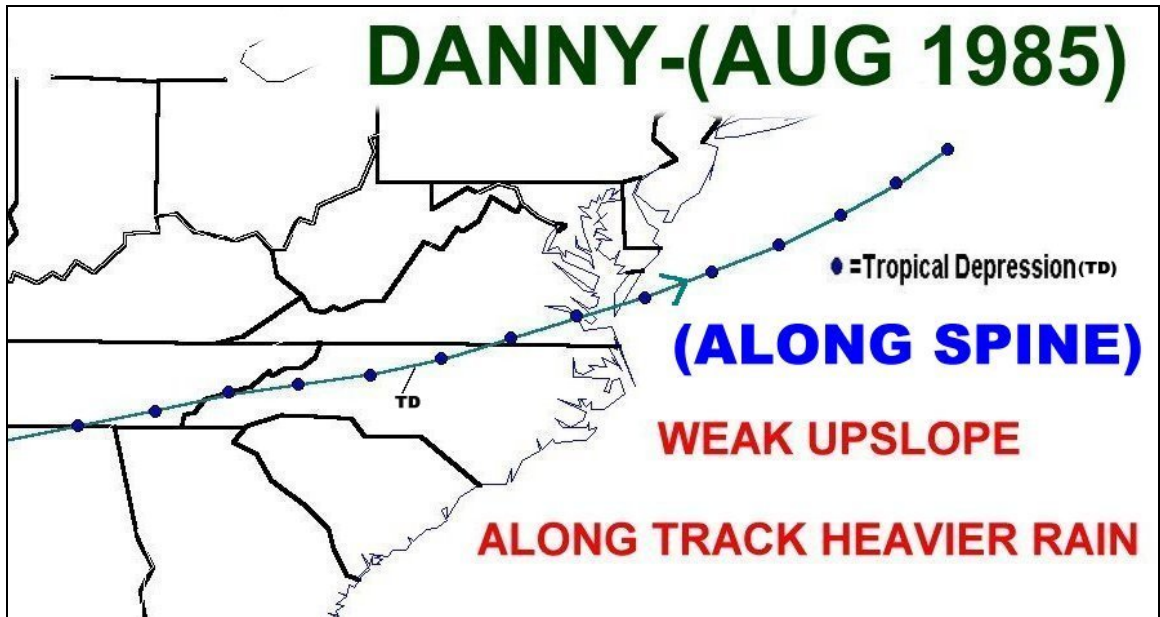


Fig. A-86: August 17-20, 1985. *DANNY*.

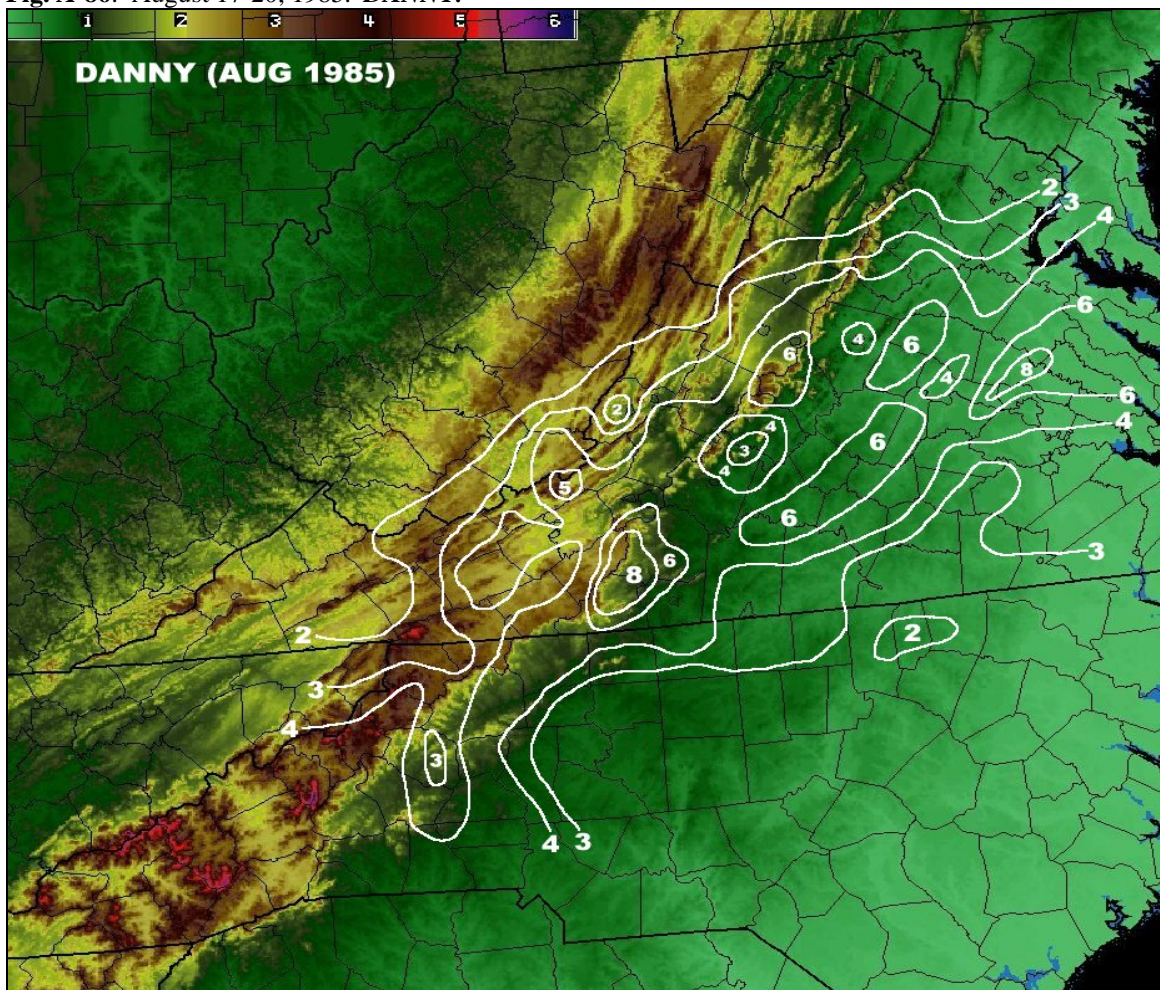


Fig. A-87: Danny rainfall in inches (white contours), August 18-19, 1985, overlaid on terrain (k ft).

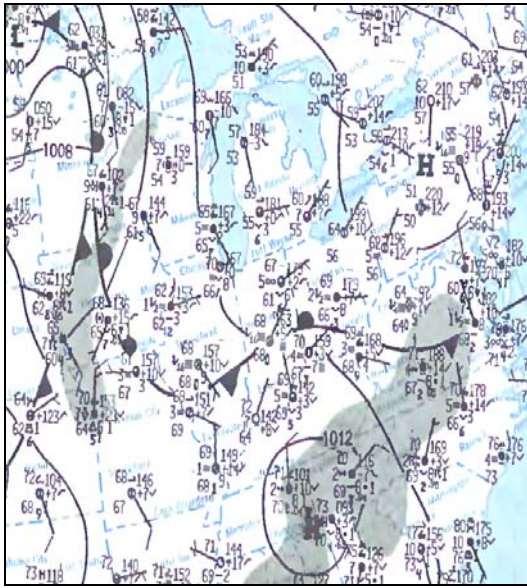


Fig. A-88: Observed standard station plot (4 mb contours), precip. (shaded), 12 UTC, August 17, 1985.

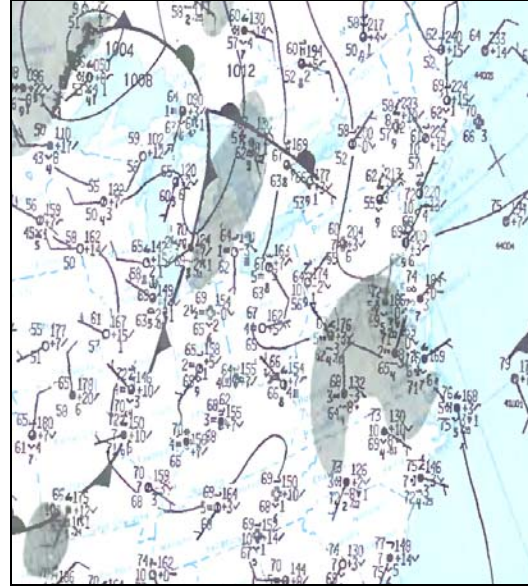


Fig. A-89: Observed standard station plot (4 mb contours), precip. (shaded), 12 UTC, August 18, 1985.

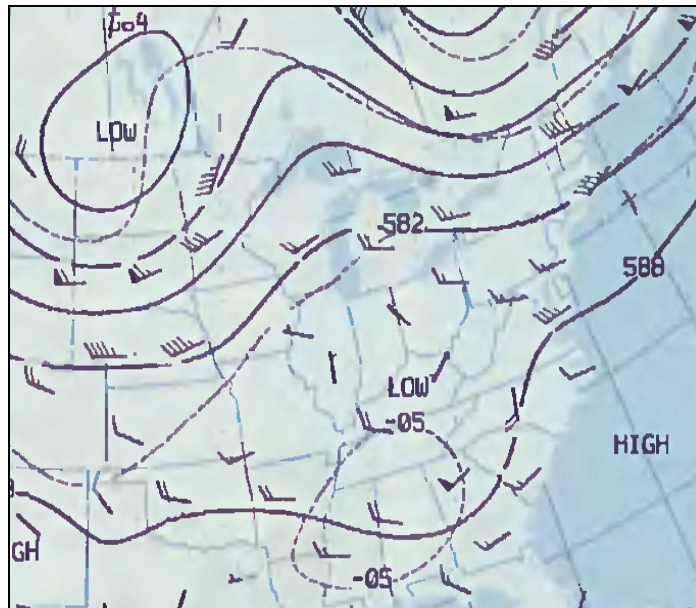


Fig. A-90: Observed 500 mb chart (60 m contours), winds (kts), temperatures (C), 12 UTC, August 17, 1985.

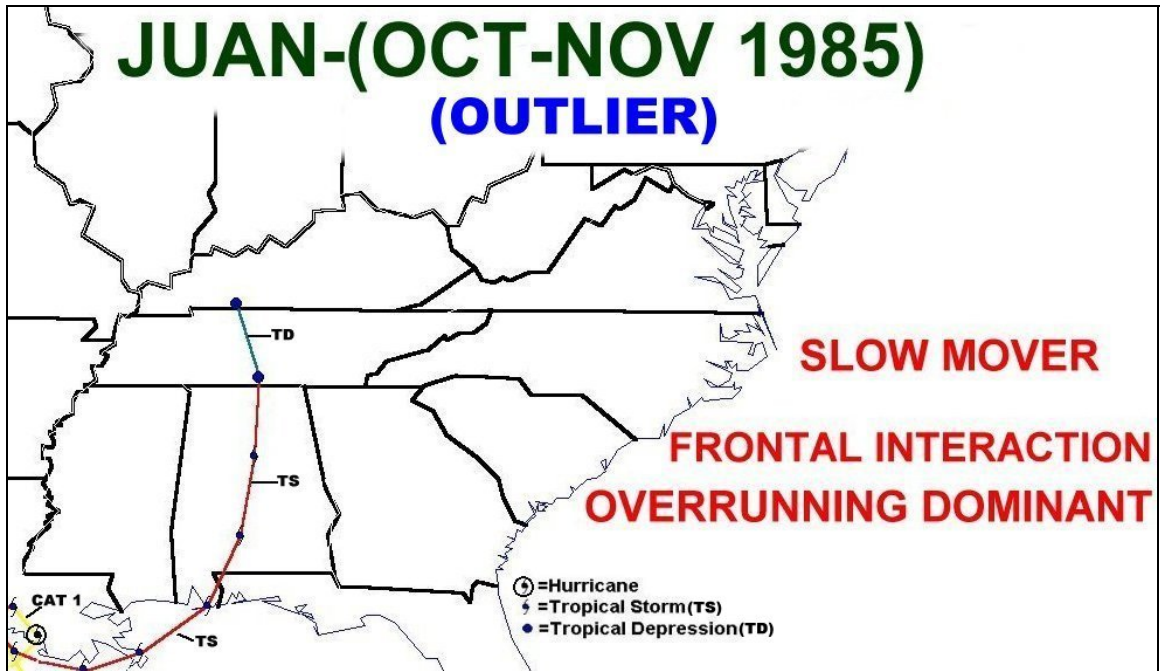


Fig. A-91: October 28, 1985- November 2, 1985. *JUAN*.

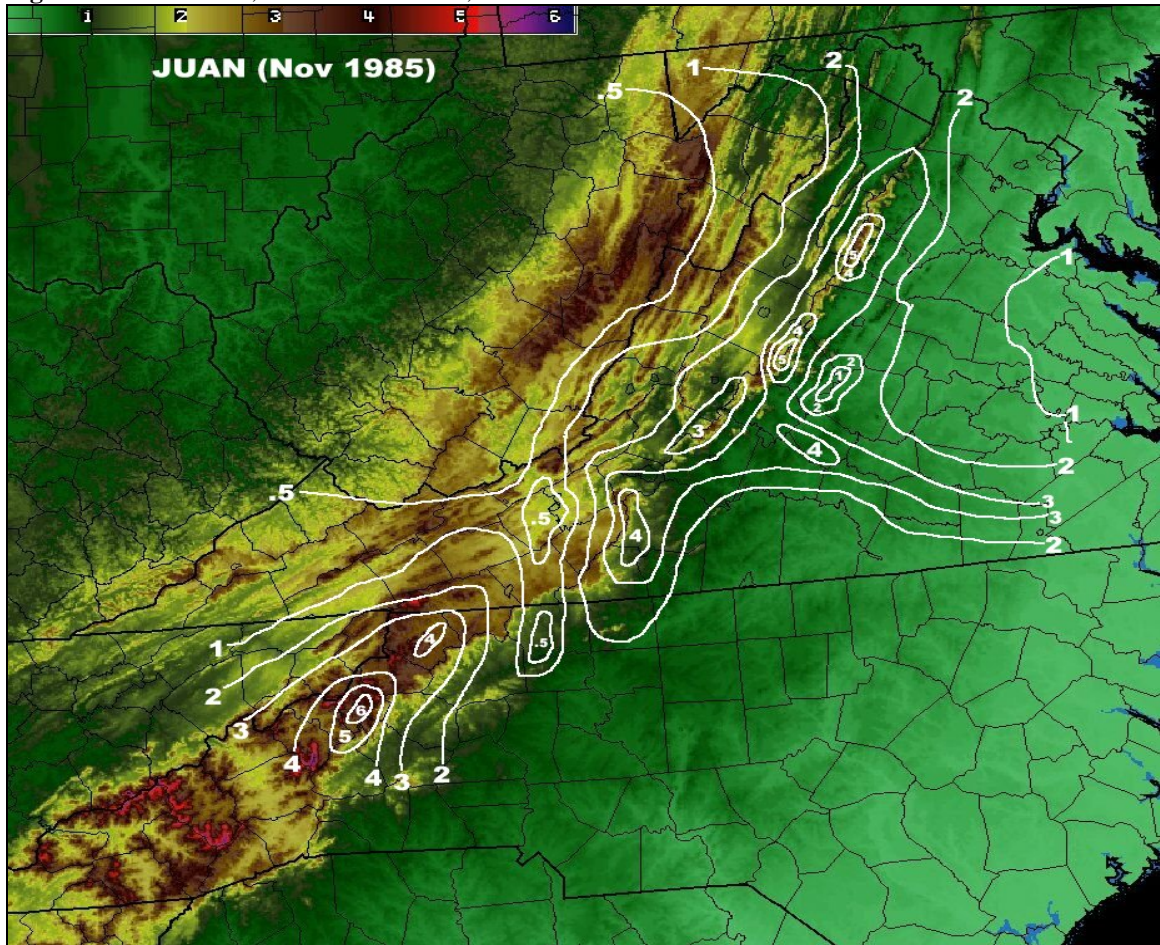


Fig. A-92: Juan rainfall in inches (white contours), November 1-2, 1985, overlaid on terrain (k ft).

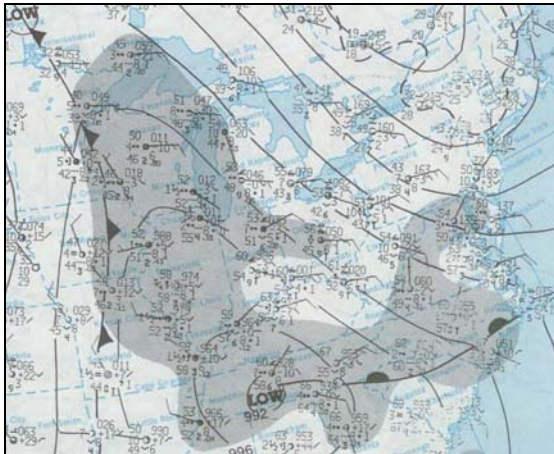


Fig. A-93: Observed standard station plot (4 mb contours), precipitation (shaded), 12 UTC, November 1, 1985.



Fig. A-94: Observed standard station plot (4 mb contours), precipitation (shaded), 12 UTC, November 2, 1985.

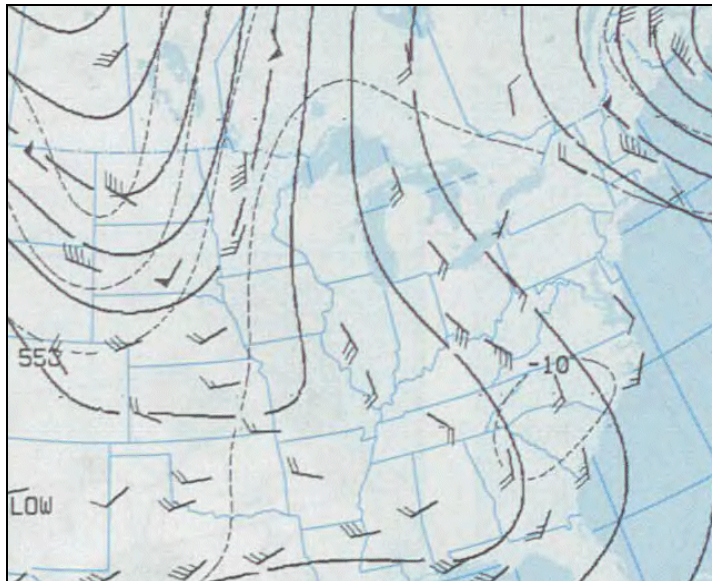


Fig. A-95: Observed 500 mb chart (60 m contours), winds (kts), temperatures (C), 12 UTC, Nov. 1, 1985.



Fig. A-96: August 28-29, 1988. *CHRIS*.

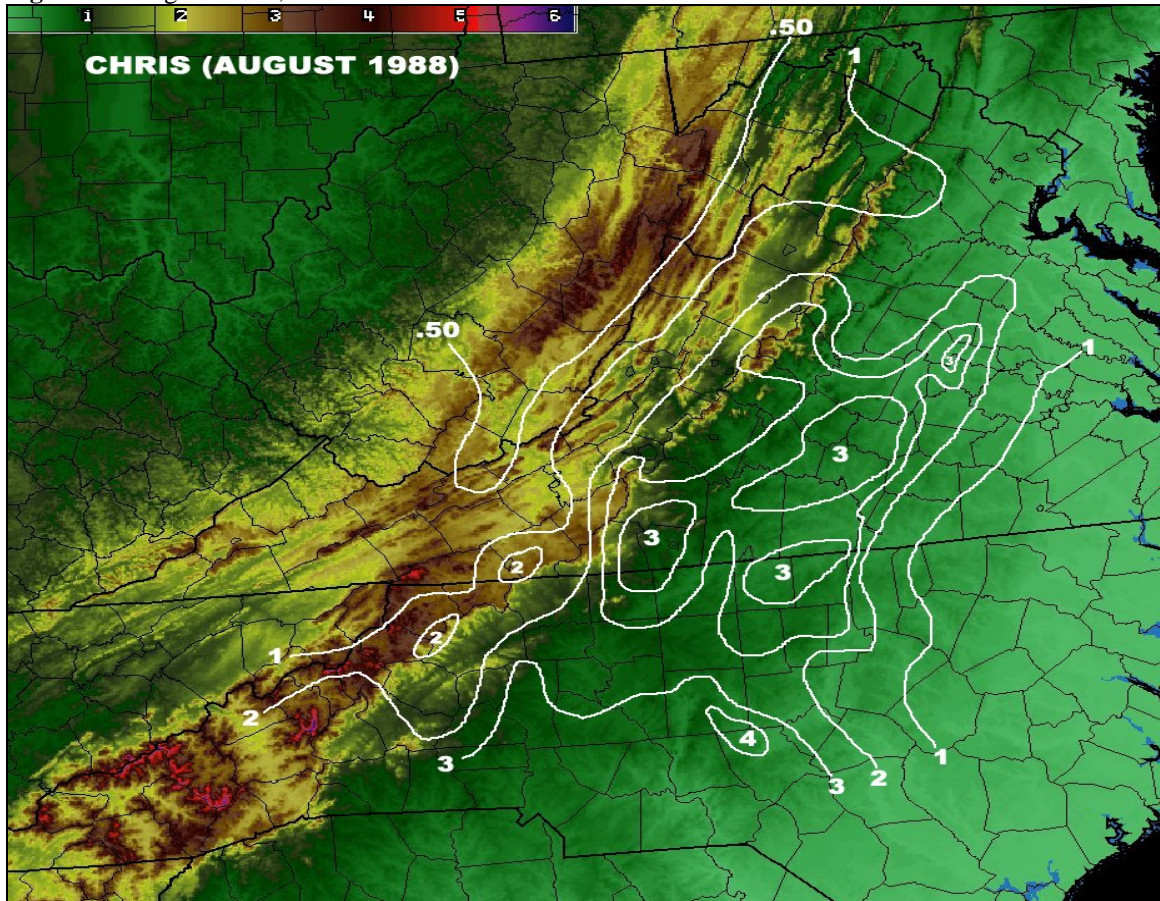


Fig. A-97: Chris rainfall in inches (white contours), August 28-29, 1988, overlaid on terrain (k ft).

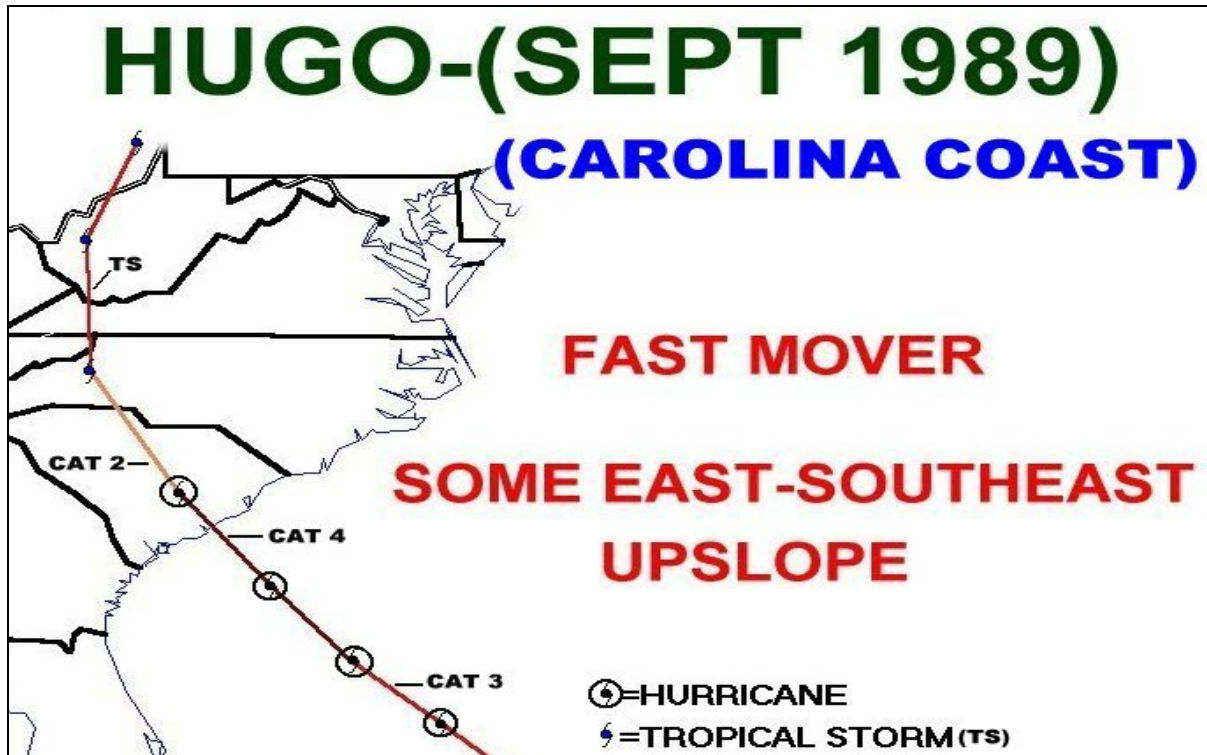


Fig. A-101: September 21-23, 1989. *HUGO*.

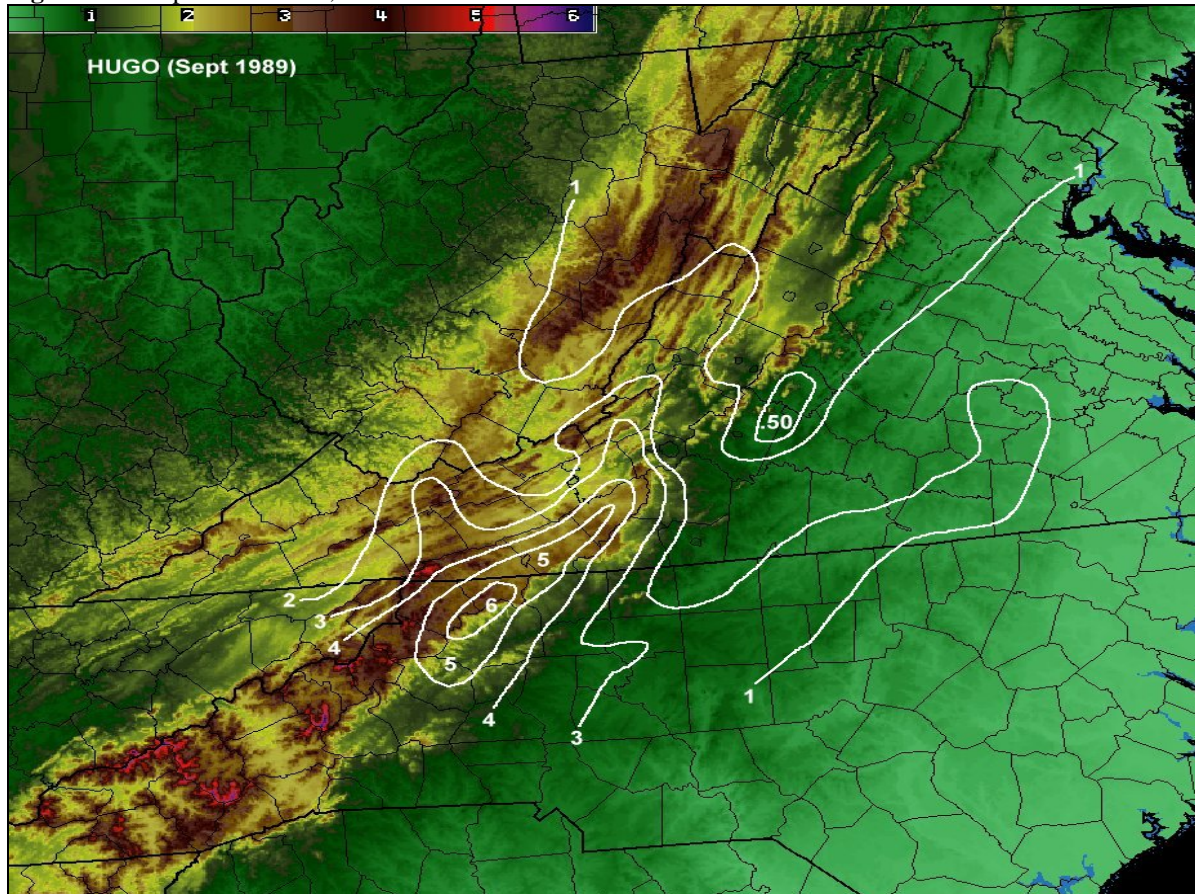


Fig. A-102: Hugo rainfall in inches (white contours), September 21-22, 1989, overlaid on terrain (k ft).

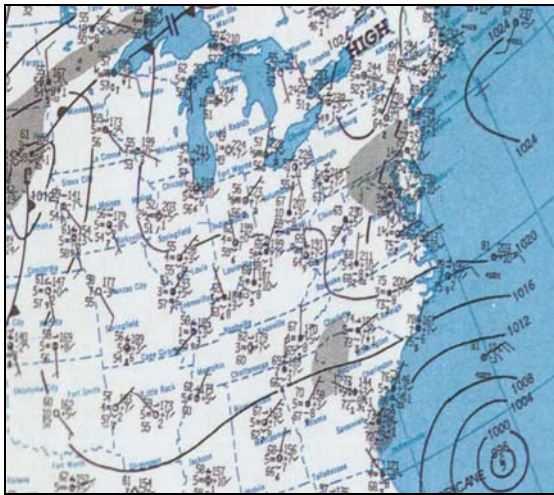


Fig. A-103: Observed standard station plot (4 mb contours), precip. (shaded), 12 UTC, September 21, 1989.

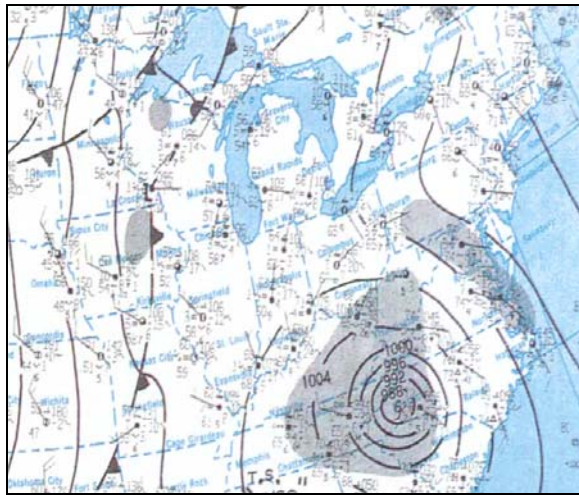


Fig. A-104: Observed standard station plot (4 mb contours), precipitation (shaded), 12 UTC, September 22, 1989.

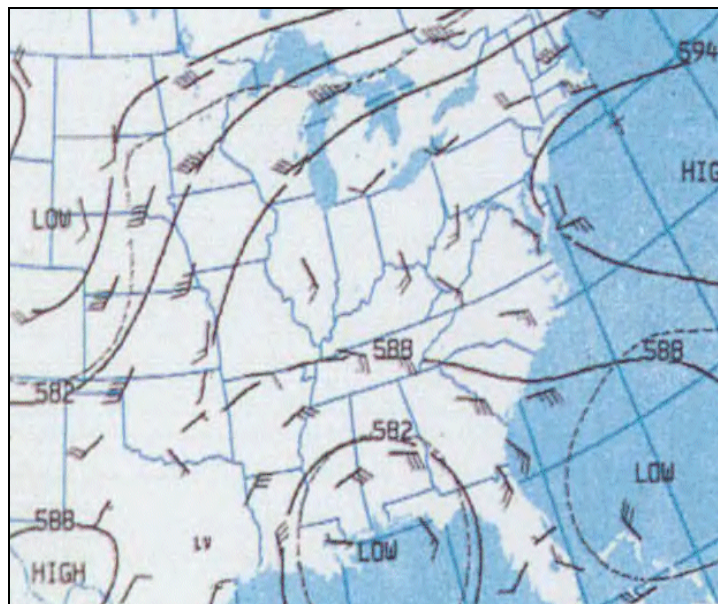


Fig. A-105: Observed 500 mb chart (60 m contours), winds (kts), temperatures (C), 12 UTC, September 21, 1989.

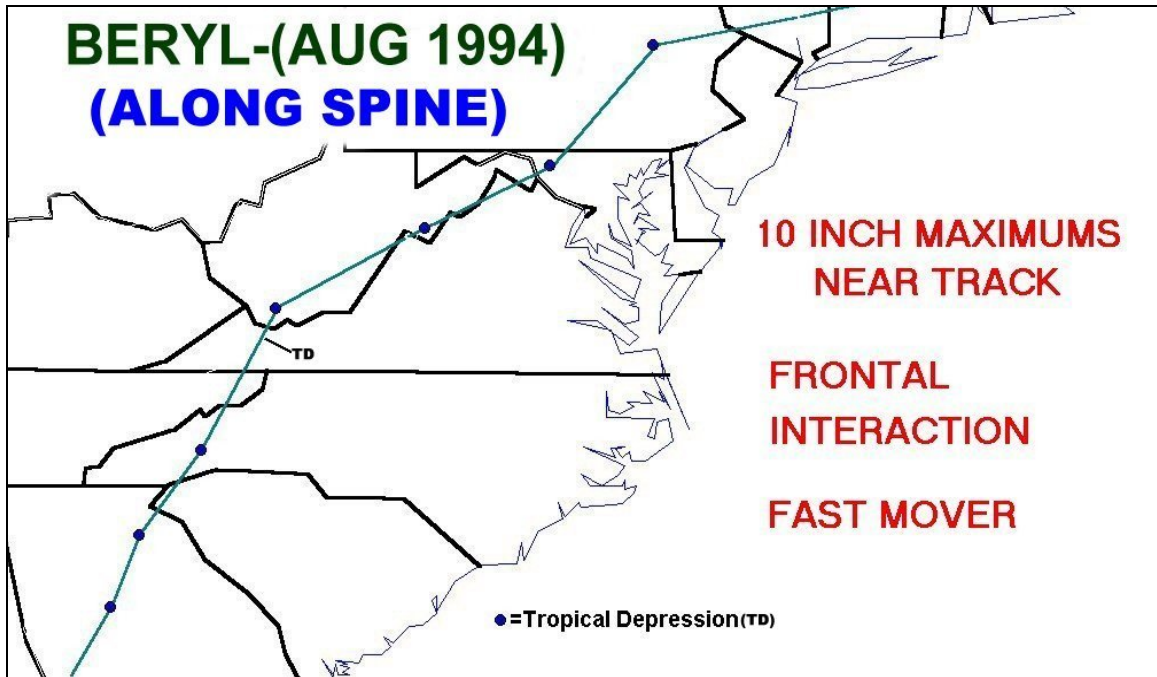


Fig. A-106: August 16-18, 1994. *BERYL*.

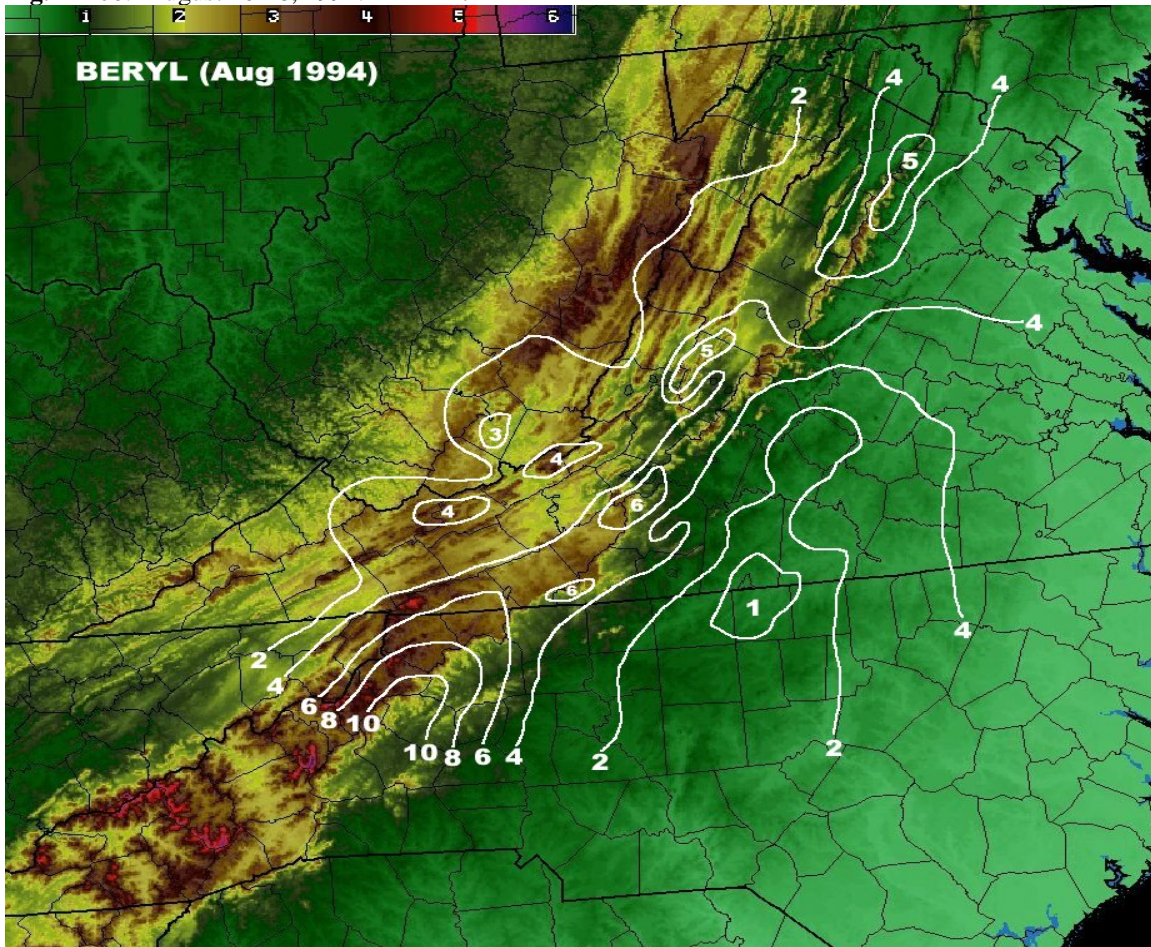


Fig. A-107: Beryl rainfall in inches (white contours), August 16-17, 1994, overlaid on terrain (k ft).

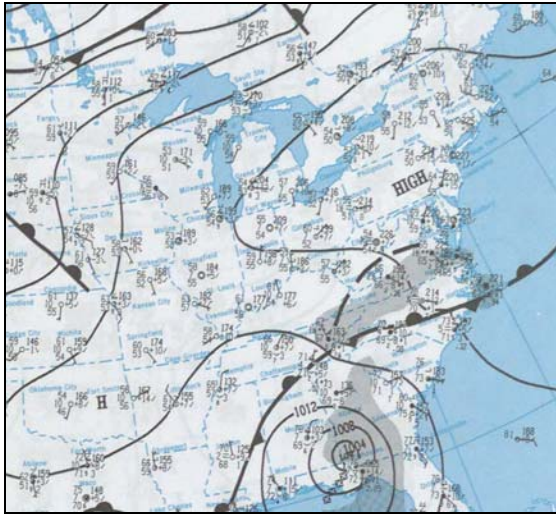


Fig. A-108: Observed standard station plot (4 mb contours), precip. (shaded), 12 UTC, August 16, 1994.

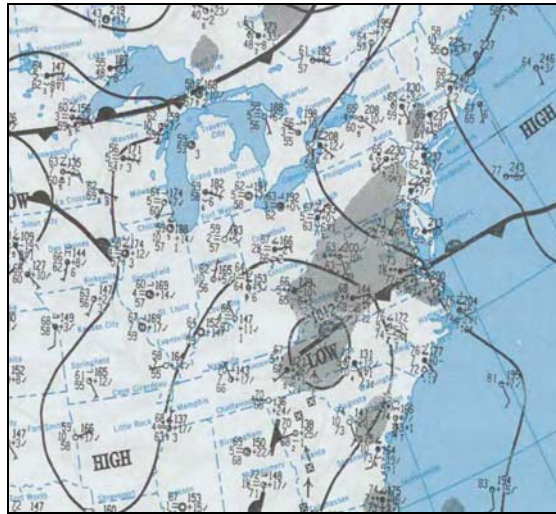


Fig. A-109: Observed standard station plot (4 mb contours), precip. (shaded), 12 UTC, August 17, 1994.

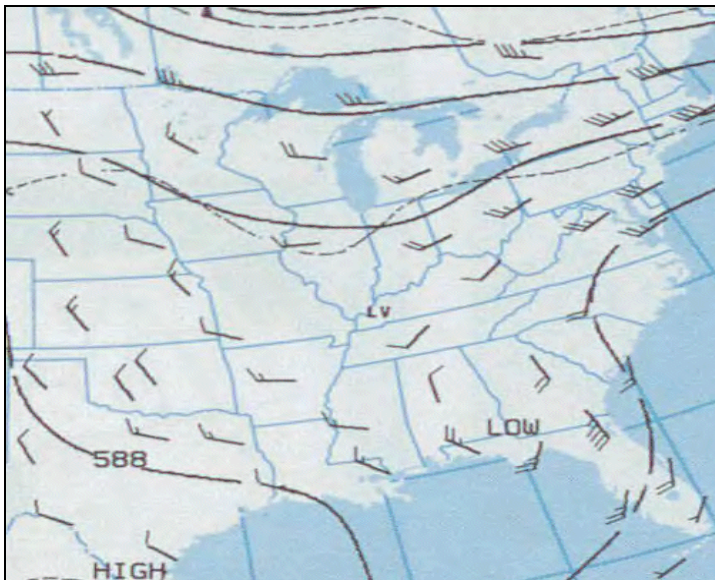


Fig. A-110: Observed 500 mb chart (60 m contours), winds (kts), temperatures (C), 12 UTC, August 16, 1994.

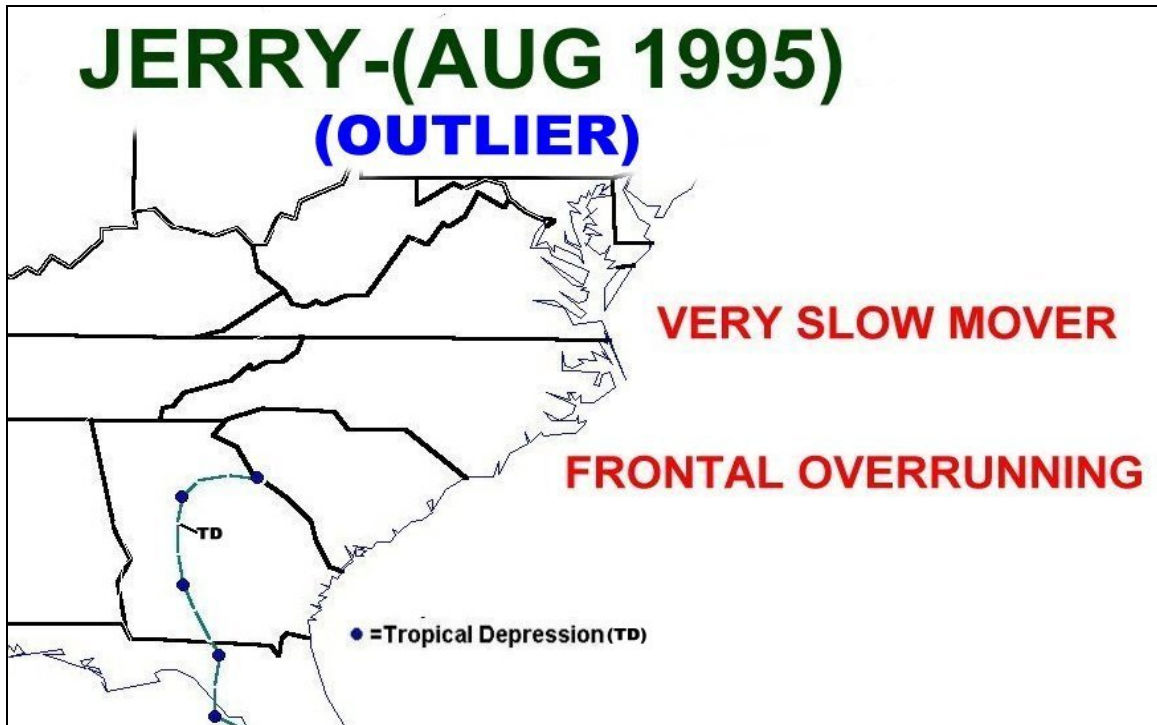


Fig. A-111: August 25-27, 1995. *JERRY*.

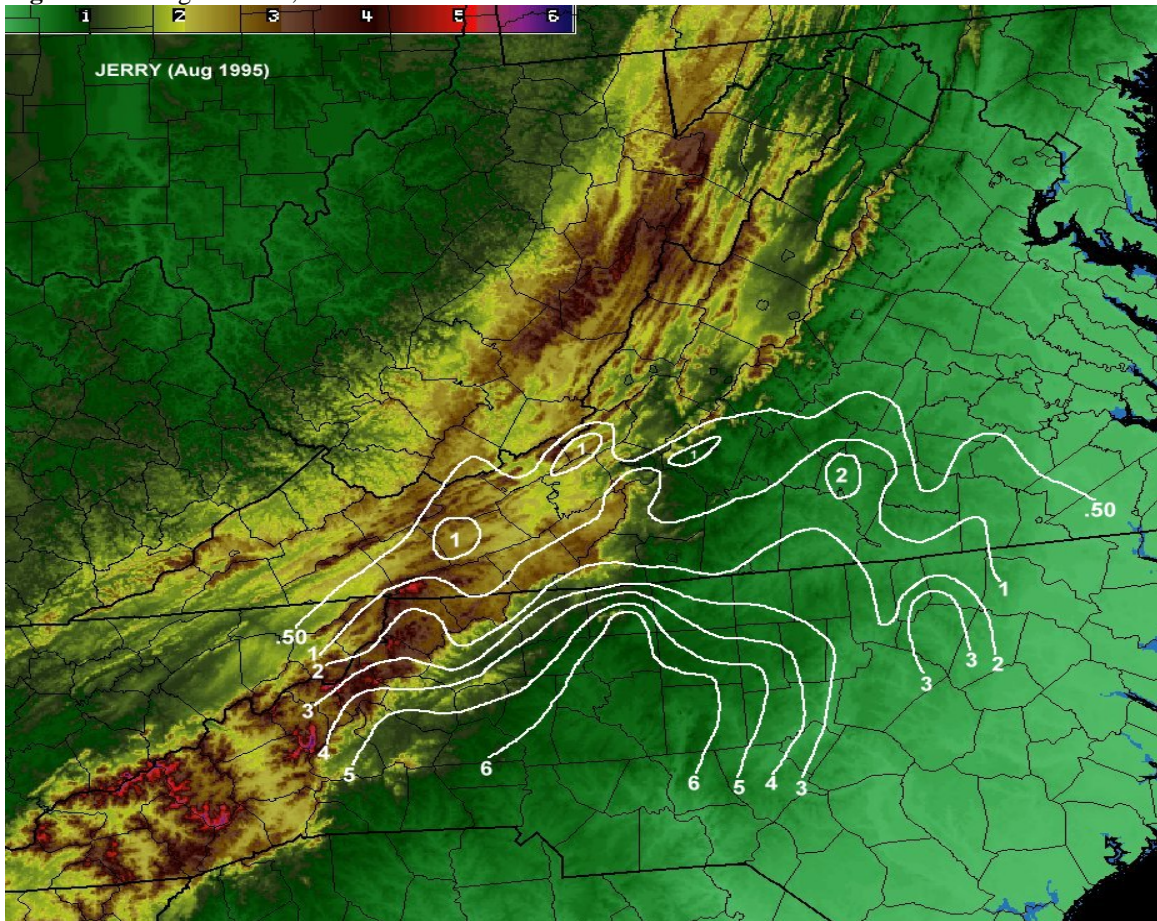


Fig. A-112: Jerry rainfall in inches (white contours), August 26-27, 1995, overlaid on terrain (k ft).

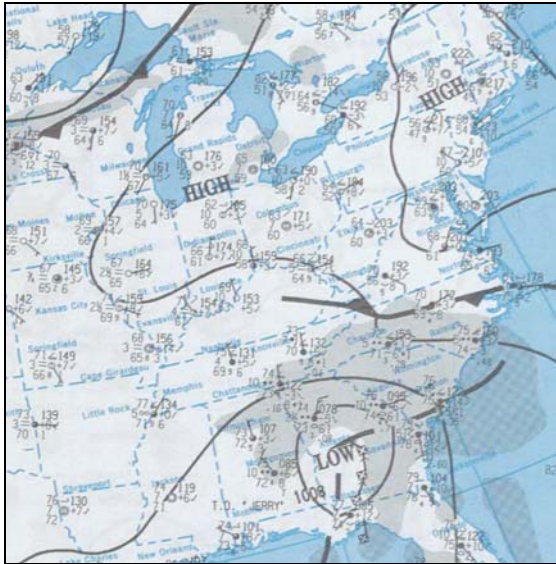


Fig. A-113: Observed standard station plot (4 mb contours), precip. (shaded), 12 UTC, August 26, 1995.

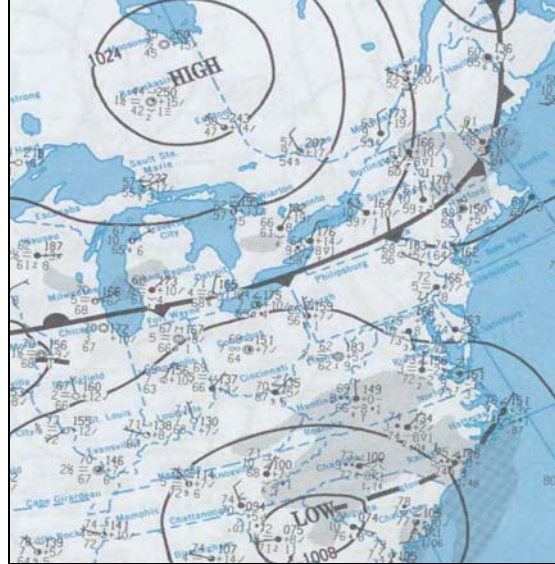


Fig. A-114: Observed standard station plot (4 mb contours), precip. (shaded), 12 UTC, August 27, 1995.

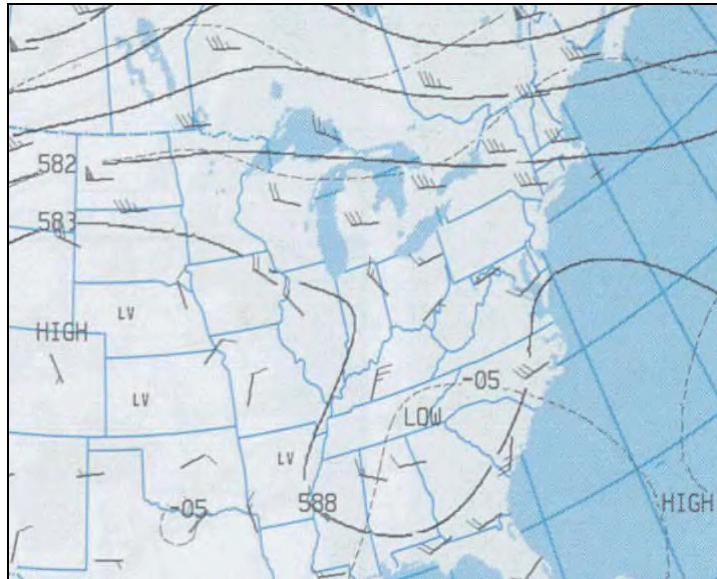


Fig. A-115: Observed 500 mb chart (60 m contours), winds (kts), temperatures (C), 12 UTC, August 27, 1995.

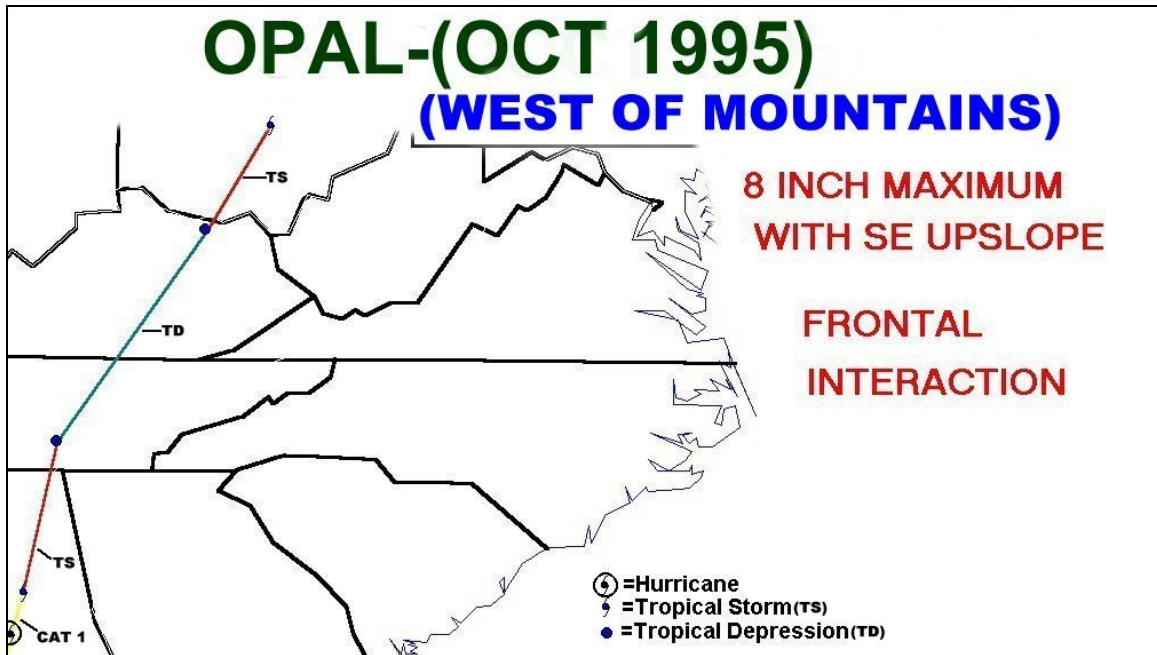


Fig. A-116: October 5-6, 1995. *OPAL*.

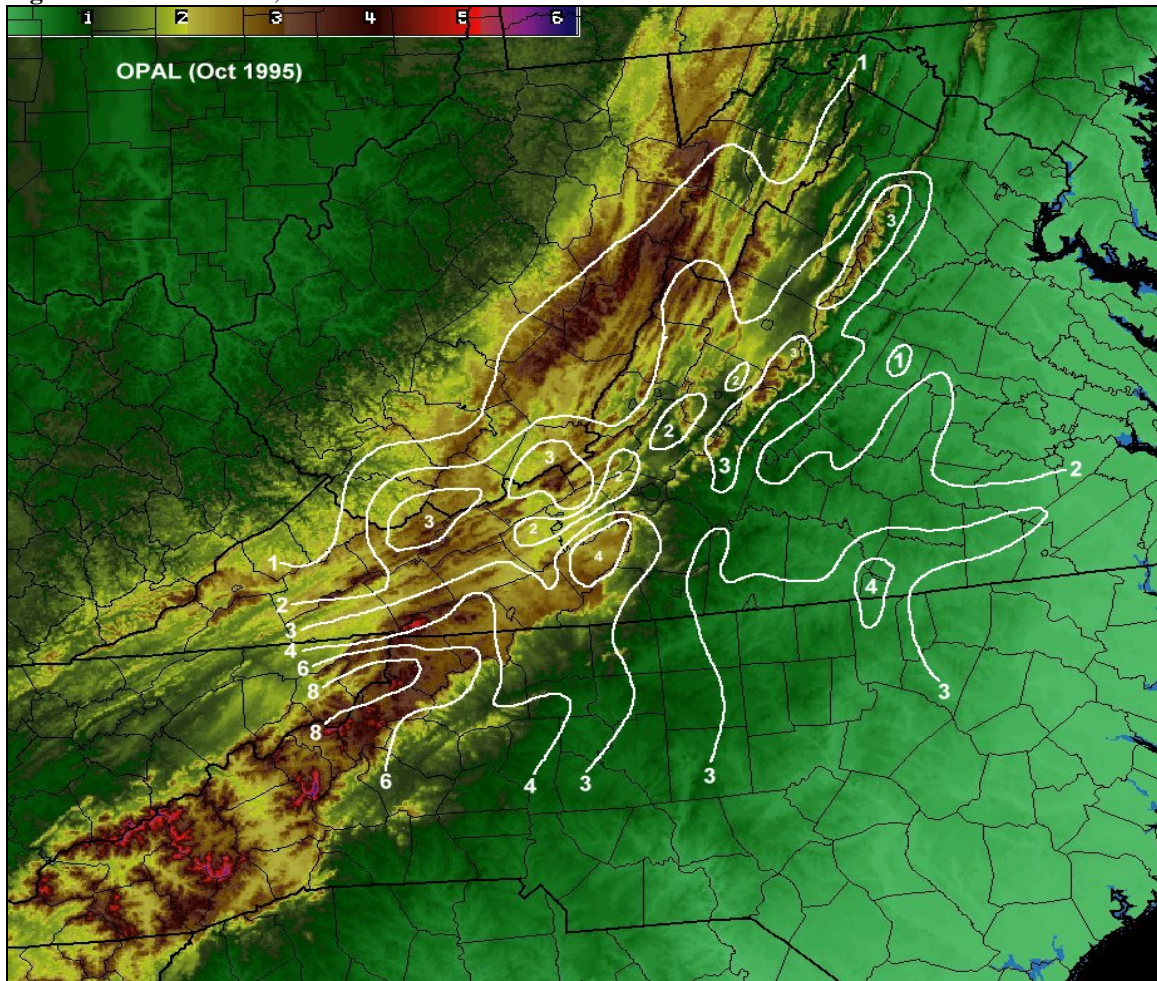


Fig. A-117: Opal rainfall in inches (white contours), October 5, 1995, overlaid on terrain (k ft).

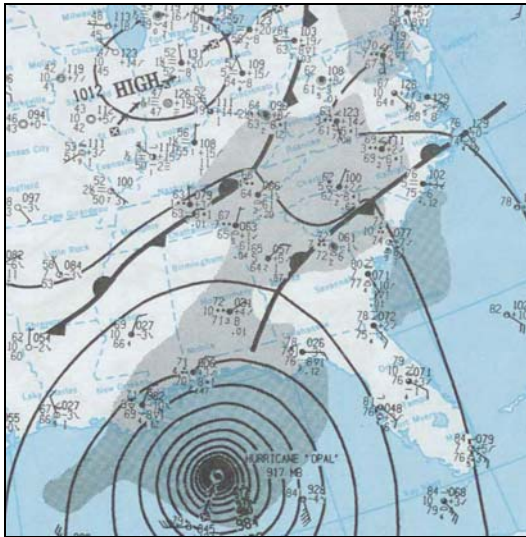


Fig. A-118: Observed standard station plot (4 mb contours), precip. (shaded), 12 UTC, October 4, 1995. .

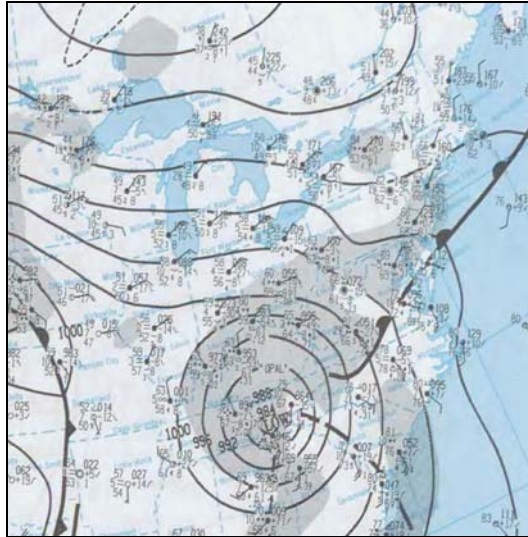


Fig. A-119: Observed standard station plot (4 mb contours), precip. (shaded), 12 UTC, October 5, 1995.

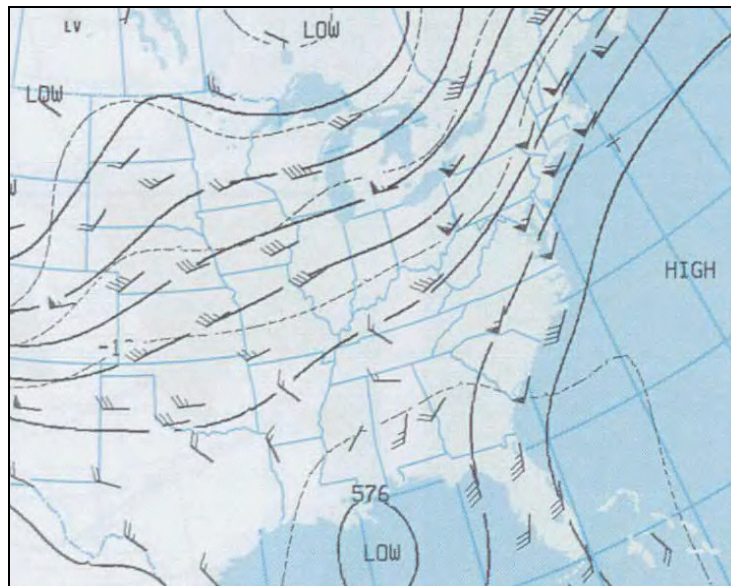


Fig. A-120: Observed 500 mb chart (60 m contours), winds (kts), temperatures (C), 12 UTC, Oct. 4, 1995.

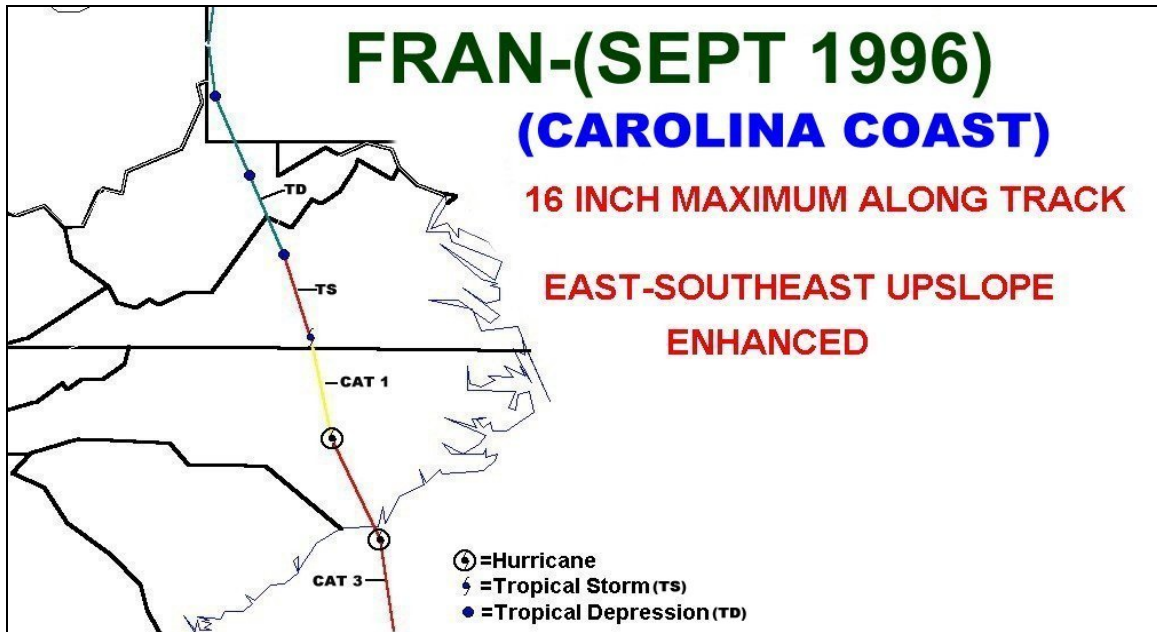


Fig. A-121: September 4-6, 1996. *FRAN*.

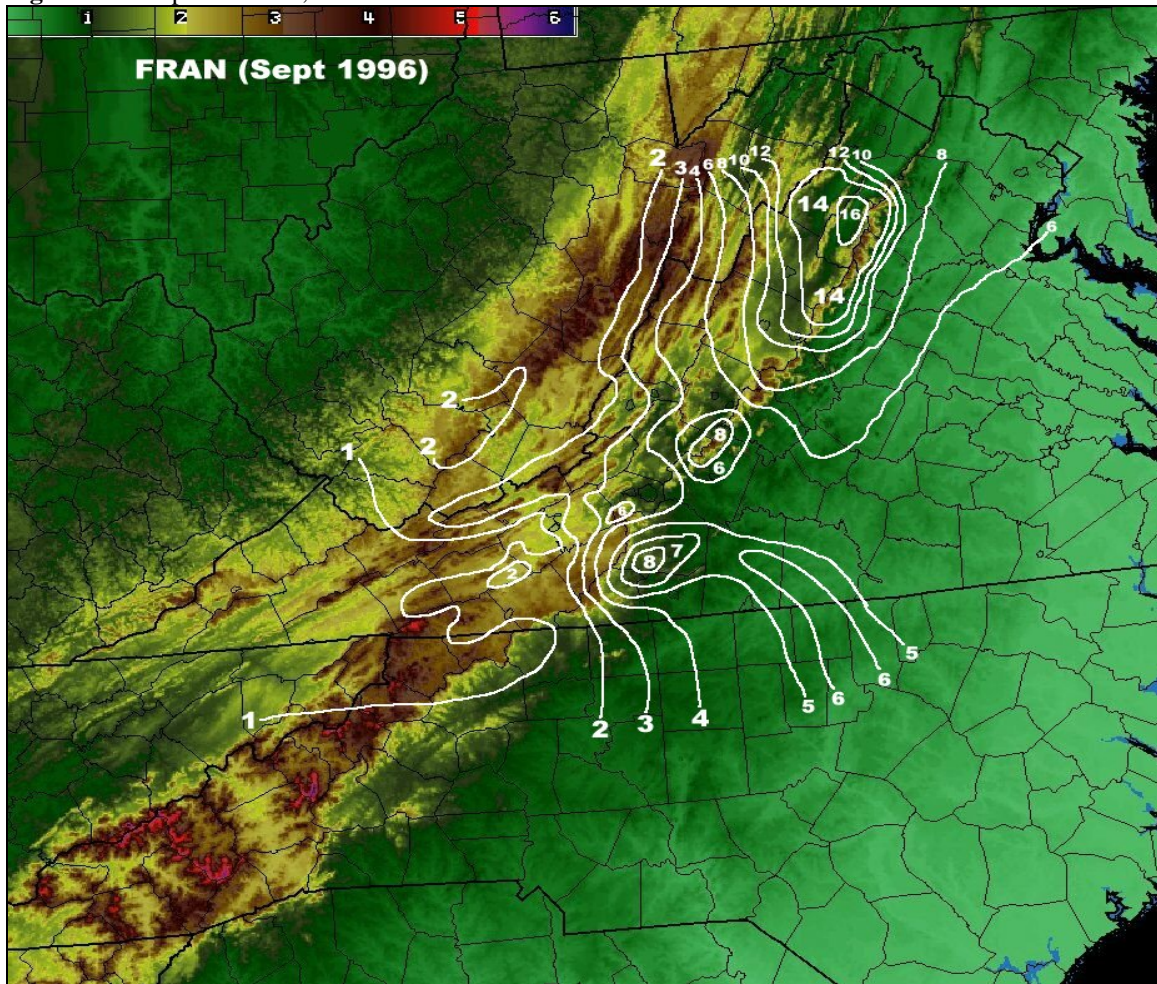


Fig. A-122: Fran rainfall in inches (white contours), September 5-6, 1996, overlaid on terrain (k ft).

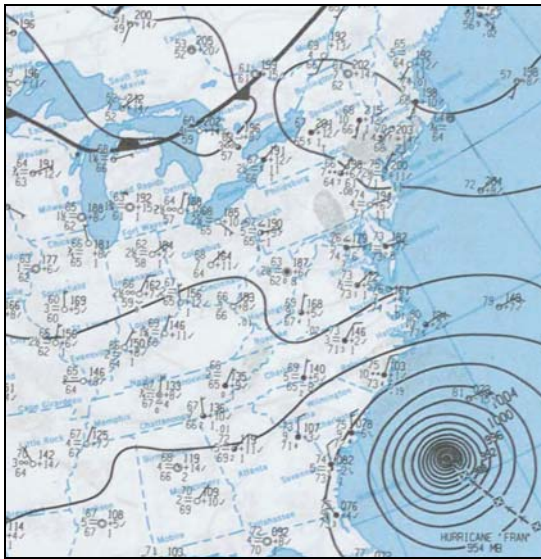


Fig. A-123: Observed standard station plot (4 mb contours), precip. (shaded), 12 UTC, September 5, 1996.

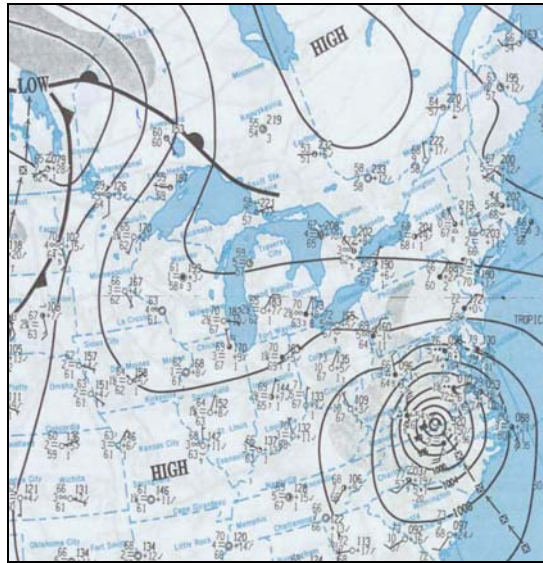


Fig. A-124: Observed standard station plot (4 mb contours), precip. (shaded), 12 UTC, September 6, 1996.

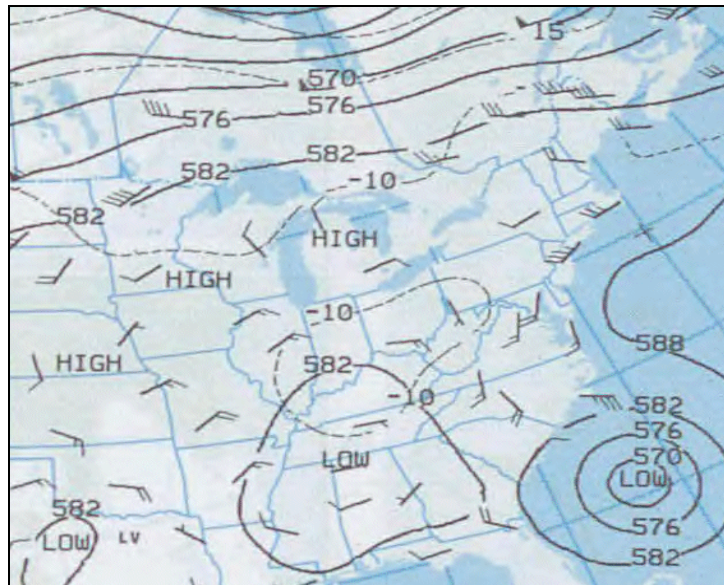


Fig. A-125: Observed 500 mb chart (60 m contours), winds (kts), temperatures (C), 12 UTC, Sept 5, 1996.

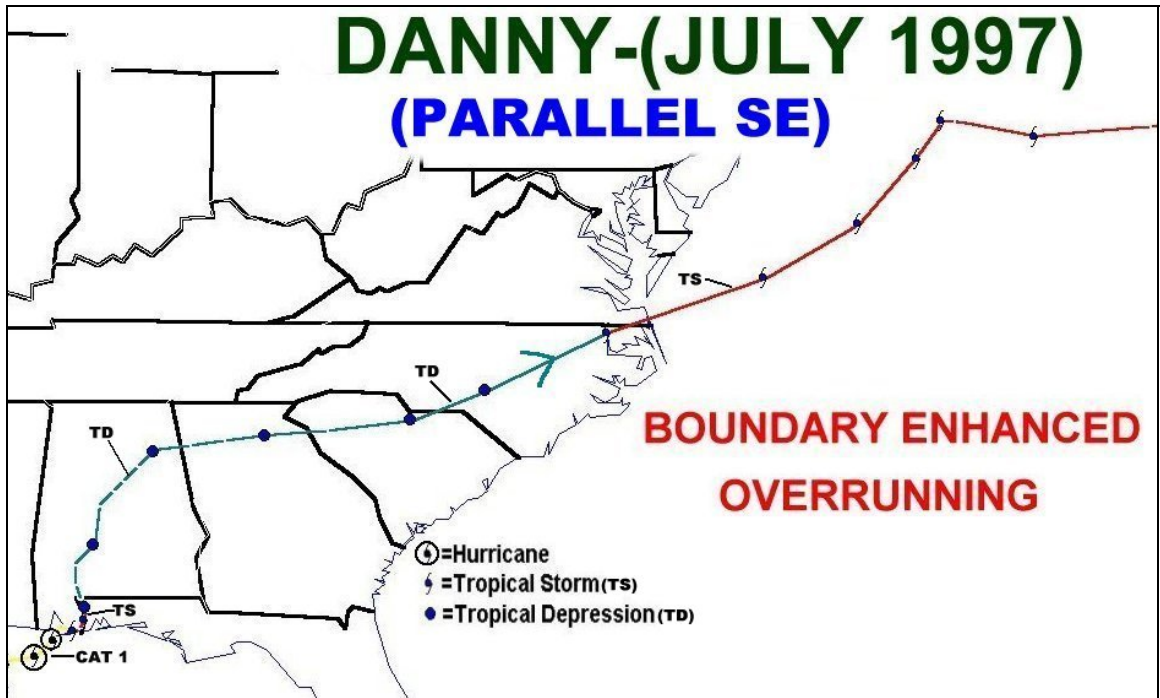


Fig. A-126: July 19-27, 1997. *DANNY*.

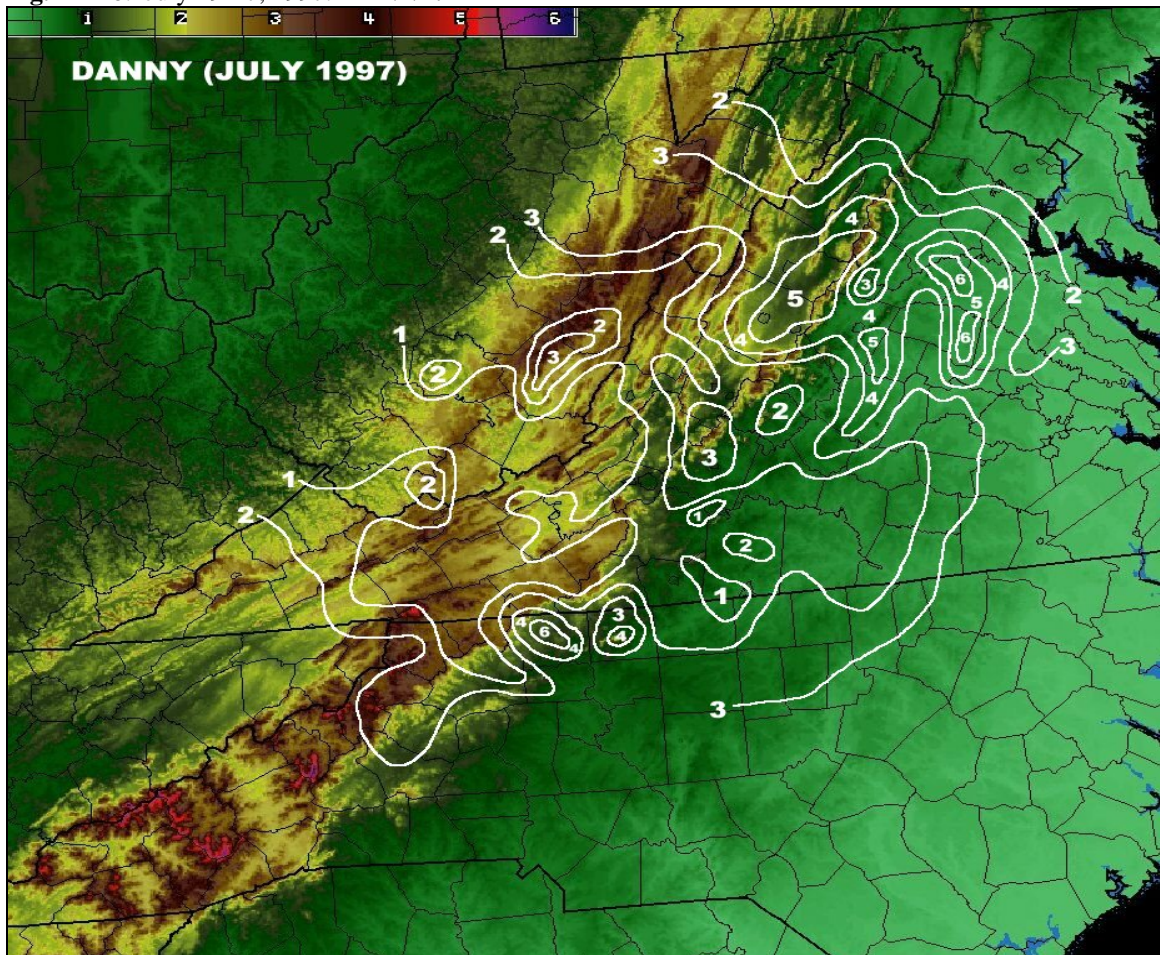


Fig. A-127: Danny rainfall in inches (white contours), July 23-24, 1997, overlaid on terrain (k ft).

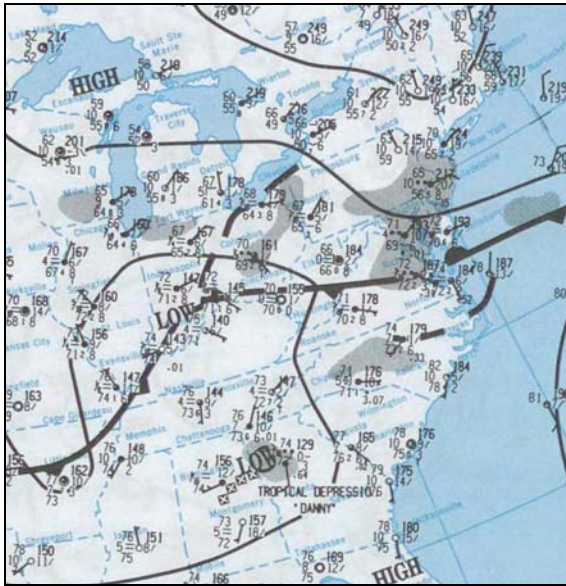


Fig. A-128: Observed standard station plot (4 mb contours), precip. (shaded), 12 UTC, July 23, 1997.

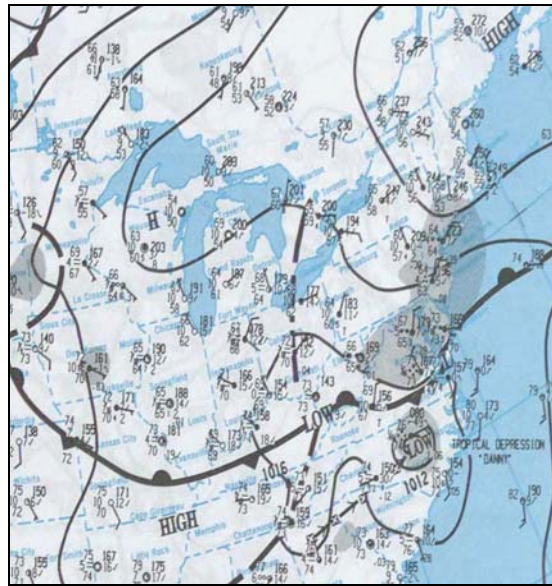


Fig. A-129: Observed standard station plot (4 mb contours), precip. (shaded), 12 UTC, July 24, 1997.

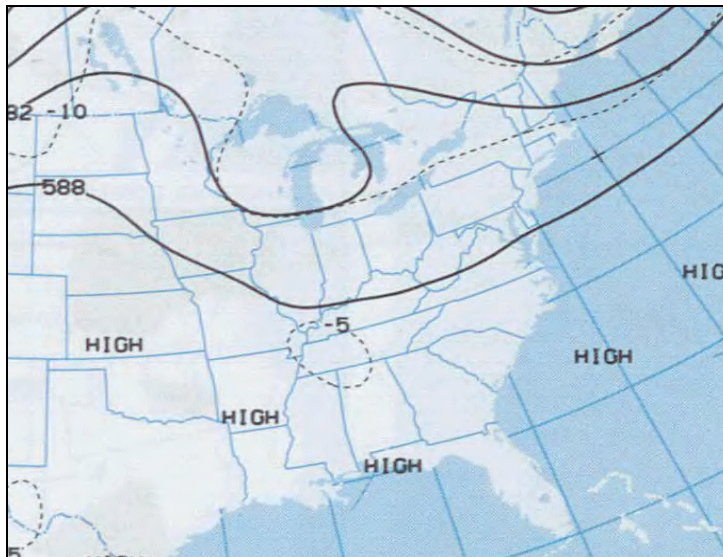


Fig. A-130: Observed 500 mb chart (60 m contours), winds (kts), temperatures (C), 12 UTC, July 23, 1997.

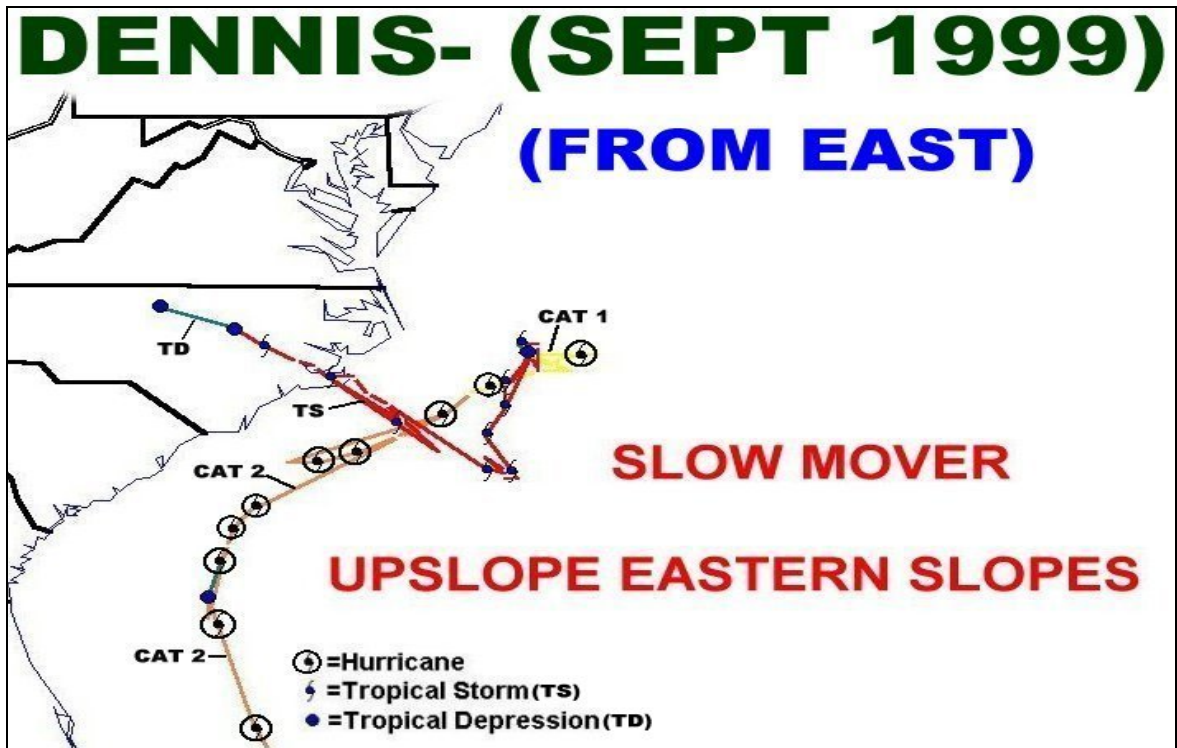


Fig. A-131: August 29-September 6, 1999. *DENNIS*.

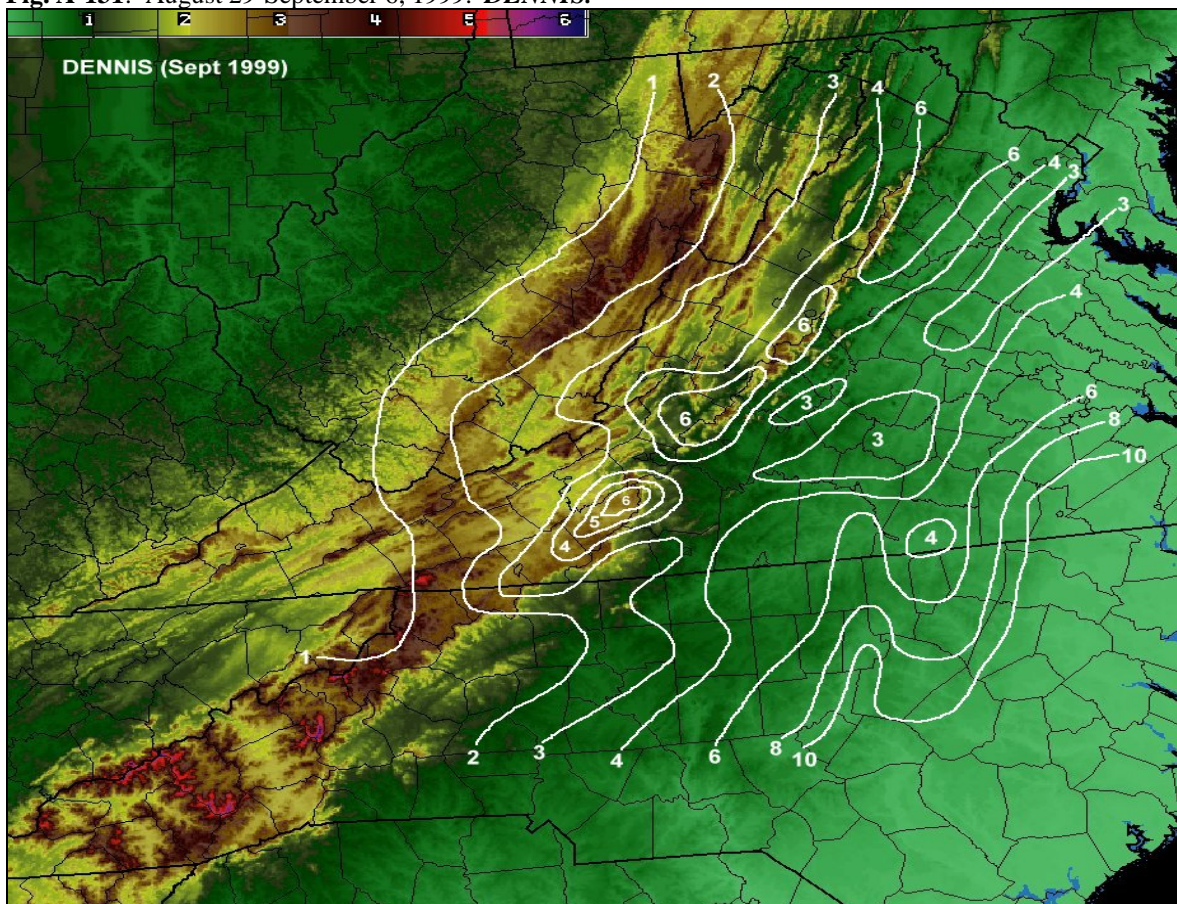


Fig. A-132: Dennis rainfall in inches (white contours), September 5-6, 1999, overlaid on terrain (k ft).

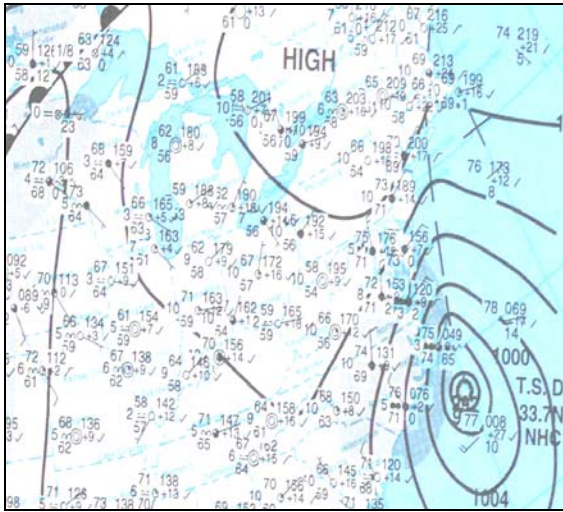


Fig. A-133: Observed standard station plot (4 mb contours), precip. (shaded), 12 UTC, September 4, 1999.

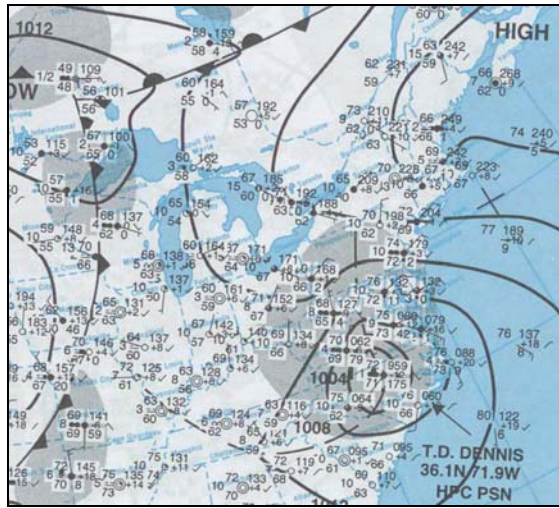


Fig. A-134: Observed Standard Station Plot, 12 (4 mb contours), precip. (shaded), 12 UTC, September 5, 1999.

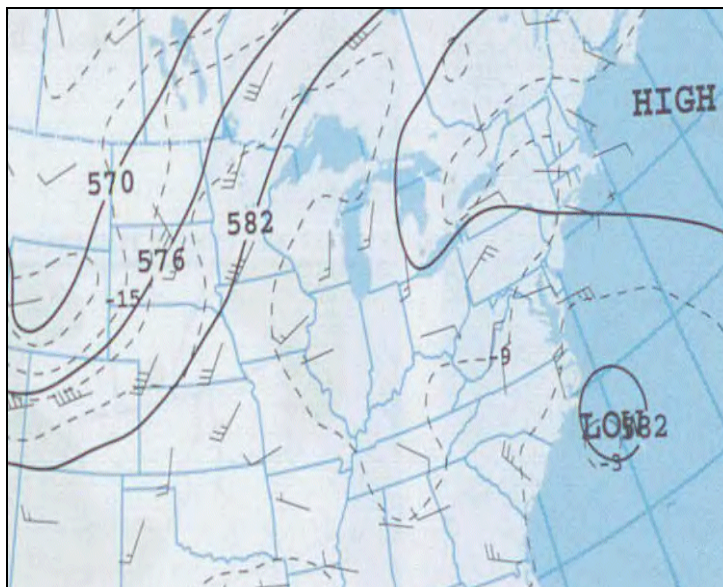


Fig. A-135: Observed 500 mb chart (60 m contours), winds (kts), temperatures (C), 12 UTC, Sept 4, 1999.

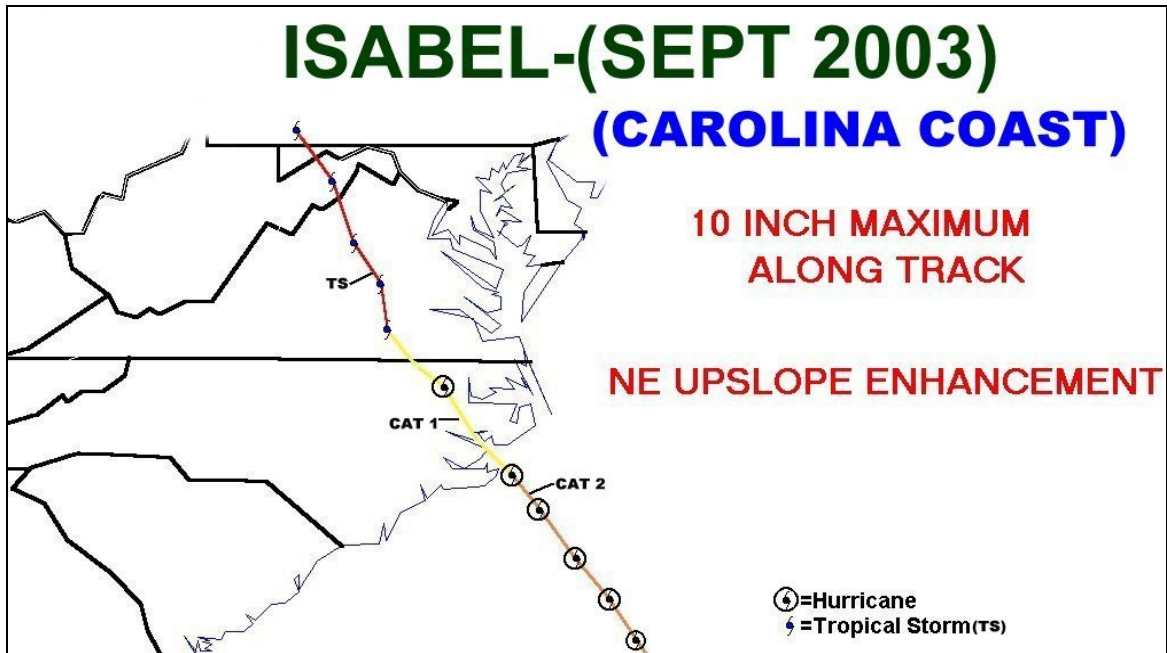


Fig. A-136: September 17-19 2003. *ISABEL*.

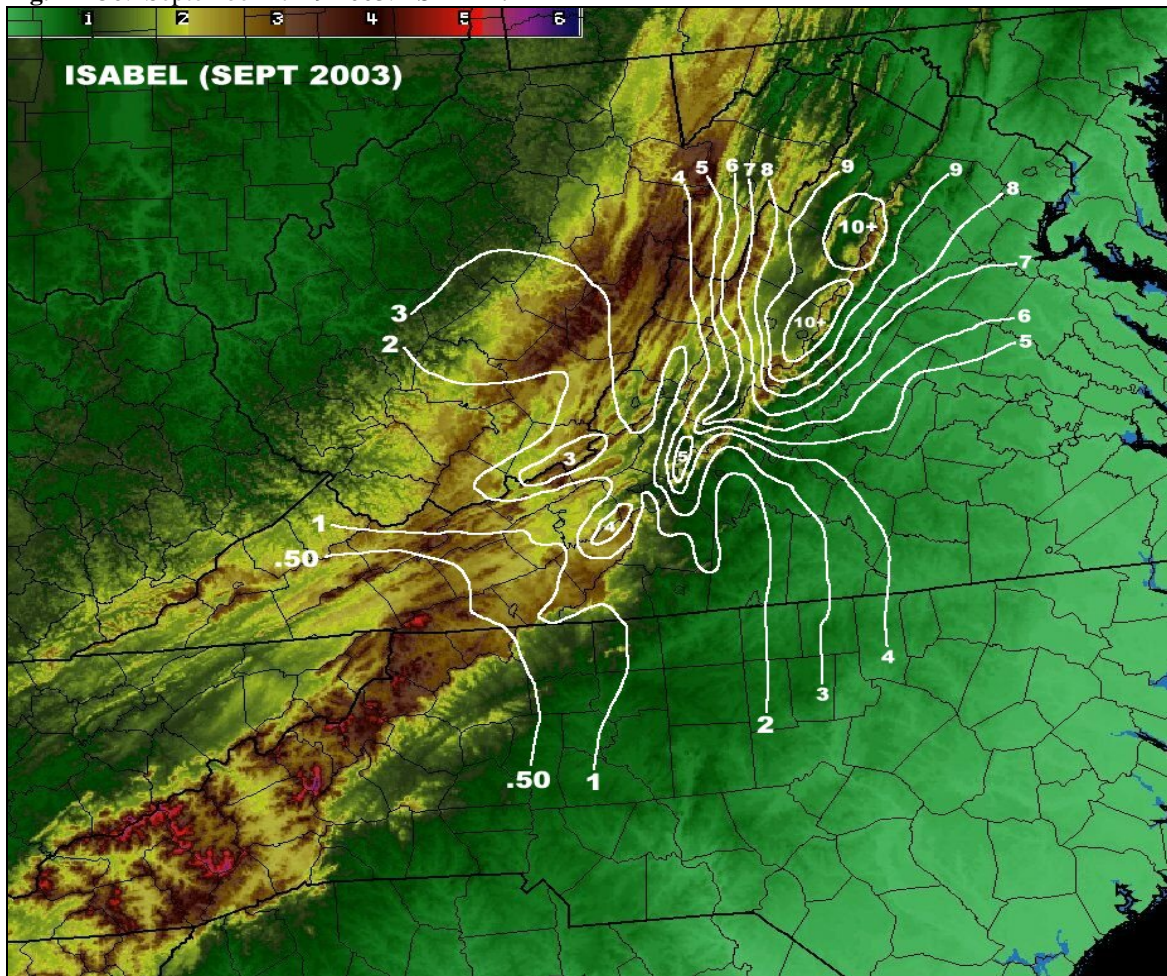


Fig. A-137: Isabel rainfall in inches (white contours), September 18, 2003, overlaid on terrain (k ft).

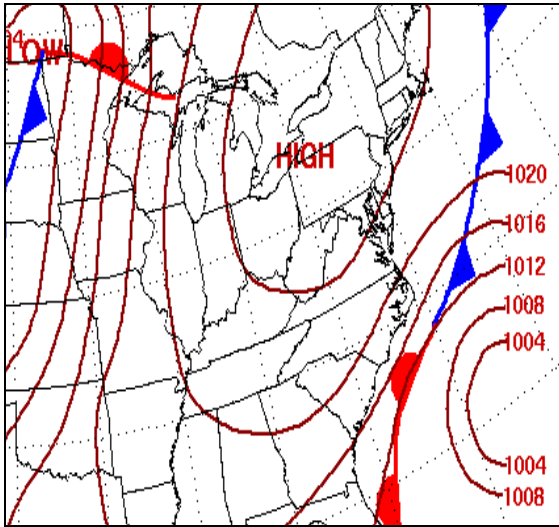


Fig. A-138: Observed standard station plot, (4 mb contours), precip. (shaded), 12 UTC, September 17, 2003.

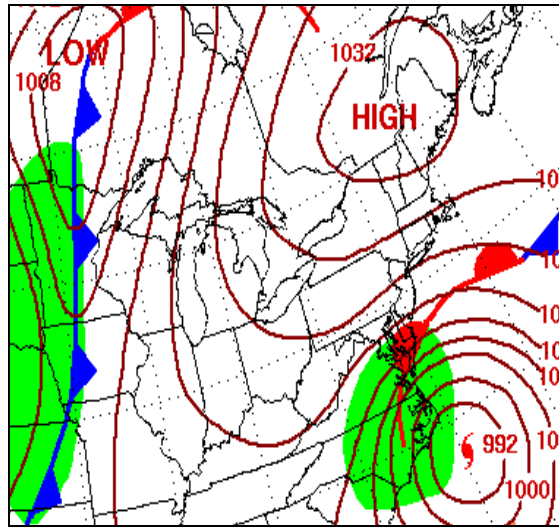


Fig. A-139: Observed standard station plot (4 mb contours), precip. (shaded), 12 UTC, September 18, 2003.

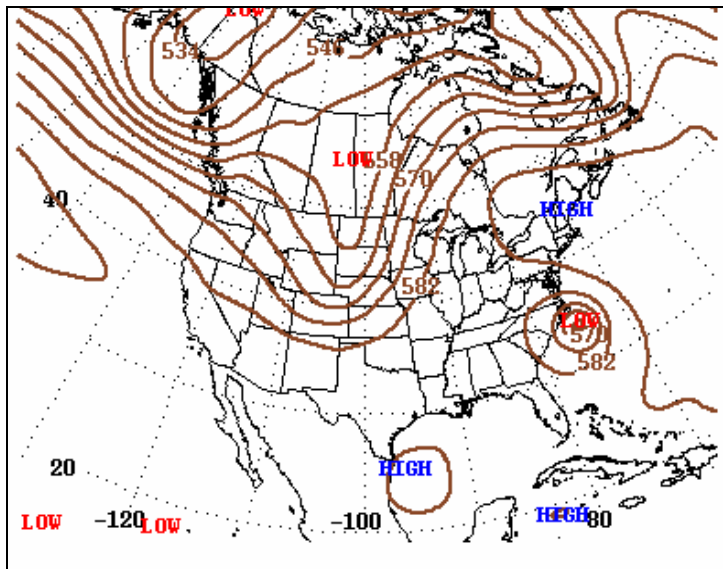


Fig. A-140: Observed 500 mb chart (60 m contours), winds (kts), temperatures (C), 12 UTC, Sept 18, 2003.

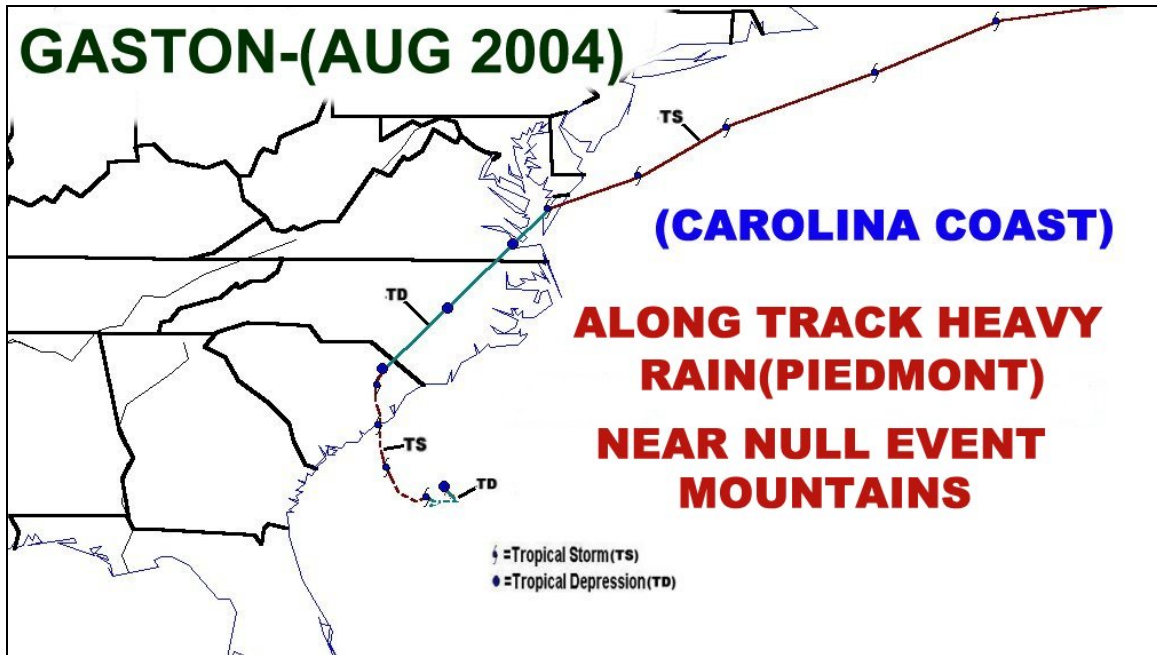


Fig. A-141: August 28-30, 2004. *GASTON*.

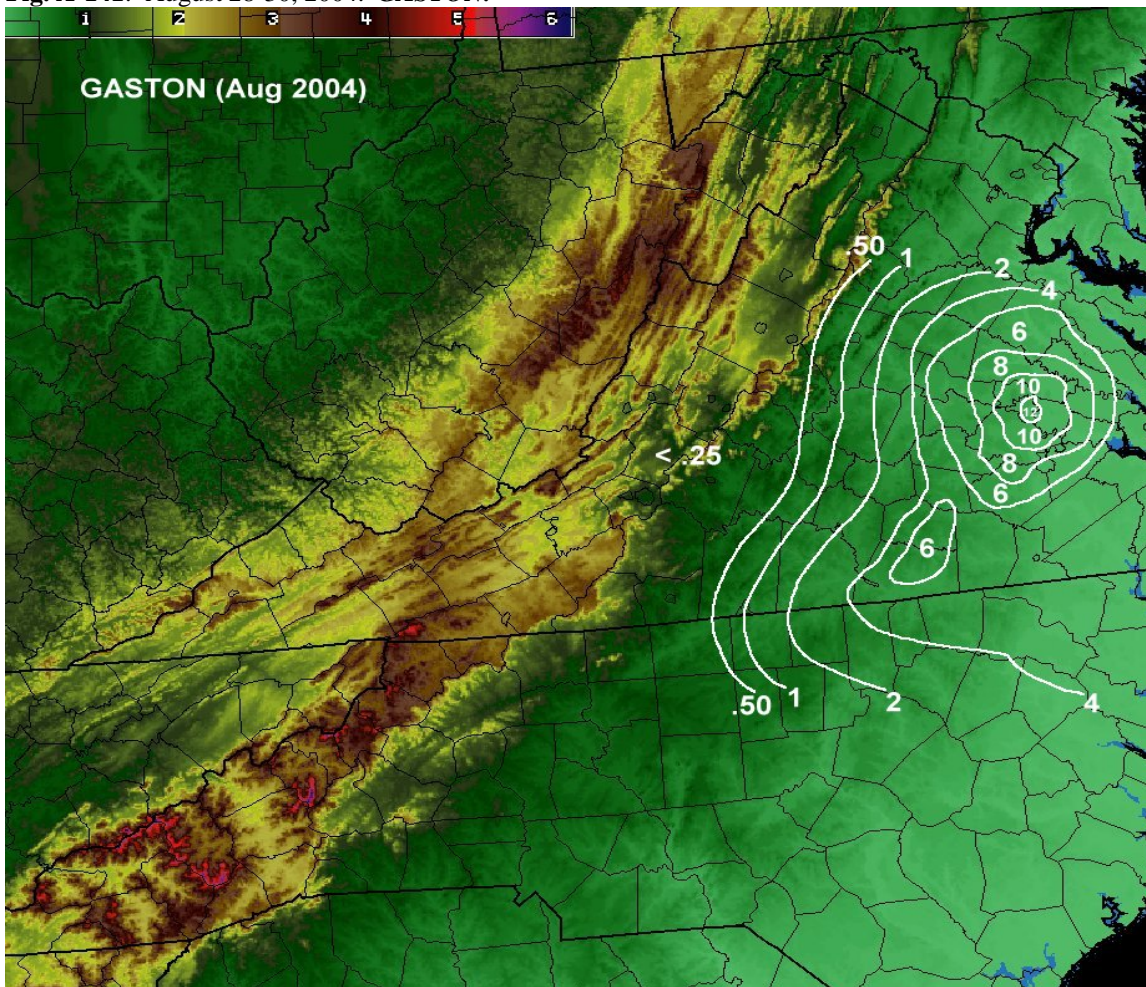


Fig. A-142: Gaston rainfall in inches (white contours), August 30, 2004, overlaid on terrain (k ft).

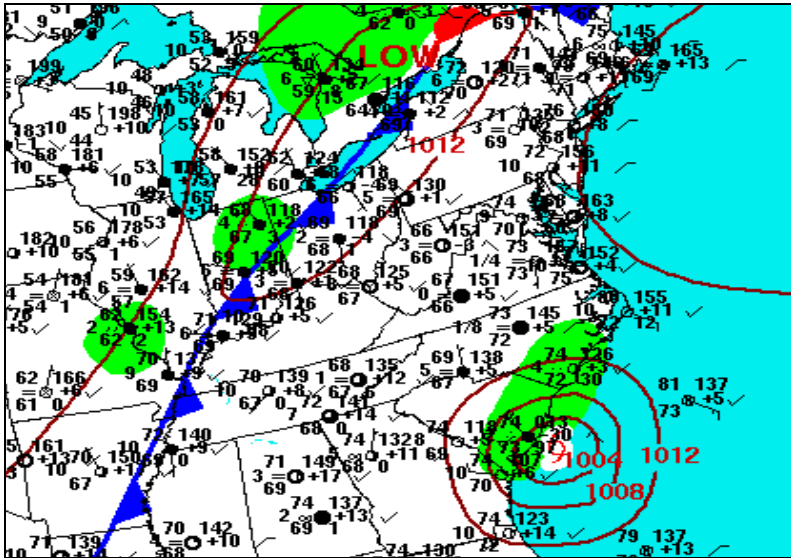


Fig. A-143: Observed standard station plot (4 mb contours), precip (shaded), 12 UTC, August 29, 2004.

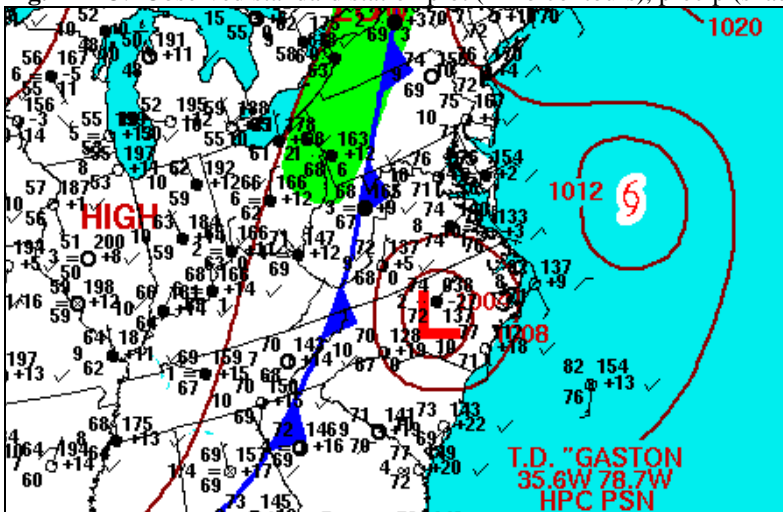


Fig. A-144: Observed standard station plot (4 mb contours), precip (shaded), 12 UTC, August 30, 2004.

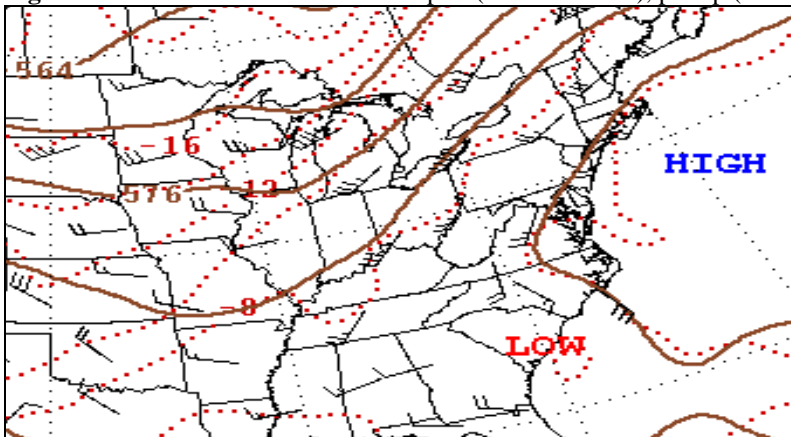


Fig. A-145: Observed 500 mb chart (60 m contours), winds (kts), temperatures (C), 12 UTC, August 29, 2004.

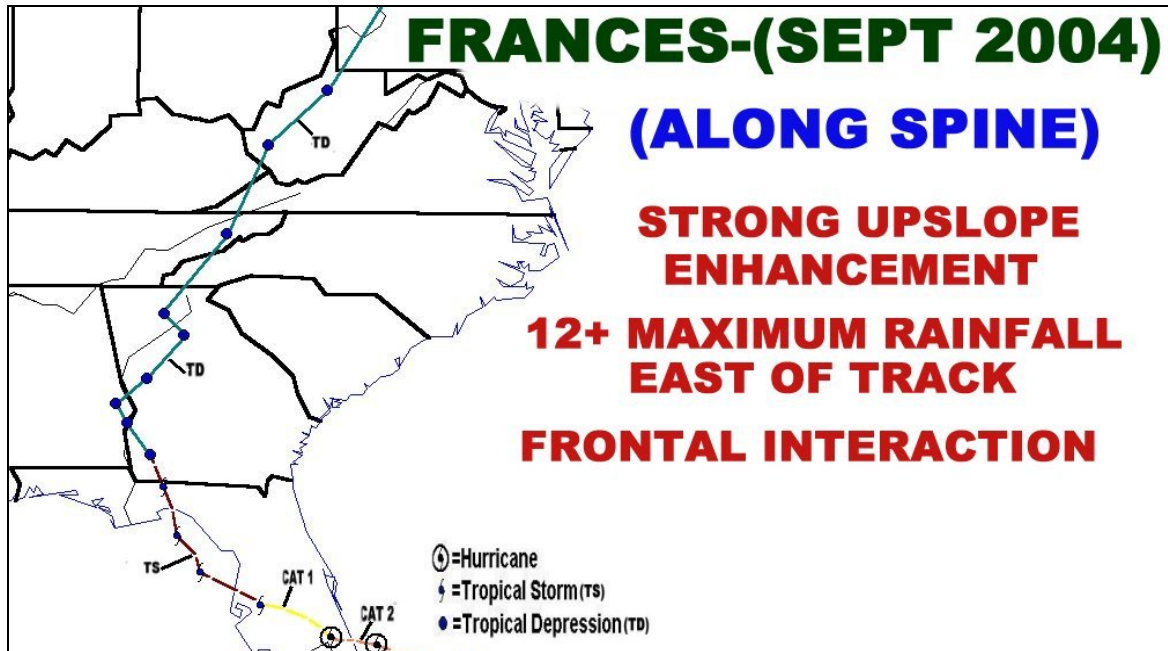


Fig. A-146: September 5-8, 2004. *FRANCES*.

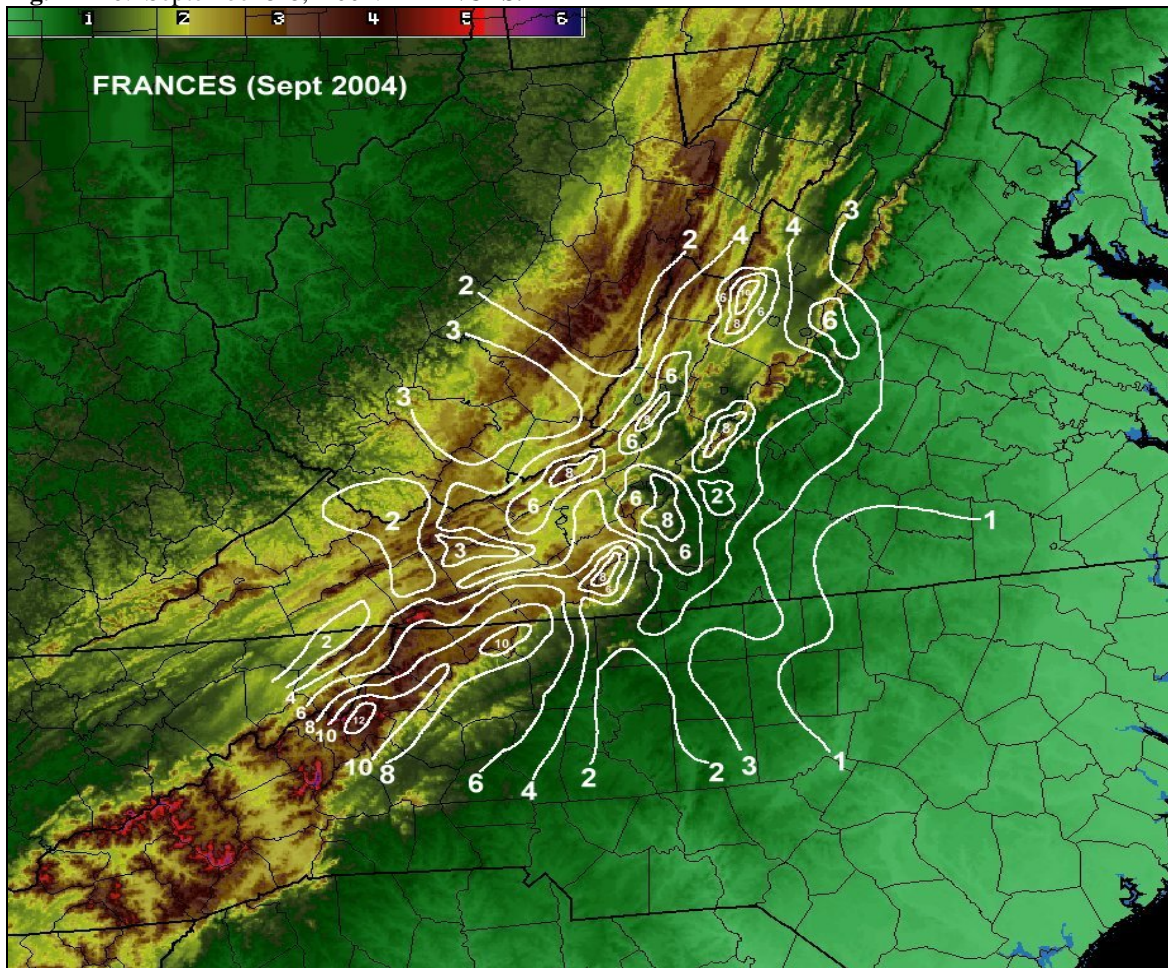


Fig. A-147: Frances rainfall in inches (white contours), Sept. 7-8, 2004, overlaid on terrain (k ft).

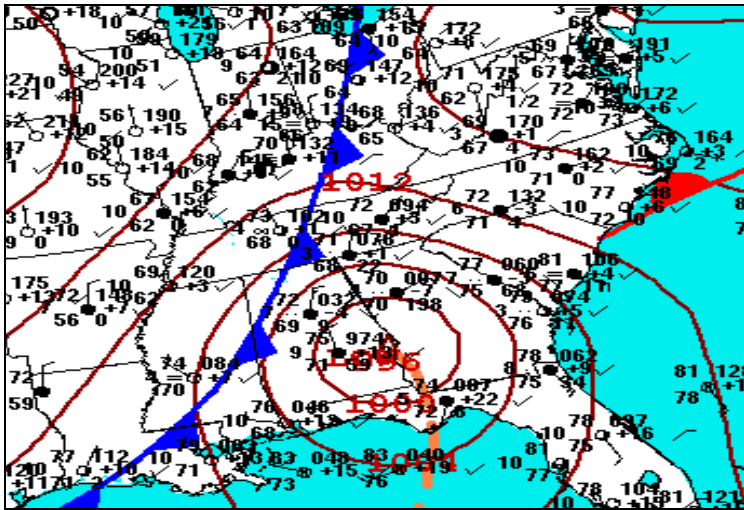


Fig. A-148: Observed standard station plot (4 mb contours), precip. (shaded), 12 UTC, Sept. 7, 2004.

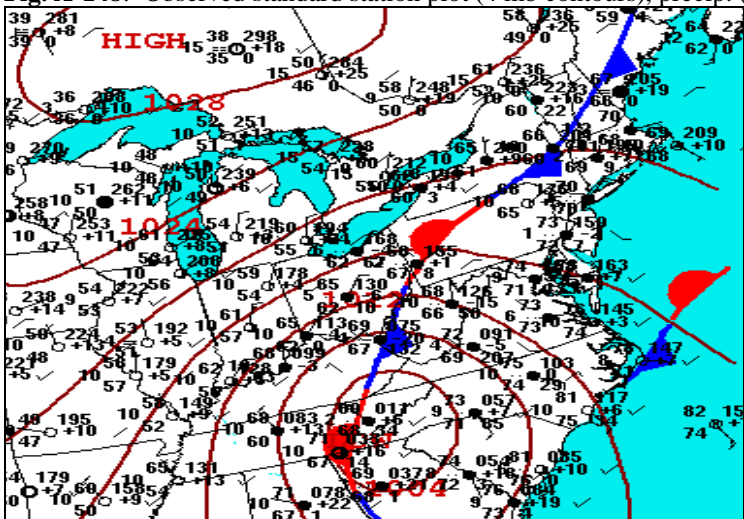


Fig. A-149: Observed standard station plot (4 mb contours), precip. (shaded), 12 UTC, Sept. 8, 2004.

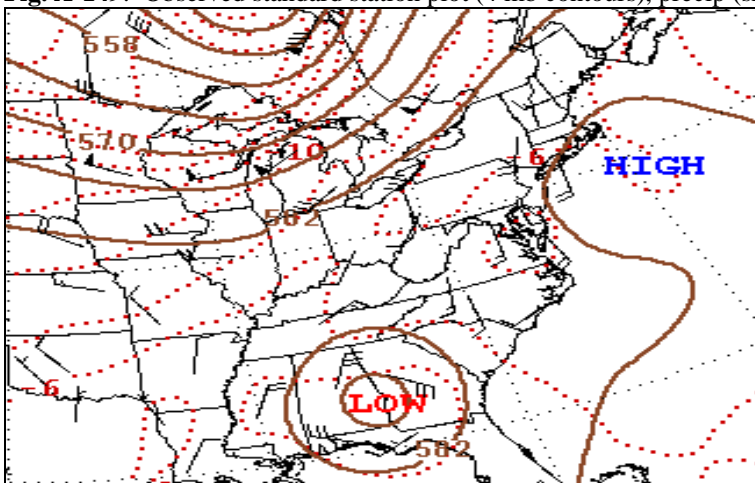


Fig. A-150: Observed 500 mb chart (60 m contours), winds (kts), temperatures (C), 12 UTC, Sept. 7, 2004.

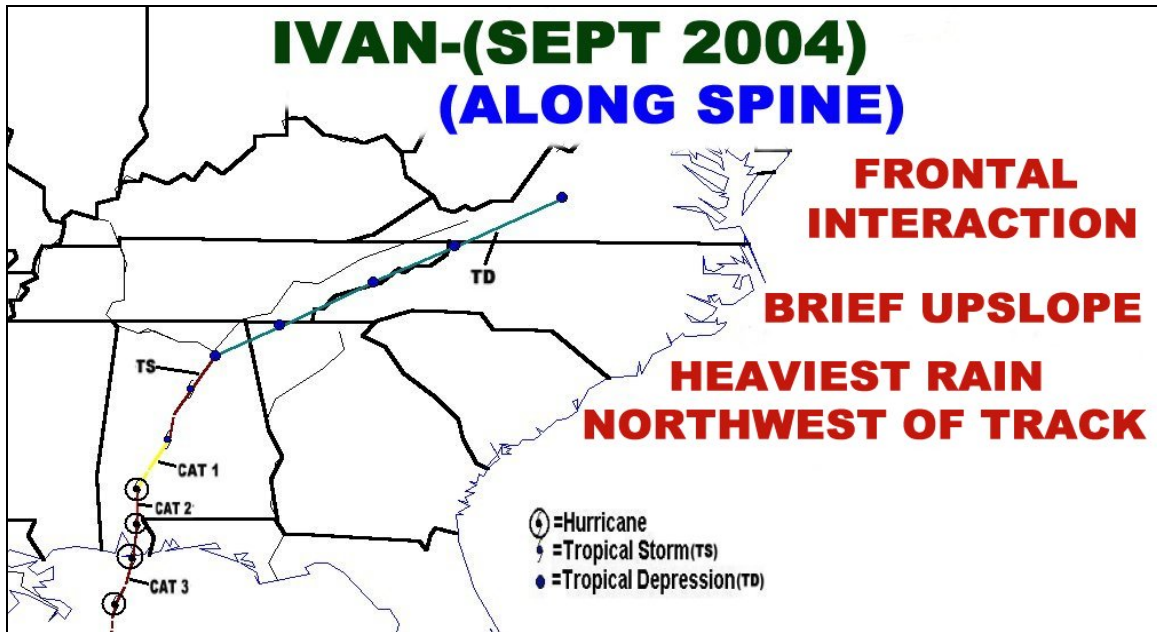


Fig. A-151: September 15-17, 2004. *IVAN*.

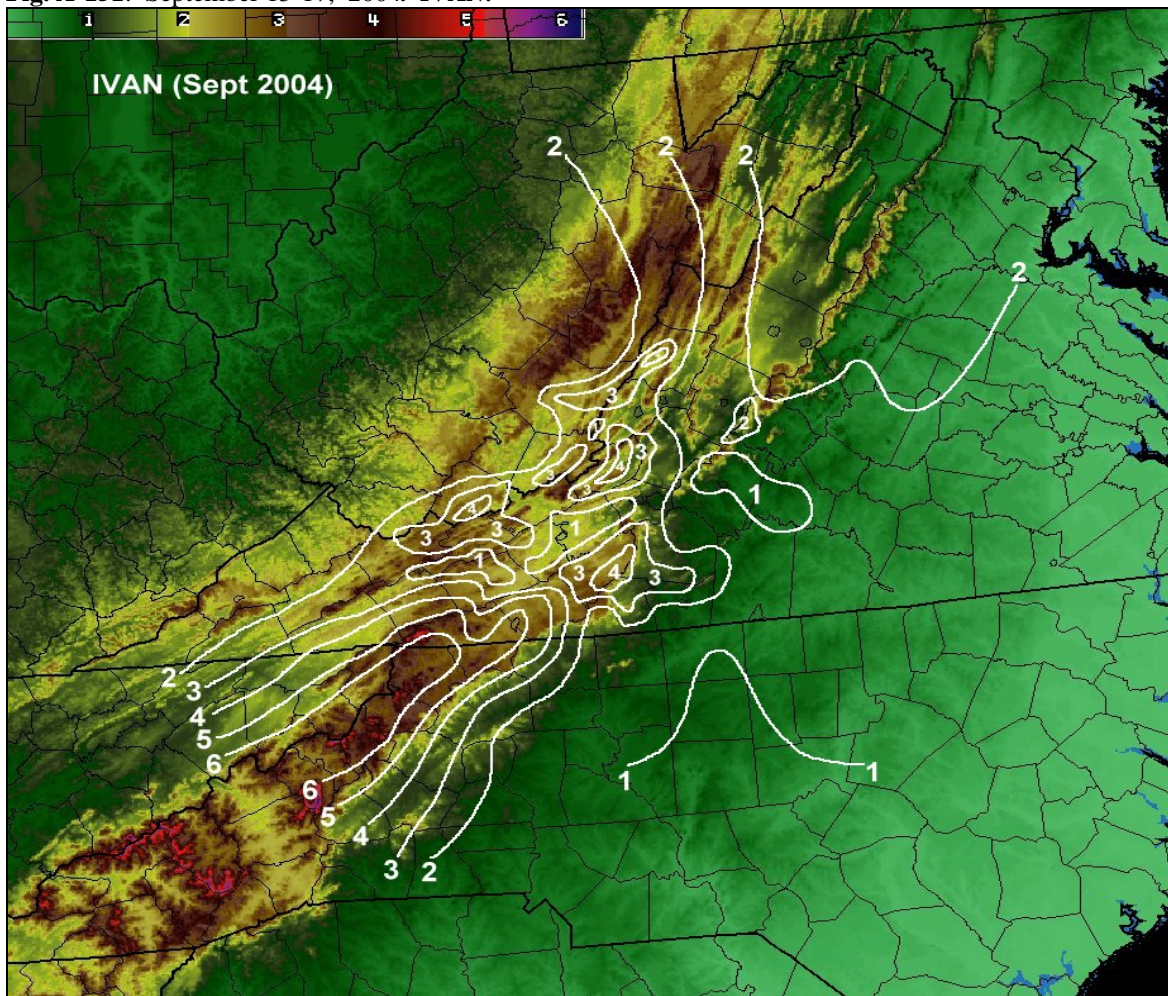


Fig. A-152: Ivan rainfall in inches (white contours), Sept. 16-17, 2004, overlaid on terrain (k ft).

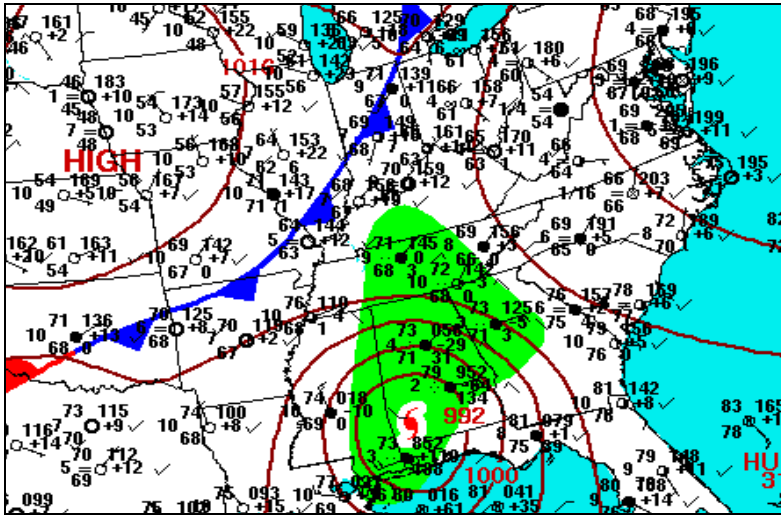


Fig. A-153: Observed standard station plot (4 mb contours), precip (shaded), 12 UTC, Sept. 16, 2004.

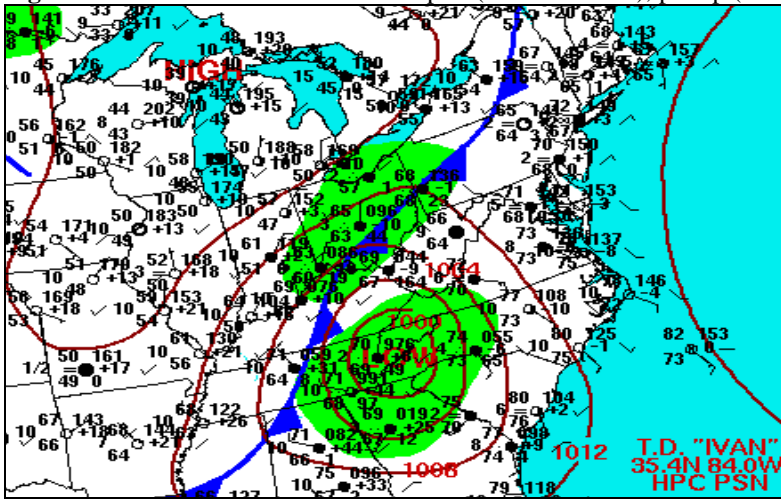


Fig. A-154: Observed standard station plot (4 mb contours), precip (shaded), 12 UTC, Sept. 17, 2004.

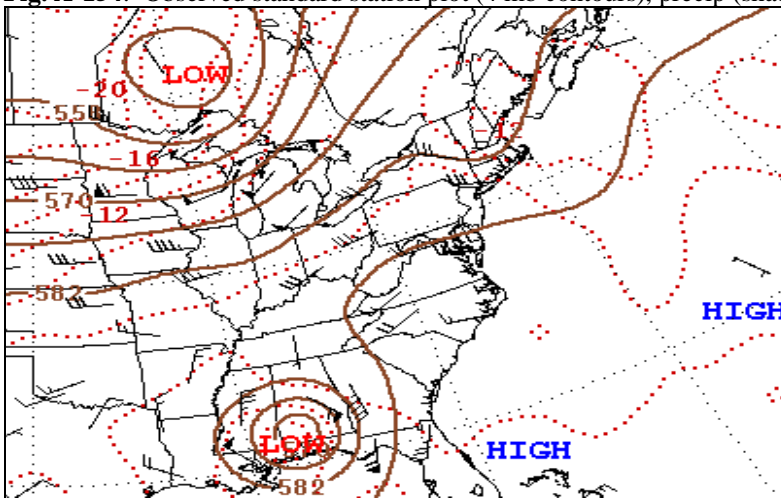


Fig. A-155: Observed 500 mb chart (60 m contours), winds (kts), temperatures (C), 12 UTC, Sept. 16, 2004.

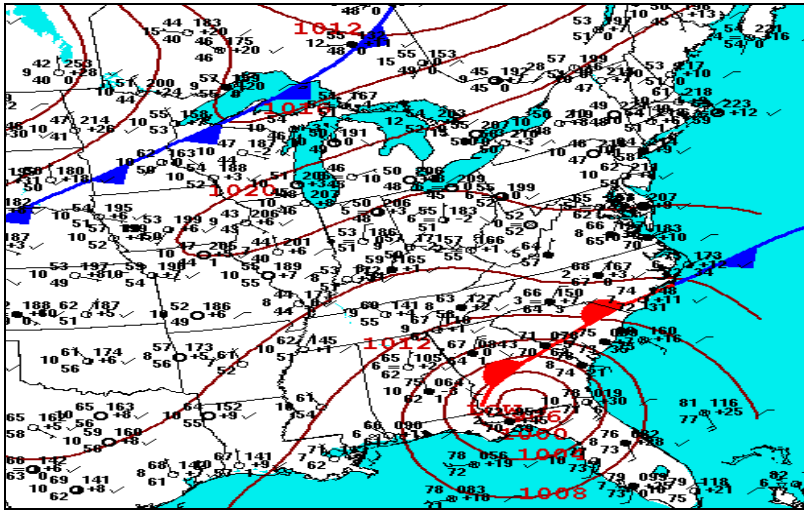


Fig. A-158: Observed standard station plot (4 mb contours), precip (shaded), 12 UTC, Sept. 27 , 2004.

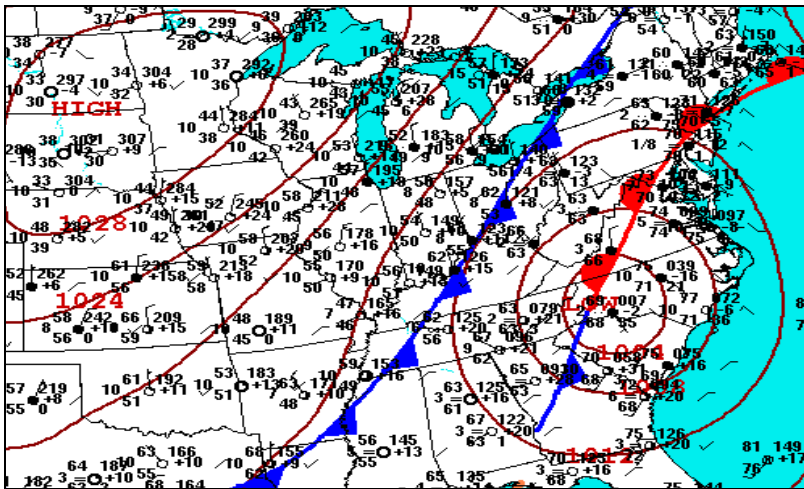


Fig. A-159: Observed standard station plot (4 mb contours), precip (shaded), 12 UTC, Sept. 28 , 2004.

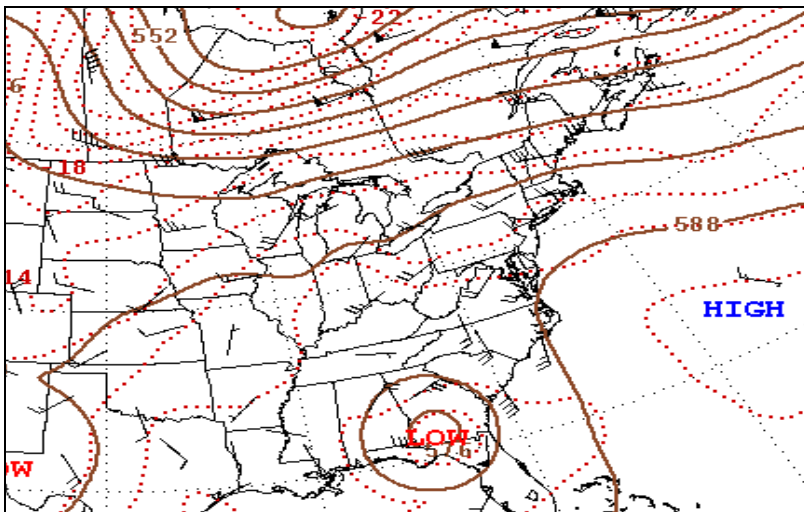


Fig. A-160: Observed 500 mb chart (60 m contours), winds (kts), temperatures (C), 12 UTC, Sept. 27, 2004

NWS ER 46 An Objective Method of Forecasting Summertime Thunderstorms. John F. Townsend and Russell J. Younkin. May 1972. (COM-72-10765).

NWS ER 47 An Objective Method of Preparing Cloud Cover Forecasts. James R. Sims. August 1972. (COM-72-11382).

NWS ER 48 Accuracy of Automated Temperature Forecasts for Philadelphia as Related to Sky Condition and Wind Direction. Robert B. Wassall. September 1972. (COM-72-11473).

NWS ER 49 A Procedure for Improving National Meteorological Center Objective Precipitation Forecasts. Joseph A. Ronco, Jr. November 1972. (COM-73-10132).

NWS ER 50 PEATMOS Probability of Precipitation Forecasts as an Aid in Predicting Precipitation Amounts. Stanley E. Wasserman. December 1972. (COM-73-10243).

NWS ER 51 Frequency and Intensity of Freezing Rain/Drizzle in Ohio. Marvin E. Miller. February 1973. (COM-73-10570).

NWS ER 52 Forecast and Warning Utilization of Radar Remote Facsimile Data. Robert E. Hamilton. July 1973. (COM-73-11275).

NWS ER 53 Summary of 1969 and 1970 Public Severe Thunderstorm and Tornado Watches Within the National Weather Service, Eastern Region. Marvin E. Miller and Lewis H. Ramey. October 1973. (COM-74-10160)

NWS ER 54 A Procedure for Improving National Meteorological Center Objective Precipitation Forecasts - Winter Season. Joseph A. Ronco, Jr. November 1973. (COM-74-10200).

NWS ER 55 Cause and Prediction of Beach Erosion. Stanley E. Wasserman and David B. Gilhousen. December 1973.(COM-74-10036).

NWS ER 56 Biometeorological Factors Affecting the Development and Spread of Plant Diseases. V.J. Valli. July 1974. (COM-74-11625/AS).

NWS ER 57 Heavy Fall and Winter Rain In The Carolina Mountains. David B. Gilhousen. October 1974. (COM-74-11761/AS).

NWS ER 58 An Analysis of Forecasters' Propensities In Maximum/Minimum Temperature Forecasts. I. Randy Racer. November 1974. (COM-75-10063/AS).

NWS ER 59 Digital Radar Data and its Application in Flash Flood Potential. David D. Sisk. March 1975. (COM-75-10582/AS).

NWS ER 60 Use of Radar Information in Determining Flash Flood Potential. Stanley E. Wasserman. December 1975. (PB250071/AS).

NWS ER 61 Improving Short-Range Precipitation Guidance During the Summer Months. David B. Gilhousen. March 1976. (PB256427).

NWS ER 62 Locally Heavy Snow Downwind from Cooling Towers. Reese E. Otts. December 1976. (PB263390/AS).

NWS ER 63 Snow in West Virginia. Marvin E. Miller. January 1977. (PB265419/AS).

NWS ER 64 Wind Forecasting for the Monongahela National Forest. Donald E. Risher. August 1977. (PB272138/AS).

NWS ER 65 A Procedure for Spraying Spruce Budworms in Maine during Stable Wind Conditions. Monte Glovinsky. May 1980. (PB80-203243).

NWS ER 66 Contributing Factors to the 1980-81 Water Supply Drought, Northeast U.S. Solomon G. Summer. June 1981. (PB82-172974).

NWS ER 67 A Computer Calculation and Display System for SLOSH Hurricane Surge Model Data. John F. Townsend. May 1984. (PB84-198753).

NWS ER 68 A Comparison Among Various Thermodynamic Parameters for the Prediction of Convective Activity. Hugh M. Stone. April 1985. (PB85-206217/AS).

NWS ER 69 A Comparison Among Various Thermodynamic Parameters for the Prediction of Convective Activity, Part II. Hugh M. Stone. December 1985. (PB86-142353/AS).

NWS ER 70 Hurricane Gloria's Potential Storm Surge. Anthony G. Gigi and David A. Wert. July 1986. (PB86-226644/AS).

NWS ER 71 Washington Metropolitan Wind Study 1981-1986. Clarence Burke, Jr. and Carl C. Ewald. February 1987. (PB87-151908/AS).

NWS ER 72 Mesoscale Forecasting Topics. Hugh M. Stone. March 1987. (PB87-180246/AS).

NWS ER 73 A Procedure for Improving First Period Model Output Statistics Precipitation Forecasts. Antonio J. Lacroix and Joseph A. Ronco, Jr. April 1987. (PB87-180238/AS).

NWS ER 74 The Climatology of Lake Erie's South Shoreline. John Kwiatkowski. June 1987. (PB87-205514/AS).

NWS ER 75 Wind Shear as a Predictor of Severe Weather for the Eastern United States. Hugh M. Stone. January 1988. (PB88-157144).

NWS ER 76 Is There A Temperature Relationship Between Autumn and the Following Winter? Anthony Gigi. February 1988. (PB88-173224).

NWS ER 77 River Stage Data for South Carolina. Clara Cillentine. April 1988. (PB88-201991/AS).

NWS ER 78 National Weather Service Philadelphia Forecast Office 1987 NOAA Weather Radio Survey & Questionnaire. Robert P. Wanton. October 1988. (PB89-111785/AS).

NWS ER 79 An Examination of NGM Low Level Temperature. Joseph A. Ronco, Jr. November 1988. (PB89-122543/AS).

NWS ER 80 Relationship of Wind Shear, Buoyancy, and Radar Tops to Severe Weather 1988. Hugh M. Stone. November 1988. (PB89-1222419/AS).

NWS ER 81 Relation of Wind Field and Buoyancy to Rainfall Inferred from Radar. Hugh M. Stone. April 1989. (PB89-208326/AS).

NWS ER 82 Second National Winter Weather Workshop, 26-30 Sept. 1988: Postprints. Laurence G. Lee. June 1989.(PB90-147414/AS).

NWS ER 83 A Historical Account of Tropical Cyclones that Have Impacted North Carolina Since 1586. James D. Stevenson. July 1990. (PB90-259201).

NWS ER 84 A Seasonal Analysis of the Performance of the Probability of Precipitation Type Guidance System. George J. Maglaras and Barry S. Goldsmith. September 1990. (PB93-160802)

NWS ER 85 The Use of ADAP to Examine Warm and Quasi-Stationary Frontal Events in the Northeastern United States. David R. Vallee. July 1991. (PB91-225037)

NWS ER 86 Rhode Island Hurricanes and Tropical Storms A Fifty-Six Year Summary 1936-0991. David R. Vallee. March 1993. (PB93-162006)

NWS ER 87 Post-print Volume, Third National Heavy Precipitation Workshop, 16-20 Nov. 1992. April 1993. (PB93-186625)

NWS ER 88 A Synoptic and Mesoscale Examination of the Northern New England Winter Storm of 29-30 January 1990. Robert A. Marine and Steven J. Capriola. July 1994. (PB94-209426)

NWS ER 89 An Initial Comparison of Manual and Automated Surface Observing System Observations at the Atlantic City, New Jersey, International Airport. James C. Hayes and Stephan C. Kuhl. January 1995.

NWS ER 90 Numerical Simulation Studies of the Mesoscale Environment Conductive to the Raleigh Tornado. Michael L. Kaplan, Robert A. Rozumalski, Ronald P. Weglarz, Yuh-Lang Lin, Steven Businger, and Rodney F. Gonski. November 1995.

NWS ER 91 A Climatology of Non-convective High Wind Events in Western New York State. Thomas A. Niziol and Thomas J. Paone. April 2000.

NWS ER 92 Tropical Cyclones Affecting North Carolina Since 1586 - An Historical Perspective. James E. Hudgins. April 2000.

NWS ER 93 A Severe Weather Climatology for the Wilmington, NC WFO County Warning Area. Carl R., Morgan. October 2001.

NWS ER 94 Surface-based Rain, Wind, and Pressure Fields in Tropical Cyclones over North Carolina since 1989. Joel Cline. June 2002.

NWS ER 95 A Severe Weather Climatology for the Charleston, South Carolina, WFO County Warning Area. Stephen Brueske, Lauren

NWS ER 96 A Severe Weather Climatology for the WFO Wakefield, VA County Warning Area. Brian T. Cullen. May 2003. (PB2003-105462)

NWS ER 97 Severe Weather Climatology for the Columbia, SC WFO County Warning Area. Leonard C. Vaughan. September 2003. (PB2004-100999)

NWS ER 98 Climatology of Heavy Rainfall Associated with Tropical Cyclones Affecting the Central Appalachians. James Hudgins, Steve Keighton, Kenneth Kostura, Jan Jackson. September 2005. (PB2005-110418)

NOAA SCIENTIFIC AND TECHNICAL PUBLICATIONS

The National Oceanic and Atmospheric Administration was established as part of the Department of Commerce on October 3, 1970. The mission responsibilities of NOAA are to assess the socioeconomic impact of natural and technological changes in the environment and to monitor and predict the state of the solid Earth, the oceans and their living resources, the atmosphere, and the space environment of the Earth.

The major components of NOAA regularly produce various types of scientific and technical information in the following kinds of publications:

PROFESSIONAL PAPERS--Important definitive research results, major techniques, and special investigations.

CONTRACT AND GRANT REPORTS--Reports prepared by contractors or grantees under NOAA sponsorship.

ATLAS--Presentation of analyzed data generally in the form of maps showing distribution of rainfall, chemical and physical conditions of oceans and atmosphere, distribution of fishes and marine mammals, ionospheric conditions, etc.

TECHNICAL SERVICE PUBLICATIONS--Reports containing data, observations, instructions, etc. A partial listing includes data serials; prediction and outlook periodicals; technical manuals, training papers, planning reports, and information serials; and miscellaneous technical publications.

TECHNICAL REPORTS--Journal quality with extensive details, mathematical developments, or data listings.

TECHNICAL MEMORANDUMS--Reports of preliminary, partial, or negative research or technology results, interim instructions, and the like.



Information on availability of NOAA publications can be obtained from:

NATIONAL TECHNICAL INFORMATION SERVICE
U.S. DEPARTMENT OF COMMERCE
5285 PORT ROYAL ROAD
SPRINGFIELD, VA 22161

